

PHENOMENOLOGICAL ANALYSIS OF MECHANICAL AND OPTICAL BEHAVIOUR OF RHEO-OPTICALLY SIMPLE MATERIALS

P. S. THEOCARIS

Summary

Classical photoelasticity can be extended to encompass the study of time dependent phenomena. For viscoelastic materials it is necessary to record the complete time history of their mechanical and optical characteristic properties. The mechanical properties can be expressed by the creep compliances and relaxation moduli in shear, extension and bulk deformation, as well as the lateral contraction functions in creep and relaxation. The optical properties are described by the stress-optical and strain-optical coefficients in creep or relaxation. Therefore, the main requirement for a photoviscoelastic analysis is the optical and mechanical characterization of the material. It is the purpose of this paper to review the principles and laws expressing the mechanical and optical behaviour of rheo-optically simple substances and to show important intimate relations between these characteristic functions as the time, frequency or temperature are varying during the tests.

INTRODUCTION

It has been well established that for a perfectly elastic high polymer used in photoelasticity principal stress—, strain—, and dielectric susceptibility-directions are always coincident. Since there is always an immediate response in strain or stress and birefringence for a suddenly applied external load or prescribed displacement in a perfectly elastic material, the equilibrium state for stress, strain and birefringence is reached instantaneously, as soon as the externally applied load or displacement is established. Photoelasticity, based on this simple principle, allows the study of elastic stress and displacement fields by using the birefringence created in a transparent model submitted to similar stress or displacement configurations as in the prototype, which, according to the Maxwell-Neumann law is directly proportional to the externally applied type of disturbance in the body. Therefore, in perfectly elastic materials the stress—, strain— and birefringence isoclinics are confounded into one family of curves.

Furthermore, it is actually a common practice for many viscoelastic substances used in photoelasticity and particularly for the stiffer ones, as they are all high polymers, which are in their glassy state at ambient temperature, to use a rate averaged

value for all mechanical and optical characteristic functions. While this policy is acceptable in the glassy region, where time, temperature, or frequency variations of these functions are generally very small and sometimes imperceptible, the general adoption of this simplifying principle not only yields erroneous solutions, but also masks the intimate relationships between the properties of the material.

However, in polymeric systems the mechanical behaviour is strongly dominated by viscoelastic phenomena. This is expected because of the complicated molecular adjustments, which underlie any macroscopic mechanical deformation. In a high-polymer each flexible threadlike molecule occupies a volume much greater than atomic dimensions, and is continuously changing the shape of its contour as it squirms and writhes with its thermal energy^[1]. Alfrey^[2] has referred to these spatial relationships viewed progressively over longer ranges from orientation of bonds in the chain-backbone, up to gross long-range contour relationships, as "kinks, curls and convolutions". Rearrangements on a local scale (kinks) are relatively rapid, rearrangements on a long range scale (convolutions) are on the contrary very slow. Under stress, a new assortment of configurations is obtained, consisting of a very wide and continuous range of time scales, covering the response of the local aspects of the new distribution, which is very rapid, to the response of the long-range aspects, which is very slow.

Every polymeric substance has a distinct temperature, the so-called *glass transition temperature*, below which the writhing thermal motions essentially cease. Below this temperature only local-scale rearrangements happen, while long-range convolutional readjustments are severely restricted. Application of external loads, when the polymer is at a temperature below the glass transition temperature, modifies the secondary bonds in the macromolecule and deforms the valence angles and therefore results to an increase of the internal energy of the substance. Thus, below this temperature limit, the assumption of an elastic behaviour for the polymer is a good approximation. Above this glass transition temperature the assumption is not valid.

Similar remarks can be made for the optical behaviour of the high-polymer. Below a temperature close to the glass-transition temperature the dielectric susceptibility, defining the birefringence engendered in the material, is influenced substantially in the same way as the mechanical properties of the material by the movement of the secondary bonds and thus the material behaves mechanically and optically as a quasi-elastic body. Above the glass-transition temperature the optical viscoelastic behaviour of the high polymer does not always follow the corresponding mechanical behaviour. The mechanism defining the birefringence may be different to the mechanism defining the mechanical viscoelastic behaviour of the material.

Parallelism between the optical and mechanical viscoelastic behaviour is not a general law, but an expression of the particular behaviour of a class of high polymers. This class of materials may be called *rheo-optically simple materials*. However, there exist many polymeric substances, whose optical and mechanical viscoelastic behaviours do not develop parallelly. Indeed, for the simple case of a creep experiment in

simple tension, the deformation developed in the specimen under isothermal conditions always increases and this results from thermodynamic reasons. On the contrary, there is no thermodynamic condition implying that the birefringence must always increase in the same type of creep test. The relations connecting the mechanical and optical behaviour of a high polymer are not conjugated thermodynamically. Only a phenomenological study for each particular substance may establish a relation between the mechanical and optical behaviour of the substance, and this relation may be of any type.

Furthermore, for the case of a viscoelastic material subjected to any type of loading or displacement, the correspondence between stress-, strain-, and dielectric susceptibility-tensors is not in advance known to be so simple as for perfectly elastic materials. Even for rheo-optically simple materials the interrelation of these three tensors is not very simple, especially at the transition region of the viscoelastic spectrum above the glass transition temperature, where strong time-dependent variations in stress, strain and birefringence are expected to happen.

It is the purpose of this paper to give a critical review of the principles and laws which express the mechanical and optical behaviour of linear viscoelastic materials. Since the most important high polymers used in photoelasticity are of the type of rheo-optically simple materials, we restrict ourselves to this group of high polymers. This restriction is also justified by the fact that all other high polymers, which do not comply with the rheo-optically simple materials, present a mechanical and optical behaviour which is particular for each substance, and it is difficult to derive general laws for their viscoelastic behaviour valid for a large group of materials.

Characterization of material Properties

In a viscoelastic body the state of deformation at a generic point is specified by the strain tensor. Similarly, the state of stress is specified by the stress tensor. Furthermore the refractive index variation in the body, due to the created optical anisotropy because of the external loading, is specified by the refractive index tensor or the dielectric susceptibility tensor. Both the latter tensors are independent of the particular loading programme of the viscoelastic substance, the geometric characteristics of the specimen used in the tests, and the optical set-up. However, since birefringence is what we measure in a photoelastic test we will use in the following the birefringence tensor keeping always in mind that this tensor is dependent also on the particular characteristics of the material used, the type of test and the experimental arrangement. If the strains are small the components of the three tensors are related in a simple manner by certain moduli or compliances of elasticity, which are properties of the material alone. These moduli for viscoelastic substances are time dependent, and the nature of this dependence is the primary interest of the phenomenological study of viscoelasticity.

In the following it is assumed that the material is initially isotropic, homogeneous,

and elastic and that the strains are small compared with unity. These definitions are the same for elastic and viscoelastic substances in all respects except that for the viscoelastic materials the moduli and compliances will be functions of time and the previous stress history.

Two basic types of deformation may be created in a deformable body. These are simple shear, which creates a change only of shape, and bulk deformation, which corresponds to a change of volume with no change in shape. All other types of deformation may be created by superposition of these two simple types. The molecular adjustments, which accompany a macroscopic response to stress, are different in these two simple cases, and physical measurements of the two types of deformation yield different kinds of information concerning the molecular motions and interactions. The simplest way to describe the viscoelastic behaviour of a polymer is to define at least two of its elastic compliances or moduli along the whole range of time, frequency and temperature.

Three types of compliances and moduli exist, which correspond to the different modes of static or dynamic loading of specimens, i.e., the extension, the shear and the bulk compliances, [$D(t)$, $J(t)$ and $B(t)$ respectively] and moduli [$E(t)$, $G(t)$ and $K(t)$ respectively]. These quantities describe the mechanical properties of each material. The optical properties of the transparent materials are related to the variation of birefringence with stress and strain through the stress-optical and strain-optical coefficients in creep and relaxation [$C_\sigma(t)$, $C_\varepsilon(t)$].

A great part of the viscoelastic materials manifesting accidental birefringence and used in photoelastic analysis may be classed as *rheo-optically simple materials*. The linearity in their mechanical and optical behaviour may be shown experimentally by satisfying Boltzmann's superposition principle^[3]. A linear behaviour implies that the viscoelastic laws may be expressed by linear differential or integral operators which, when properly chosen, may reproduce any arbitrary creep or relaxation function for any time-dependent input loading. There are many ways of specifying these sets of differential or integral operators. Linear-differential operators are related to various finite viscoelastic models, which are mere pictorial representations of the differential relationships.

A more general representation in terms of the creep compliances or relaxation moduli functions is given by using viscoelastic operators in integral form. The relations holding between normal stresses (σ_i) and strains (ε_i), their deviatoric components (s_{ij} , e_{ij}), the mean normal stresses and strains (σ_{kk} , ε_{kk}), the maximum shear stresses and strains (σ_m , γ_m) the birefringence due to an applied constant maximum shear stress or strain (N_σ , N_ε) are expressed by the relations:

$$\varepsilon_i(t) = \int_0^t D(t-\tau) \frac{d\sigma_i(\tau)}{d\tau} d\tau, \quad \sigma_i(t) = \int_0^t E(t-\tau) \frac{d\varepsilon_i(\tau)}{d\tau} d\tau, \quad (1)$$

$$e_{ij}(t) = \frac{1}{2} \int_0^t J(t-\tau) \frac{ds_{ij}(\tau)}{d\tau} d\tau, \quad s_{ij}(t) = 2 \int_0^t G(t-\tau) \frac{de_{ij}(\tau)}{d\tau} d\tau, \quad (2)$$

$$e_{kk}(t) = \frac{1}{3} \int_0^t B(t-\tau) \frac{d\sigma_{kk}(\tau)}{d\tau} d\tau, \quad \sigma_{kk}(t) = 3 \int_0^t K(t-\tau) \frac{de_{kk}(\tau)}{d\tau} d\tau, \quad (3)$$

$$\gamma_m(t) = \int_0^t C_s(t-\tau) \frac{d}{d\tau} \left[N_s(\tau) \cos 2\theta(\tau) \right] d\tau, \quad 2\sigma_m(t) = \int_0^t C_\sigma(t-\tau) \frac{d}{d\tau} \left[N_\sigma(\tau) \cos 2\theta(\tau) \right] d\tau, \quad (4)$$

where $\theta(\tau)$ is the angle made between the principal axes of birefringence and the principal axes of stress and strain. The integral equations (1-4) express Boltzmann's superposition principle in the case of a continuous stress or strain history. It is assumed in these formulas that all prescribed stress- and strain-components are step functions of time. They are assumed applied at non-negative time, the body remaining undisturbed for any negative value of time. The quantities $D(t)$, $J(t)$ and $B(t)$ are the *extention*, *shear* and *bulk compliances* respectively. Similarly, $E(t)$, $G(t)$ and $K(t)$ are the *respective moduli*. These moduli are connected with the corresponding compliances by the integral equations of the convolution type:

$$\int_0^t E(t-\tau) D(\tau) d\tau = t,$$

$$\int_0^t G(t-\tau) J(\tau) d\tau = t,$$

$$\int_0^t K(t-\tau) B(\tau) d\tau = t.$$

The quantities $E(t)$, $D(t)$, $G(t)$, $J(t)$ and $K(t)$, $B(t)$ are interrelated by the following inequalities:

$$E(t) D(t) \leq 1, \quad G(t) J(t) \leq 1, \quad K(t) B(t) \leq 1. \quad (6)$$

The validity of the last three inequalities was indicated by Schwarzl[4] and shown experimentally by Theocaris[5].

If we consider the variation with time of the lateral strain $-\varepsilon_y(t)$ due to the longitudinal strain $\varepsilon_x(t)$ of a viscoelastic tension specimen under creep or relaxation, we define two types of lateral contraction ratio functions of the material $\nu_c(t)$ and $\nu_r(t)$ corresponding to a creep or relaxation mode of loading. These two functions are in principle different in the physical plane and they coincide only in the transform plane. They have been introduced in this form by Theocaris[5], and they are expressed by the integral equations :

$$-\varepsilon_y(t) = \int_0^t \nu_c(t-\tau) D(t-\tau) \frac{d\sigma_x(\tau)}{d\tau} d\tau, \quad (7a)$$

$$-\varepsilon_y(t) = \int_0^t \nu_r(t-\tau) \frac{d\varepsilon_x(\tau)}{d\tau} d\tau. \quad (7b)$$

The function $\nu_c(t)$ defined from a creep test [$\sigma(t) = \sigma_0 H(t)$, $H(t)$ is a step function] is in principle different than the function $\nu_r(t)$ defined from a relaxation test. Again, the following integral relation of the convolution type holds between the two lateral contraction ratio functions :

$$\int_0^t \nu_r(t-\tau) \nu_c^{-1}(\tau) d\tau = t, \quad (8)$$

which indicates that, in the physical plane, it is valid that :

$$\nu_c^{-1}(t) \cdot \nu_r(t) \leq 1. \quad (9)$$

For a uniaxial tension test both the lateral strain $-\varepsilon_y(t)$ and the mean normal strain must be positive and it is then valid that :

$$3D(t) \geq J(t) > 2D(t) \quad \text{or} \quad E(t)/3 \leq G(t) < E(t)/2 \quad (10a)$$

and

$$\frac{1}{2} \geq \nu_{c,r}(t) > 0. \quad (10b)$$

The lateral contraction ratio functions are dimensionless and may vary between 0 and 1/2. Unlike the compliances and the moduli, it cannot be claimed in advance that the lateral contraction ratio functions are monotonically varying functions. However, there is sufficient experimental evidence, covering an extended range of polymeric substances, and showing that both lateral contraction ratio functions are monotonically increasing functions with time and temperature.

The compliances and the corresponding moduli, as well as the two lateral contraction ratio functions are interrelated by Volterra's integral equations of the second kind :

$$D(t) = J(t)/3 + B(t)/9 \quad (11)$$

$$J(t) = 2D(t) \left[1 + \nu_{r0} \right] + 2 \int_0^t \dot{\nu}_r(t-\tau) D(\tau) d\tau \quad (12)$$

$$B(t) = 3D(t) \left[1 - 2\nu_{r0} \right] - 6 \int_0^t \dot{\nu}_r(t-\tau) D(\tau) d\tau \quad (13)$$

$$E(t) = 2G(t) \left[1 + \nu_{r0} \right] + 2 \int_0^t \dot{\nu}_r(t-\tau) G(\tau) d\tau \quad (14)$$

$$E(t) = 3K(t) \left[1 - 2\nu_{r0} \right] - 6 \int_0^t \dot{\nu}_r(t-\tau) K(\tau) d\tau \quad (15)$$

$$\nu_r(t) = \frac{1}{2} \left[J_0 E(t) - 1 \right] + \frac{1}{2} \int_0^t \dot{J}(t-\tau) E(\tau) d\tau \quad (16)$$

$$v_r(t) = \left[\frac{1}{2} - \frac{1}{6} B_0 E(t) \right] - \frac{1}{6} \int_0^t \dot{B}(t-\tau) E(\tau) d\tau \quad (17)$$

$$v_c(t) D(t) = v_{r0} D(t) + \int_0^t \dot{v}_r(t-\tau) D(\tau) d\tau. \quad (18)$$

These are the simplest of the integral equations interrelating every three characteristic functions(*). It is generally accepted that one pair of independent functions specifies the whole viscoelastic behaviour and every other characteristic function can be calculated from any pair of functions known. Some of the above mentioned relations will be used later for the derivation of further interrelations.

In order to supplement the transient experiments and simultaneously to provide data corresponding to very short times, experiments with periodically varying external excitations may be executed. A periodic test at radian frequency ω is qualitatively equivalent to a transient test at time $t = 1/\omega$. For linear viscoelastic materials all compliances and moduli consist of a complex quantity decomposed into a real part (*the storage compliance or modulus*) and an imaginary part (*the loss compliance or modulus*). Thus, we have :

$$\begin{aligned} D^* &= (D' - iD'') & E^* &= (E' + iE'') \\ J^* &= (J' - iJ'') & G^* &= (G' + iG'') \\ B^* &= (B' - iB'') & K^* &= (K' + iK'') \\ v_c^* &= (v_c' - i v_c'') & v_r^* &= (v_r' + i v_r''). \end{aligned} \quad (19) \quad (20)$$

If the ratio of the peak stress to the peak strain (F^*) and the phase angle δ , ($\tan \delta = F''/F'$), are measured the well known relations hold:

$$\left[F^*(\omega) \right] = \left\{ \left[F'(\omega) \right]^2 + \left[F''(\omega) \right]^2 \right\}^{1/2}, \quad \tan \delta = F''(\omega) / F'(\omega) \quad (21)$$

where F^* , F' and F'' express all complex storage or loss moduli and compliances.

Although it is valid that $D^*(\omega) = 1/E^*(\omega)$, $J^*(\omega) = 1/G^*(\omega)$ and $B^*(\omega) = 1/K^*(\omega)$ their individual components are connected by:

$$D'(\omega) = \frac{E'(\omega)}{[E'(\omega)]^2 + [E''(\omega)]^2} = \frac{1}{1 + \tan^2 \delta} \frac{1}{E'(\omega)}$$

(*) In previous papers by the author similar relations to Equs (12)-(18) were given where all three interrelated viscoelastic functions in each integral equation were either creep or relaxation functions. These relations were derived from the above exact relations by introducing either of the approximate relations $D(t) \approx 1/E(t)$, $J(t) \approx 1/G(t)$, $B(t) \approx 1/K(t)$ and $v_c(t) = v_r(t)$. This was done in order to obtain integral equations interrelating exclusively either creep or relaxation functions. Experimental evidence proves the validity of these simple functions as a first approximation[^{21, 30, 38, 39, 44, 46, 49}].

$$D''(\omega) = \frac{E''(\omega)}{[E'(\omega)]^2 + [E''(\omega)]^2} = \frac{1/E''(\omega)}{1 + (\tan^2 \delta)^{-1}} \quad (21a)$$

$$E'(\omega) = \frac{D'(\omega)}{[D'(\omega)]^2 + [D''(\omega)]^2} = \frac{1/D'(\omega)}{1 + \tan^2 \delta},$$

$$E''(\omega) = \frac{D''(\omega)}{[D'(\omega)]^2 + [D''(\omega)]^2} = \frac{1/D''(\omega)}{1 + (\tan^2 \delta)^{-1}},$$

and similar relations are valid for the other pairs of compliances and moduli.

By using the Laplace transform in Eqs. (1) and (4) and considering that the characteristic functions are step functions which are zero for negative arguments and positive for non-negative arguments, we obtain :

$$\bar{\sigma}_i(p) = \bar{E}(p) \bar{\varepsilon}_i(p)$$

$$2\bar{\sigma}_m(p) = \bar{C}_{\sigma r}(p) \bar{N}_\sigma(p) \cos 2\theta(p) \quad (22)$$

$$\bar{\varepsilon}_i(p) = \bar{D}(p) \bar{\sigma}_i(p)$$

$$\bar{\gamma}_m(p) = \bar{C}_{\varepsilon c}(p) \bar{N}_\varepsilon(p) \cos 2\theta(p) \quad (23)$$

$$\bar{E}(p) \bar{D}(p) = 1, \quad \bar{G}(p) \bar{J}(p) = 1, \quad \bar{K}(p) \bar{B}(p) = 1, \quad (24)$$

where bars represent the Laplace transforms of the corresponding functions with respect to time and relations (24) are derived from Eqs. (5). Furthermore, relations (12) to (18) become in the transform plane the well known elastic relations between moduli and compliances. Particularly, relations expressing the lateral contraction ratios in the transform plane are the well known elastic relations. Thus $\bar{\nu}_c(p)$ and $\bar{\nu}_r(p)$ in terms of the extension and bulk compliances and moduli are given by :

$$\bar{\nu}_c(p) = \left[\frac{1}{2} - \frac{\bar{B}(p)}{6\bar{D}(p)} \right], \quad \bar{\nu}_r(p) = \left[\frac{1}{2} - \frac{\bar{E}(p)}{6\bar{K}(p)} \right].$$

These relations because of Eqs. (24) yield :

$$\bar{\nu}_c(p) = \bar{\nu}_r(p)$$

and by applying Lerch's theorem we have that :

$$\nu_c(t) = \nu_r(t). \quad (25)$$

Therefore the LCR functions in creep and relaxation are equal and we may use indifferently either of them in any of the integral equations (12) to (18). Experimental evidence with a highly cross-linked polymer (pure epoxy resin) showed a discrepancy between measured values of $\nu_c(t)$ and $\nu_r(t)$ which was always less than 5 percent at maximum. This discrepancy may be attributed to experimental error in measuring the two couples of strains for each test[5].

The constitutive equations for the isothermal deformation of a linear viscoelastic substance may be expressed by the integral operator relation :

$$\sigma_{ij} = 3\delta_{ij} \int_0^t K(t-\tau) \dot{\varepsilon}_{kk}(\tau) d\tau + 2 \int_0^t G(t-\tau) \dot{e}_{ij}(\tau) d\tau \quad (26)$$

or its inverse :

$$\varepsilon_{ij} = \frac{\delta_{ij}}{3} \int_0^t B(t-\tau) \dot{\sigma}_{kk}(\tau) d\tau + \frac{1}{2} \int_0^t J(t-\tau) \dot{s}_{ij}(\tau) d\tau \quad (27)$$

where δ_{ij} is the Kronecker delta, and dots mean differentiation with time. These relations in the transform plane become :

$$\overline{\sigma}_{ij}(p) = 3\delta_{ij} \overline{K}(p) \varepsilon_{kk}(p) + 2\overline{G}(p) \dot{e}_{ij}(p) \quad (28)$$

$$\overline{\varepsilon}_{ij}(p) = \frac{\delta_{ij}}{3} \overline{B}(p) \dot{\sigma}_{kk}(p) + \frac{1}{2} \overline{J}(p) \dot{s}_{ij}(p). \quad (29)$$

For the dynamic moduli and compliances it can be readily derived that the elastic stress-strain relationships hold with moduli or compliances of the complex quantities. Then, the interrelations between dynamic complex moduli and compliances are the simple elastic relations.

The Viscoelastic Spectra and Their Approximations

For the study of the relations interconnecting the various viscoelastic functions, it has been proved useful to introduce two series of additional derived functions the *retardation* and *relaxation spectra* in extension, shear, bulk and LCR functions. These spectra were derived from the different models, introduced to visualize the viscoelastic behaviour of high polymers. Although both the models and the derived spectra are not quite essential for the purpose of mathematical definition, they are useful to reveal the intimate viscoelastic behaviour of each polymer and yield important indications concerning the interdependence of the characteristic functions.

Although we shall present the general equations of these spectra, we will not be concerned with the mechanical models, which lie behind them, since we consider that the presentation of the viscoelastic behaviour by an infinite series of models is objectionable. This is due to the fact that, while a certain type or combination of mechanical models can be adjusted to fit one characteristic function of the material, it is generally impossible to succeed to obtain reasonable results by the same model for the remaining viscoelastic functions. Indeed, Freudenthal and Henry^[6] studied theoretically the variation of LCR for a number of typical viscoelastic models. They found that for a Maxwell and a four-parameter body, LCR varies between 0.33 and 0.50, in the case where it is assumed that $3K = 8G$. A Kelvin body, and the so-called standard solid under the same assumption are rather unrealistic since they vary between $-\infty$ and 0.33 and 0.20 and 0.33 respectively. This proves

that, while an infinite number of models may fit satisfactorily one characteristic property of the material, (say the extension compliance or modulus), this does not imply that it also satisfies all others (say the LCR function), and thus it does not describe properly and accurately the viscoelastic behaviour of the substance.

The continuous retardation spectrum for the extension creep compliance $D(t)$ is defined by :

$$D(t) = Dg + \int_0^{\infty} L_e(\ln\tau) (1 - e^{-t/\tau}) d(\ln\tau), \quad (30)$$

where the instantaneous compliance Dg is added to introduce a discrete contribution with $t = 0$. Similarly, the relaxation spectrum for the extension relaxation modulus is given as:

$$E(t) = E_r + \int_0^{\infty} H_e(\ln\tau) (e^{-t/\tau}) d(\ln\tau), \quad (31)$$

where the instantaneous modulus E_r is introduced to encounter the discrete contribution with $t = \infty$.

Similar relations to Eqs. (30) and (31) exist, which express the retardation and relaxation spectra in shear (subscript s) in bulk deformation (subscript v), as well as the lateral contraction ratio in creep or relaxation (subscript v). These equations, relating a viscoelastic function with its spectrum, although accurate within the assumptions of linear viscoelasticity, fail to meet practical purposes as they stand, because an integration from 0 to $+\infty$ is required for a function, which is not known analytically all over the viscoelastic range.

Following the development by Schwarzl and Staverman^[7-9] we introduce the approximations for the retardation (L_k) and relaxation (H_k) spectra :

$$L_k = \int_0^{\infty} f_k(t/\tau) L(\ln\tau) d(\ln\tau), \quad (32)$$

$$H_k = \int_0^{\infty} g_k(t/\tau) H(\ln\tau) d(\ln\tau), \quad (33)$$

where the approximations L_k and H_k are expressed as integrals over the exact spectra (L or H), multiplied by the intensity functions f_k or g_k of order k . The intensity functions must be positive for $\tau > 0$, they are functions of (t/τ) possessing only one maximum in the region $\tau = t$, they are normalized, and they decrease to zero at both sides of the maximum. With the spectrum not varying in the region where f_k or g_k are noticeably different from zero, the following approximations hold, if we take into consideration the normalization properties of f_k and g_k respectively :

$$L_k(\ln t) = L_k(\ln\tau) \int_0^{\infty} f_k(t/\tau) d(\ln\tau) = L(\ln t) \quad (34)$$

$$H_k(\ln t) = H(\ln \tau) \int_0^\infty g_k(t/\tau) d(\ln \tau) = H(\ln t).$$

In order that relations (34) hold exactly, the corresponding intensity functions f_k and g_k must be delta functions. Then, the closer the resemblance of the intensity function to a delta function the higher the approximation.

If we take

$$f_k = f_1 = \left[\frac{t}{\tau} e^{-t/\tau} \right] \quad (35)$$

we obtain the so-called *first approximation for the retardation or relaxation spectra*. This approximation is generally rather poor, yielding a maximum at the neighbourhood of the characteristic times at which retardation or relaxation processes occur. However, the overall shape of the spectra is given without details.

To obtain better approximations it is necessary to construct expressions for Eqs. (32) and (33) with more pronounced intensity functions. Following Schwarzl and Staverman^[8, 9] we can define the spectra :

$$L(t) = L_k(t) = (-1)^{k-1} / (k-1)! \quad k^k t^{(k-1)} \psi^{(k)}(kt) \quad (36)$$

$$H(t) = H_k(t) = (-1)^{k-1} / (k-1)! \quad k^k t^{(k-1)} \varphi^{(k)}(kt), \quad (37)$$

where k is the order of approximation sought for the spectra and $\psi^{(k)}(kt)$ and $\varphi^{(k)}(kt)$ the k^{th} order derivatives of the characteristic creep (ψ) or relaxation (φ) functions, the spectra of which are investigated.

From the above relations the following approximation spectra in the log time scale can be readily derived :

$$L_1(\log t) = 0.434 \left[\frac{d\psi(\tau)}{d(\log \tau)} \right] \quad (38)$$

$$L_2(\log t/2) = \left[0.434 \frac{d\psi(\tau)}{d(\log \tau)} - 0.189 \frac{d^2 \psi(\tau)}{d(\log \tau)^2} \right] \quad (39)$$

$$L_3(\log t/3) = \left[0.434 \frac{d\psi(\tau)}{d(\log \tau)} - 0.282 \frac{d^2 \psi(\tau)}{d(\log \tau)^2} + 0.041 \frac{d^3 \psi(\tau)}{d(\log \tau)^3} \right]. \quad (40)$$

Similar relations exist for the corresponding approximations of the relaxation spectra where the general function ψ is replaced by the φ -function for relaxation and the plus sign before brackets is changed to minus sign.

It may be concluded from the above relations that, in order to find the k^{th} approximation of a spectrum at time $\log t$, the experimental function must be known at time $k \log t$. This remark indicates the range along which experimental

data are needed to calculate certain approximations. It has been shown by Schwarzl and Staverman^[9] that, in general, the higher the approximation the more details of the real spectrum are reproduced in right proportions. It has been also shown that the approximations of increasing order correspond to intensity functions of increasing sharpness.

Figs 1 and 2 present the first, second and third approximation spectra for the creep compliance in extension of a cold-setting pure epoxy polymer and the relaxation modulus in extension for the N.B.S. polyisobutylene as they have been calculated by the formulas (38)-(40). Since the creep-compliance and relaxation modulus curves are slowly varying smooth curves the difference between approximations of spectra are minimized.

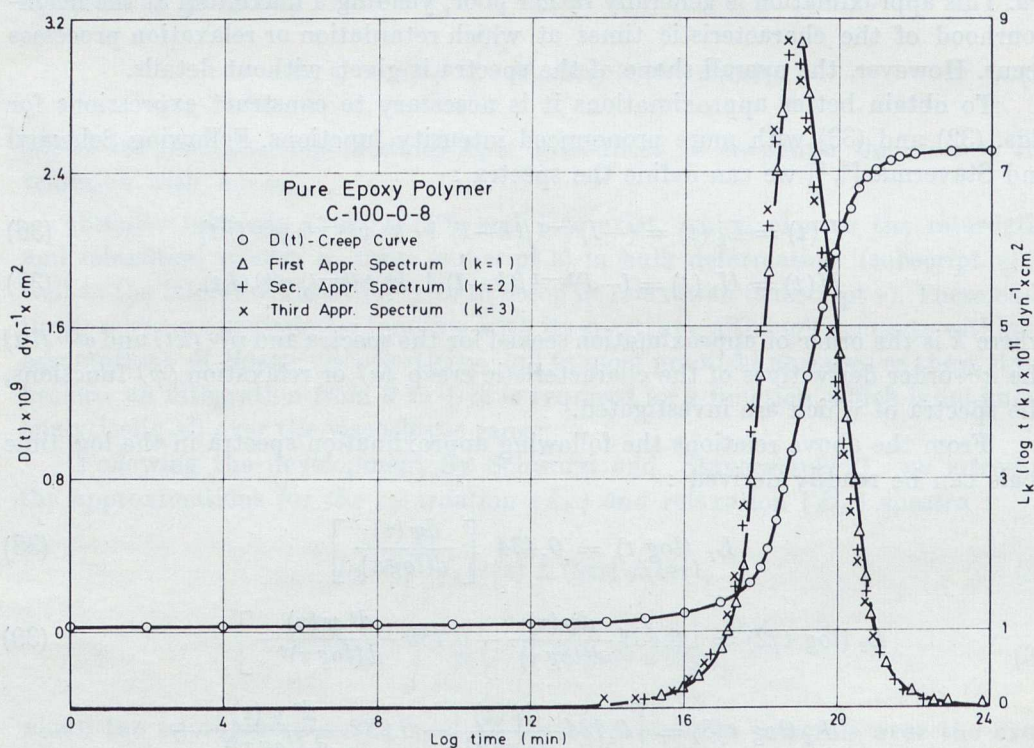


Fig. 1 First, second and third approximation spectra for the creep compliance in extension of a cold-setting pure epoxy polymer (C-100-0-8).

If one spectrum is known over the entire range of the time scale and certain limiting values for the compliances or moduli (D_g , E_r , etc.) for a cross-linked polymer the other spectrum can be calculated^[10]. The equations interrelating the two spectra are given by :

$$L(\ln t) = \frac{H(\ln t)}{\left[E_r - \int_{-\infty}^{\infty} \frac{H(u)}{(\tau/u-1)} d \ln u \right]^2 + \pi^2 H^2(\ln t)} \quad (41)$$

$$H(\ln t) = \frac{L(\ln t)}{\left[D_g + \int_{-\infty}^{\infty} \frac{L(u)}{(1-u/\tau)} d \ln u \right]^2 + \pi^2 L^2(\ln t)} \quad (42)$$

To calculate the one spectrum, say $L(\ln t)$, from the other $H(\ln t)$, it is necessary for each point in the time scale to evaluate the integral in the denominator over the

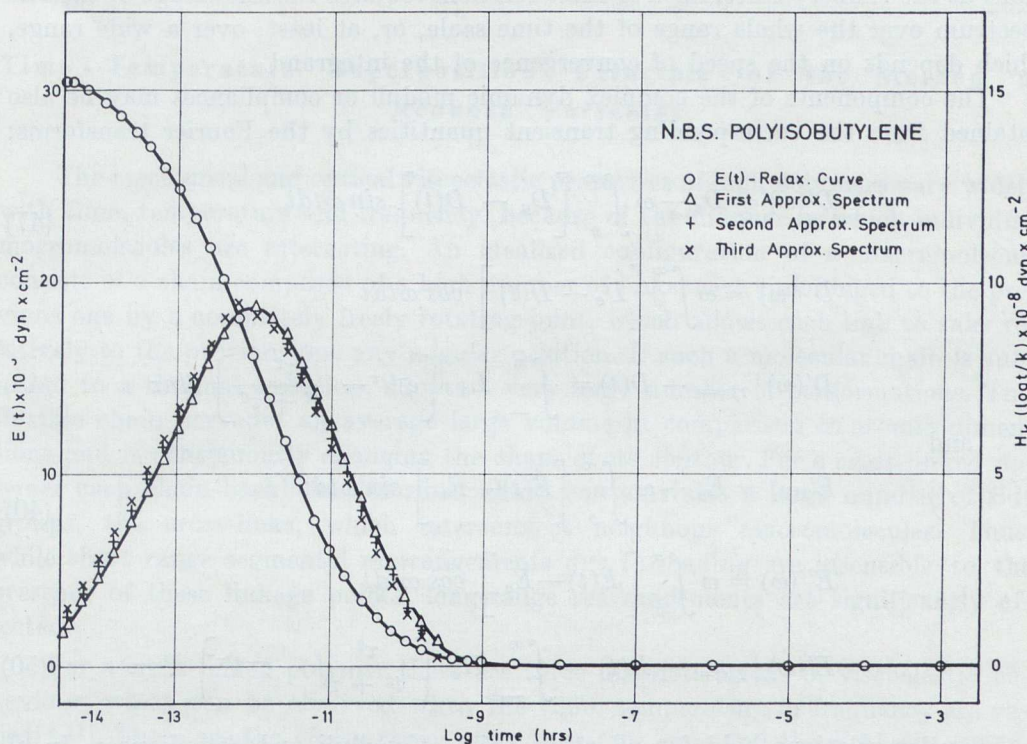


Fig. 2 First, second and third approximation spectra for the relaxation modulus in extension of the NBS polyisobutylene.

entire range. This can be done graphically or numerically from the values of $(H/\ln t)$ over the entire range. Although this calculation is not very difficult, it contains two areas of integration around the singularity, which are of similar magnitude and opposite sign. Therefore a high loss of precision is expected from this calculation.

Equations (30) and (31) can be transformed to express the storage and loss compliances and moduli in terms of their respective spectra. These are given by:

$$D' = D_g + \int_{-\infty}^{\infty} \frac{L_e(\ln \tau)}{(1 + \omega^2 \tau^2)} d \ln \tau \quad (43)$$

$$D'' = \int_{-\infty}^{\infty} \frac{L_e(\ln \tau) \omega \tau}{(1 + \omega^2 \tau^2)} d \ln \tau \quad (44)$$

and

$$E' = E_r + \int_{-\infty}^{\infty} \frac{H_e(\ln \tau) \omega^2 \tau^2}{(1 + \omega^2 \tau^2)} d \ln \tau \quad (45)$$

$$E'' = \int_{-\infty}^{\infty} \frac{H_e (\ln \tau) \omega \tau}{(1 + \omega^2 \tau^2)} d \ln \tau, \quad (46)$$

where L_e and H_e are the retardation and relaxation spectra in tension and D_g and E_r the limit values of the creep compliance at the glassy state and relaxation modulus at the rubbery state. Each of these relations requires the knowledge of the one spectrum over the whole range of the time scale, or, at least, over a wide range, which depends on the speed of convergence of the integrand.

The components of the complex dynamic moduli or compliances may be also obtained from the corresponding transient quantities by the Fourier transforms:

$$D'(\omega) = D_e - \omega \int_0^{\infty} [D_g - D(t)] \sin \omega t dt \quad (47)$$

$$D''(\omega) = \omega \int_0^{\infty} [D_e - D(t)] \cos \omega t dt$$

$$D'(\omega) |_{1/\omega=t} - D(t) = \int_{-\infty}^{\infty} L_e \left[e^{-t/\tau} - \frac{\tau^2}{t^2 + \tau^2} \right] d \ln \tau \quad (48)$$

and

$$E'(\omega) = E_e + \omega \int_0^{\infty} [E(t) - E_e] \sin \omega t dt \quad (49)$$

$$E''(\omega) = \omega \int_0^{\infty} [E(t) - E_e] \cos \omega t dt$$

$$E'(\omega) |_{1/\omega=t} - E(t) = \int_{-\infty}^{\infty} H_e \left[\frac{\tau^2}{t^2 + \tau^2} - e^{-t/\tau} \right] d \ln \tau. \quad (50)$$

Similar relations hold for all other pairs of moduli and compliances. In all these relations D_e and E_e express the equilibrium compliances and moduli. Although relations (48) and (50) contain an integral, which in general must be evaluated graphically or numerically, and a function L_e or H_e , which must also be determined approximately from whichever of the moduli or compliances is known, the right sides of these equations represent usually a minor correction, which does not need to be calculated with high precision. Therefore, these relations yield valuable results for converting the storage dynamic moduli and compliances to the transient quantities and vice versa.

In order to relate the transient compliances and moduli with the corresponding dynamic components, we use the inverse transforms and we obtain :

$$D(t) = D_g + \frac{2}{\pi} \int_0^{\infty} [D'(\omega) - D_g / \omega] \sin \omega t d\omega \quad (51)$$

$$D(t) = D_g + \frac{2}{\pi} \int_0^{\infty} \left[\frac{D''}{\omega} \right] (1 - \cos \omega t) d\omega$$

and

$$E(t) = E_e + \frac{2}{\pi} \int_0^{\infty} \left[E'(\omega) - E_e / \omega \right] \sin \omega t d\omega \quad (52)$$

$$E(t) = E_e + \frac{2}{\pi} \int_0^{\infty} (E'' / \omega) \cos \omega t d\omega.$$

Time - Temperature Superposition Principle or the Method of Reduced Variables

The mechanical and optical viscoelastic properties of high polymers vary widely with time, temperature and frequency, because of the manner in which individual macromolecules are interacting. An idealized configuration of a macromolecule consists of a chain composed of a high number of links, each link hinged to the previous one by a completely freely rotating joint, which allows each link to take relatively to the previous one any angular position. If such a molecular chain is subjected to a thermal agitation, adopts a very large number of conformations. This flexible chain pervades an average large volume in comparison to atomic dimensions and is continuously changing the shape of its contour. For a cross-linked polymer each chain-backbone described above contains also a large number of side groups, the cross-links, which interconnect neighbour macromolecules. Thus, while short range segmental rearrangements due to loading are insensible to the presence of these linkage points, long-range rearrangements are significantly affected.

For a cross-linked polymer there are three distinct regions of viscoelastic behaviour, which can be observed when the time, temperature or frequency are varied^[1, 11]. There are the *glassy region*, the *transition zone* and the *rubbery region*. It is in the transition zone, between glasslike and rubberlike behaviours, that the dependence of viscoelastic functions of time, temperature, or frequency are important. These regions can be associated qualitatively with different kinds of molecular responses and appear with different degrees of importance, depending on whether the cross-linked polymer is above or below its glass transition temperature. This temperature T_g may be defined as the point where the thermal expansion coefficient α undergoes a discontinuity in tangent. Above this temperature the thermal expansion coefficient obtains values approaching those associated with liquids. Decrease in temperature is always accompanied by a collapse of free volume of the substance, which is made possible by configurational adjustments. The reduction of the free volume is so high, that further rearrangements in the chain are extremely slow or even impossible. This results in an abrupt drop of the value for α , and the further contraction in total volume is insignificant or very small. Thus, the glass transition temperature is associated with the rate of molecular mobility. Below this temperature the mobility of the chain-backbones is insignificant and therefore the material is a *hard glass*. If there is an amount of mechanical or optical creep, this is

due only to the movement and reorientation of the side-groups (secondary bonds) between chain-backbones. This type of viscoelastic behaviour is called *glassy behaviour*. Above this temperature the configurational arrangements of the chain-backbones are possible, which alter significantly the viscoelastic behaviour, which becomes very pronounced. The material is entered into the *transition zone*. In the instantaneous elastic behaviour of the material, corresponding to its glassy behaviour, a pronounced viscoelastic behaviour is superimposed, derived from the mobility of the segments of the chain-backbones, which become flexible above the glass transition temperature. The deformation of the substance is characterized by a progressive sliding of the chains, which are in a state of permanent agitation.

Another characteristic temperature is the temperature of the rubbery plateau. This is defined as the limit where the material behaves again elastically. Indeed, as the temperature is raised, or the time is passed, the relative sliding of the chain-backbones is progressively exhausted, the thermal agitation of the substance is very high so that the new configuration of the sliding of chains is obtained quasi-instantaneously. This temperature limit is not accompanied by any change in the molecular response of the high polymer.

External loading of the material in the rubbery state modifies the orientation of the molecules, without deforming them, and brings them to a new configuration, which is statistically less probable by reducing the entropy of the system. The elastic response of a rubbery material is, therefore, due to the reduction of entropy of the substance, while the elastic response in a glass-like material is due to an accumulation of potential energy. Between the two elastic processes there is a fundamental difference. While the glass-like elasticity is mechanically and thermodynamically reversible since it is exclusively due to variation of potential energy, the rubber-like elasticity is only mechanically reversible and thermodynamically irreversible because of the dissipation of energy derived from the viscosity-like mechanism of re-orientation of the molecules. Thus, the glassy and rubbery states describe two extreme mechanisms where elastic phenomena of different nature are predominant. In-between lies the transition zone where two extreme mechanisms are in competition.

When a creep-compliance or a relaxation-modulus for a particular polymer is plotted against time or any of the dynamic functions are plotted against frequency the viscoelastic range of these materials is extended over a long time or frequency period. The variation of their magnitudes along the viscoelastic range is either very pronounced for the shear and extension moduli or compliances or it is weak for the bulk compliances and moduli and LCR functions. As a result, both coordinates are usually plotted in logarithmic scales. In order to obtain the complete range in viscoelastic properties of a high polymer it is necessary to cover several decades of the log time. Therefore, it is very important to obtain a satisfactory method of extrapolation. Such a method was first suggested by Leaderman^[12], who observed that creep recovery data, which were obtained at different temperatures, could be superimposed by a horizontal shift along the logarithmic time axis.

It has been subsequently established experimentally that the retardation or relaxation times constituting the viscoelastic spectra of many polymers decrease rapidly with increasing temperature. The temperature dependence of the viscoelastic behaviour could be expressed analytically by rather complicated forms. Then, it is simpler to introduce this dependence in the viscoelastic behaviour by a *method of reduced variables of time or frequency*, based on the *time-temperature superposition principle*. According to this principle, viscoelastic data at one temperature are transformed to another temperature by a simple multiplicative transformation of the time scale. In the case when the characteristic functions are plotted in a log time scale, this transformation degenerates to a mere parallel shift of the log time scale. Ferry[¹] has formulated this principle as follows: if the distribution of extension relaxation times at a temperature T is denoted by $E_{\tau}(\tau)$, it is related to the distribution of relaxation times at the reference temperature T_0 as follows:

$$\frac{\rho_0 T_0}{\rho T} E_T(a_T \tau) = E_{T_0}(\tau), \quad (53)$$

where the quantity a_T , called the *shift factor*, is a function of temperature only. He called this principle as the *method of reduced variables*. The quantities ρ_0 and ρ are densities at T_0 and T , and for pure polymers the ratio ρ_0/ρ is a quite small correction factor. This factor may be neglected within the accuracy of the theory. The correction factor T_0/T is introduced to correct for the kinetic theory of elasticity. Ferry[¹³] indicated also that the quantity a_T is related to the viscosities of the materials at various temperatures.

A similar formulation to that introduced by Ferry has been used by Tobolsky and Andrews[¹⁴] for both cross-linked and linear amorphous polymers. They made tests on various materials and especially in polyisobutylene. They presented the stress-relaxation data for the material as follows:

$$\begin{aligned} \frac{T_0}{T} E_{r, T}(kt) &= E_{r, T_0}(t) \\ E_{r, T_0}(t/k) &= \frac{T_0}{T} E_{r, T}(t), \end{aligned} \quad (54)$$

where $E_{r, T}(t)$ is the relaxation function at temperature T , $E_{r, T_0}(t)$ is the relaxation function at T_0 , the quantity k , which was called *time factor*, was obtained directly from the experimental relaxation curves at different temperatures, plotted against log time, by measuring the amount of shift along the log-time scale necessary to make these curves identical. Theoretically, if either Eq. (53) or (54) was completely valid, the validity of the other equation would follow. Moreover, k and a_T would be identical if they were taken as unity at the same reference temperature. The experimental equality of k and a_T was established for various high polymers[¹⁵].

Although the time-temperature superposition principle was originally developed experimentally, it has been also proved that this principle may be a conse-

quence of the kinetic theory of high-polymers. In the transition zone, where the viscoelastic behaviour is due to cooperative motions of individual chain-backbones, these motions are governed by a single average friction coefficient ζ_0 , which for the kinetic theory of Rouse^[16] is dependent on temperature T . This coefficient decreases rapidly as the friction, which is of the nature of viscosity, and which opposes segmental motions in the chain, is diminishing. Furthermore, the retardation (L) or relaxation (H) spectra, as well as their corresponding characteristic times τ_p , depend on temperature. If all these effects are lumped together into one factor, we obtain the factor $k \equiv a_T$, which describes the ratio of τ_p , at an arbitrary temperature T to that at a selected as standard temperature T_0 . We have, therefore, that:

$$a_T \equiv k = \frac{[\tau_p]_T}{[\tau_p]_{T_0}} = \frac{[a^2 \zeta_0]_T T_0}{[a^2 \zeta_0]_{T_0} T} \quad (55)$$

Since a_T is the same for all τ_p increase of temperature from T_0 to T on the log plot of the spectra corresponds to a mere shift of the curve along the ordinates by $\log(\rho T / \rho_0 T_0)$ and along the abscissas toward the origin of times by $\log a_T$. These shifts do not change the shape of the individual isothermal curve. Relation (55) is similar to equations (53) and (54). Thus, a creep or relaxation individual curve, experimentally determined at certain temperature T can be reduced to the position it would have occupied at a standard temperature T_0 by plotting $H_0/H = T_0 \rho_0 / T \rho$ versus τ / a_T and knowing the expansion coefficient $a = - \left[\frac{1}{\rho} \right] \frac{\partial \rho}{\partial T}$

and the shift factor a_T . A series of plots at different temperatures, if each of them is reduced to the standard temperature T_0 by using the appropriate value of a_T , should superimpose to give a single composite curve representing the spectrum H at temperature T_0 .

From equations (30) and (31), expressing the creep compliances and relaxation moduli as functions of their respective spectra, together with Eq. (55) it can be derived that:

$$F(t', T_0) = \frac{\rho_0 T_0}{\rho T} F(t = a_T t', T), \quad (56)$$

where $F(t, T)$ expresses any creep compliance or relaxation modulus function. Equation (56) is a statement of the time-temperature superposition principle. It indicates that any creep compliance or relaxation modulus at temperature T_0 and time t' can be obtained from the creep compliance and relaxation modulus measured at temperature T and time t . On a plot of compliance or modulus vs. logarithmic time, this amounts to a vertical shift of the magnitude $\rho_0 T_0 / \rho T$ and a horizontal shift of the magnitude $\log a_T$.

Fig. 3 presents the individual isothermal curves for the relaxation modulus in extension for the polyurethane elastomer Hysol 8705^[30].

The experimental study of the amorphous high polymers has been restricted at the beginning chiefly to the determination of their mechanical properties and especially to a simple form of stress or strain distribution, as for instance to pure shear. The results obtained in pure shear were extended to other types of simple straining.

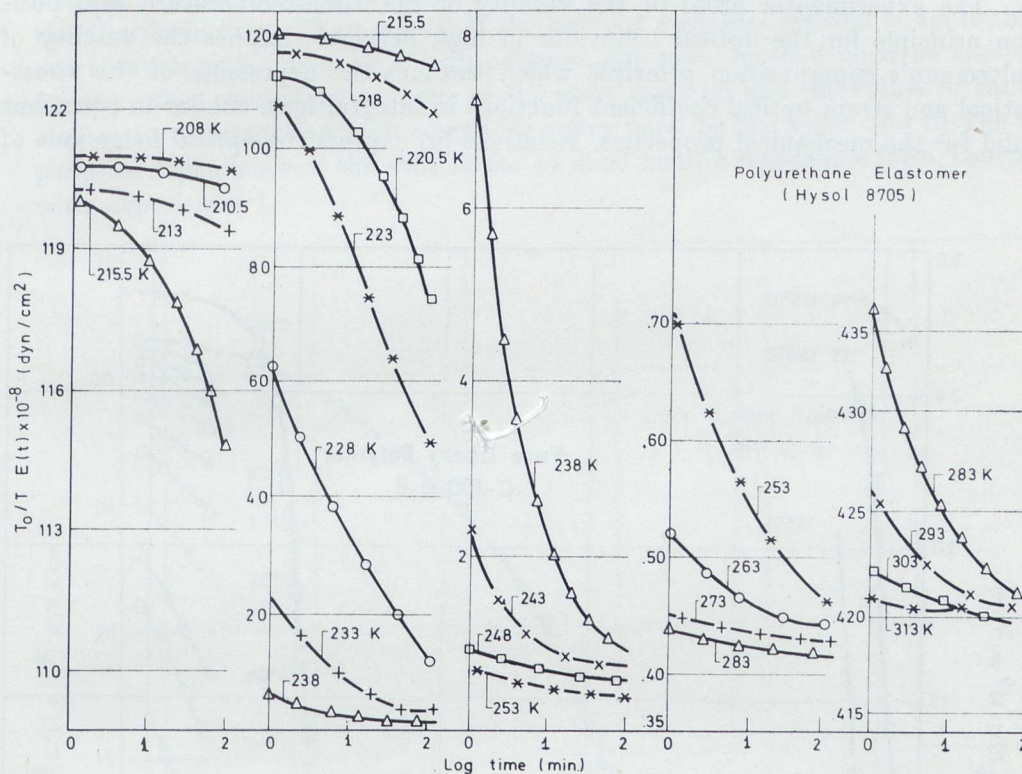


Fig. 3 Isothermal individual curves of the relaxation modulus in extension for the polyurethane elastomer Hysol 8705.

While an extensive literature exists which concerns the mechanical viscoelastic properties of high polymers, the optical viscoelastic behaviour has received less attention, at least as far as the temperature effect and the molecular orientation are concerned. The time-temperature superposition principle was shown experimentally to hold for the optical properties of high polymers by Theocaris^[17-19]. The validity of this principle was demonstrated for a series of pure and plasticized epoxy polymers. The entire response spectrum was determined for the stress- and strain-optical coefficients from the glassy up to the rubbery consistency of the materials. It was shown that the composite curves of each of these coefficients for creep and relaxation are coincident and the stress-optical coefficient curves are monotonically decreasing, while the strain-optical coefficient curves

quence of the kinetic theory of high-polymers. In the transition zone, where the viscoelastic behaviour is due to cooperative motions of individual chain-backbones, these motions are governed by a single average friction coefficient ζ_0 , which for the kinetic theory of Rouse^[16] is dependent on temperature T . This coefficient decreases rapidly as the friction, which is of the nature of viscosity, and which opposes segmental motions in the chain, is diminishing. Furthermore, the retardation (L) or relaxation (H) spectra, as well as their corresponding characteristic times τ_p , depend on temperature. If all these effects are lumped together into one factor, we obtain the factor $k \equiv a_T$, which describes the ratio of τ_p , at an arbitrary temperature T to that at a selected as standard temperature T_0 . We have, therefore, that:

$$a_T \equiv k = \frac{[\tau_p]_T}{[\tau_p]_{T_0}} = \frac{[a^2 \zeta_0]_T T_0}{[a^2 \zeta_0]_{T_0} T} \quad (55)$$

Since a_T is the same for all τ_p increase of temperature from T_0 to T on the log plot of the spectra corresponds to a mere shift of the curve along the ordinates by $\log(\rho T / \rho_0 T_0)$ and along the abscissas toward the origin of times by $\log a_T$. These shifts do not change the shape of the individual isothermal curve. Relation (55) is similar to equations (53) and (54). Thus, a creep or relaxation individual curve, experimentally determined at certain temperature T can be reduced to the position it would have occupied at a standard temperature T_0 by plotting $H_0/H = T_0 \rho_0 / T \rho$ versus τ / a_T and knowing the expansion coefficient $a = - \left(\frac{1}{\rho} \right) \frac{\partial \rho}{\partial T}$

and the shift factor a_T . A series of plots at different temperatures, if each of them is reduced to the standard temperature T_0 by using the appropriate value of a_T , should superimpose to give a single composite curve representing the spectrum H at temperature T_0 .

From equations (30) and (31), expressing the creep compliances and relaxation moduli as functions of their respective spectra, together with Eq. (55) it can be derived that:

$$F(t', T_0) = \frac{\rho_0 T_0}{\rho T} F(t = a_T t', T), \quad (56)$$

where $F(t, T)$ expresses any creep compliance or relaxation modulus function. Equation (56) is a statement of the time-temperature superposition principle. It indicates that any creep compliance or relaxation modulus at temperature T_0 and time t' can be obtained from the creep compliance and relaxation modulus measured at temperature T and time t . On a plot of compliance or modulus vs. logarithmic time, this amounts to a vertical shift of the magnitude $\rho_0 T_0 / \rho T$ and a horizontal shift of the magnitude $\log a_T$.

Fig. 3 presents the individual isothermal curves for the relaxation modulus in extension for the polyurethane elastomer Hysol 8705^[30].

The experimental study of the amorphous high polymers has been restricted at the beginning chiefly to the determination of their mechanical properties and especially to a simple form of stress or strain distribution, as for instance to pure shear. The results obtained in pure shear were extended to other types of simple straining.

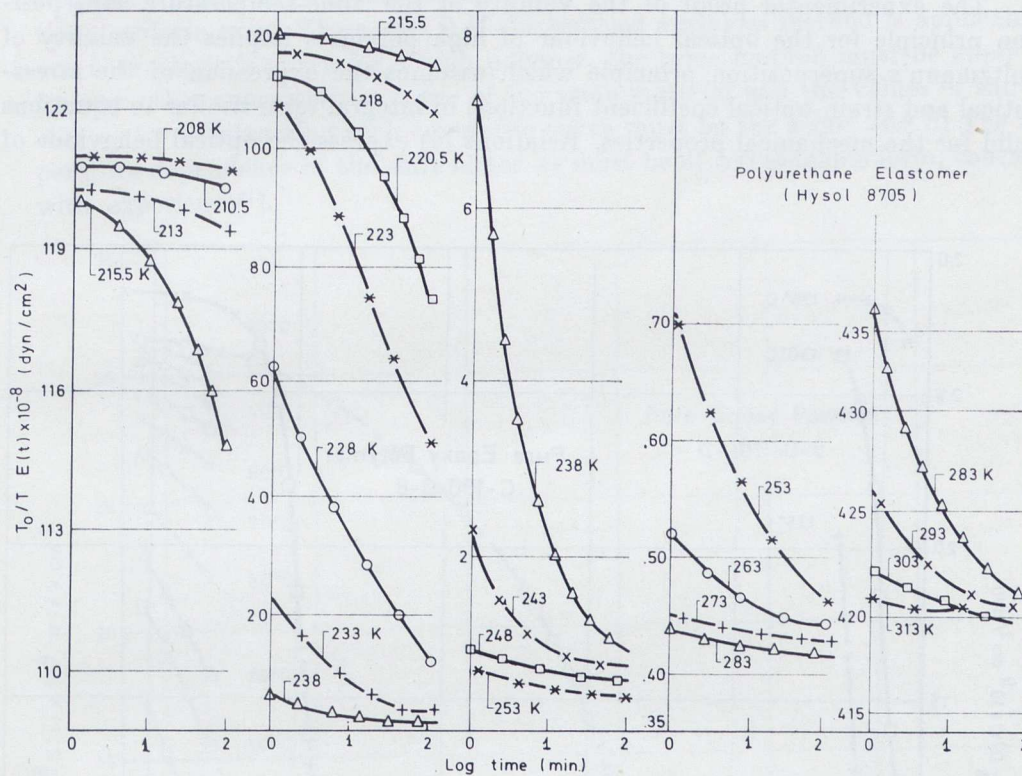


Fig. 3 Isothermal individual curves of the relaxation modulus in extension for the polyurethane elastomer Hysol 8705.

While an extensive literature exists which concerns the mechanical viscoelastic properties of high polymers, the optical viscoelastic behaviour has received less attention, at least as far as the temperature effect and the molecular orientation are concerned. The time-temperature superposition principle was shown experimentally to hold for the optical properties of high polymers by Theocaris^[17-19]. The validity of this principle was demonstrated for a series of pure and plasticized epoxy polymers. The entire response spectrum was determined for the stress- and strain-optical coefficients from the glassy up to the rubbery consistency of the materials. It was shown that the composite curves of each of these coefficients for creep and relaxation are coincident and the stress-optical coefficient curves are monotonically decreasing, while the strain-optical coefficient curves

are monotonically increasing functions. The composite curves describing the optical behaviour of cross-linked polymers were shown to belong to a standard curve presenting three distinct regions, i.e., a low-temperature glassy region and a high-temperature rubbery region where time effects are negligible. In-between lies a transition region of pronounced time dependence. These composite curves are consistent with the relative curves describing the mechanical behaviour.

The experimental proof of the validity of the time-temperature superposition principle for the optical behaviour of high polymers implies the validity of Boltzmann's superposition principle which assumes the expression of the stress-optical and strain-optical coefficient functions in integral form similar to equations valid for the mechanical properties. Relations (4) express the optical behaviour of

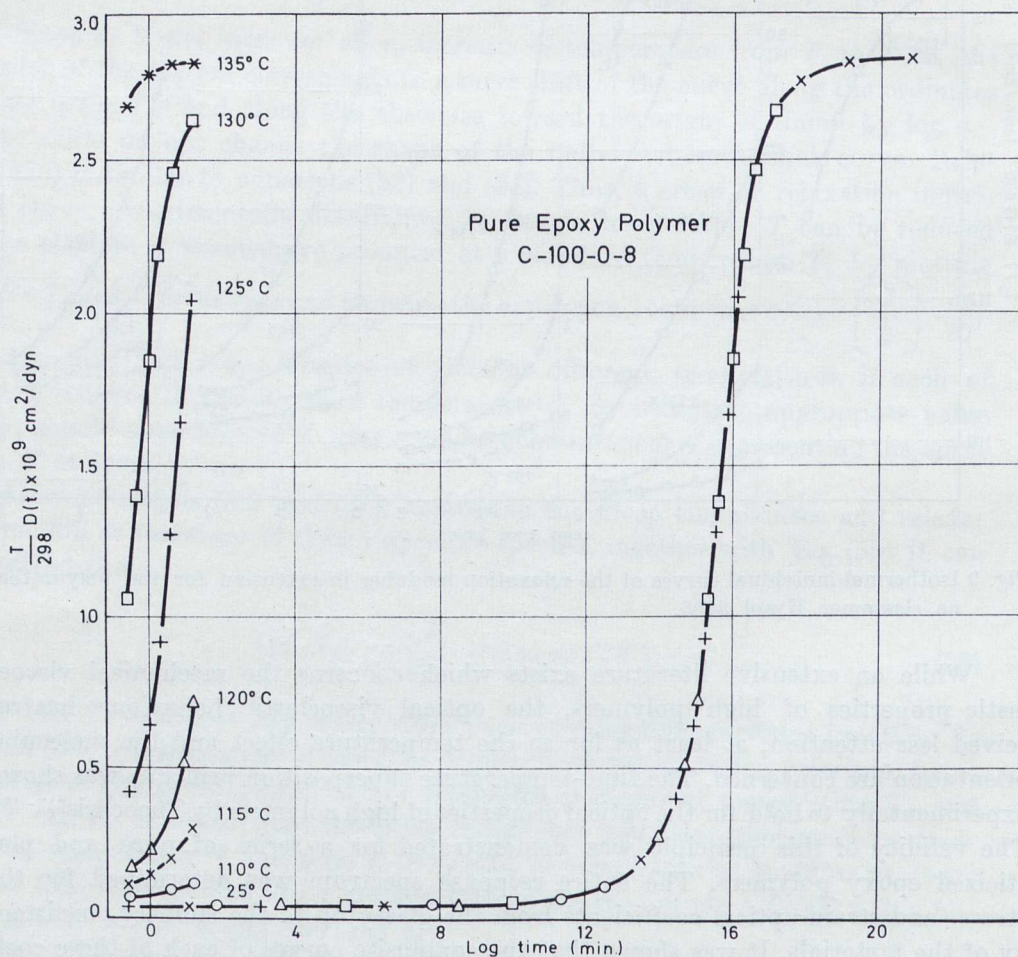


Fig. 4 Isothermal individual curves of the extension creep compliance for pure epoxy polymer C-100-0-8 and the composite curve derived by applying the method of reduced variables.

high-polymers. They are similar to relations (1-3) expressing the mechanical behaviour. Relations (4) were given explicitly by Dill^[43].

The main experimental criterion for the existence of a single composite curve expressing the viscoelastic behaviour of the substance over the entire time range is that the shapes of individual isothermal curves, taken over a substantial time or frequency range, shall match, so that they can coincide after shifting. Two additional criteria exist. These are: i) If the reduced variables method is applicable to one characteristic curve for a high polymer, the same method must be applicable for any other characteristic curve of the same material and the values of shift factor a_T for constructing each composite curve must be the same, and ii) The temperature dependence of the shift factor a_T must be of a reasonable form, consistent with experience^[1].

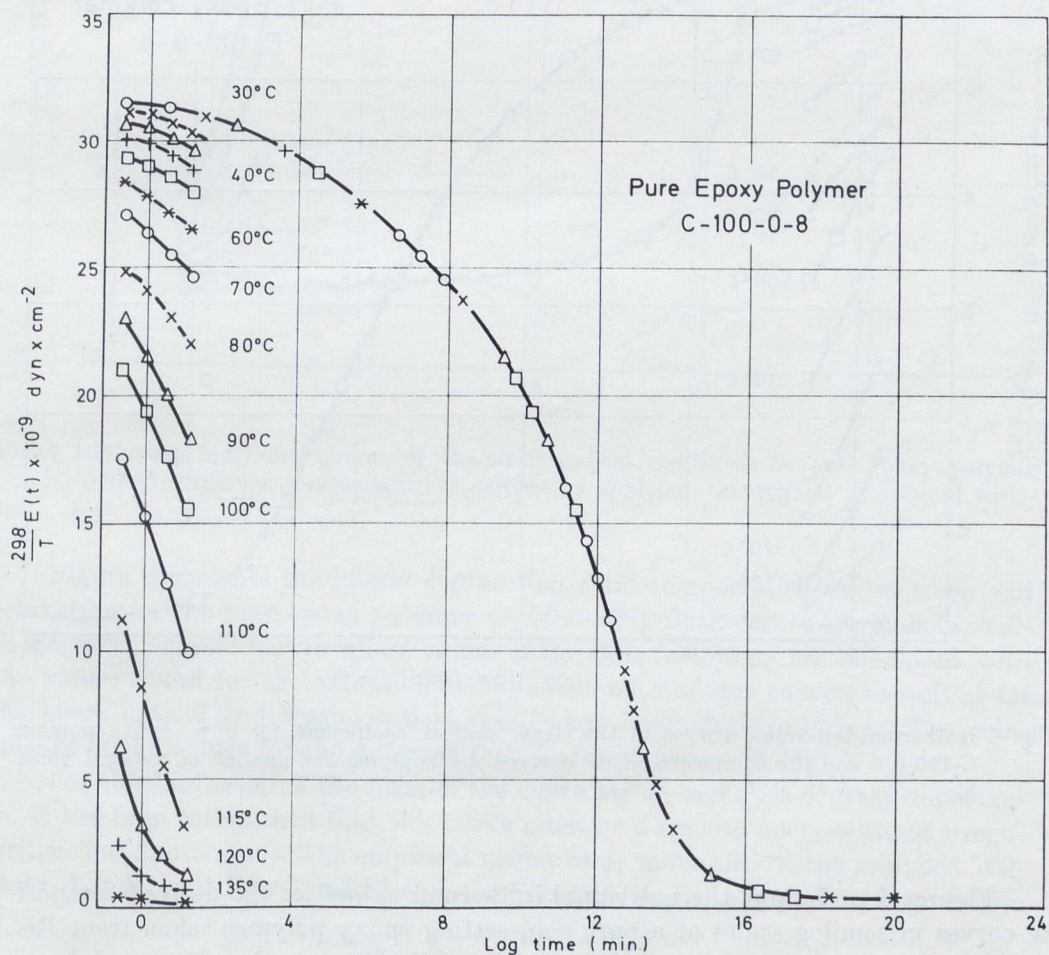


Fig. 5 Isothermal individual curves of the extension relaxation modulus for pure epoxy polymer C-100-0-8 and the composite curve derived by applying the method of reduced variables.

Experimental evidence with rheo-optically simple materials, as they are the epoxy polymers, pure or in plasticized form, show the validity of the reduced variables method and the simultaneous equality in values of the shift factor a_T for all characteristic curves expressing the mechanical and optical viscoelastic behaviour.

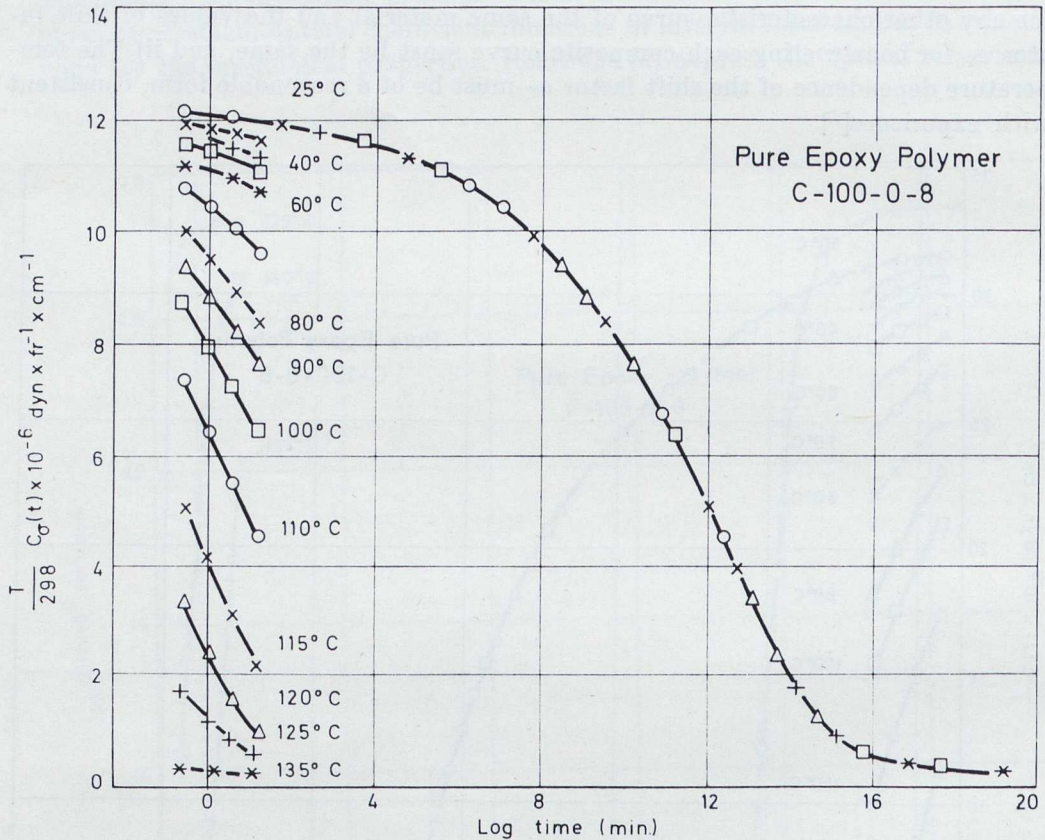


Fig. 6 Isothermal individual curves of the stress optical coefficient for pure epoxy polymer C-100-0-8 and the composite curve derived by applying the method of reduced variables.

Figures 4 to 7 show the individual isothermal as well as the derived composite curves in semilog scales of a pure cold-setting epoxy polymer taken from Ref. 17. These figures show the extension creep compliance and relaxation modulus as well as the stress- and strain- optical coefficients of the materials. The zero temperature in the log scale corresponds to a temperature at 25° C.

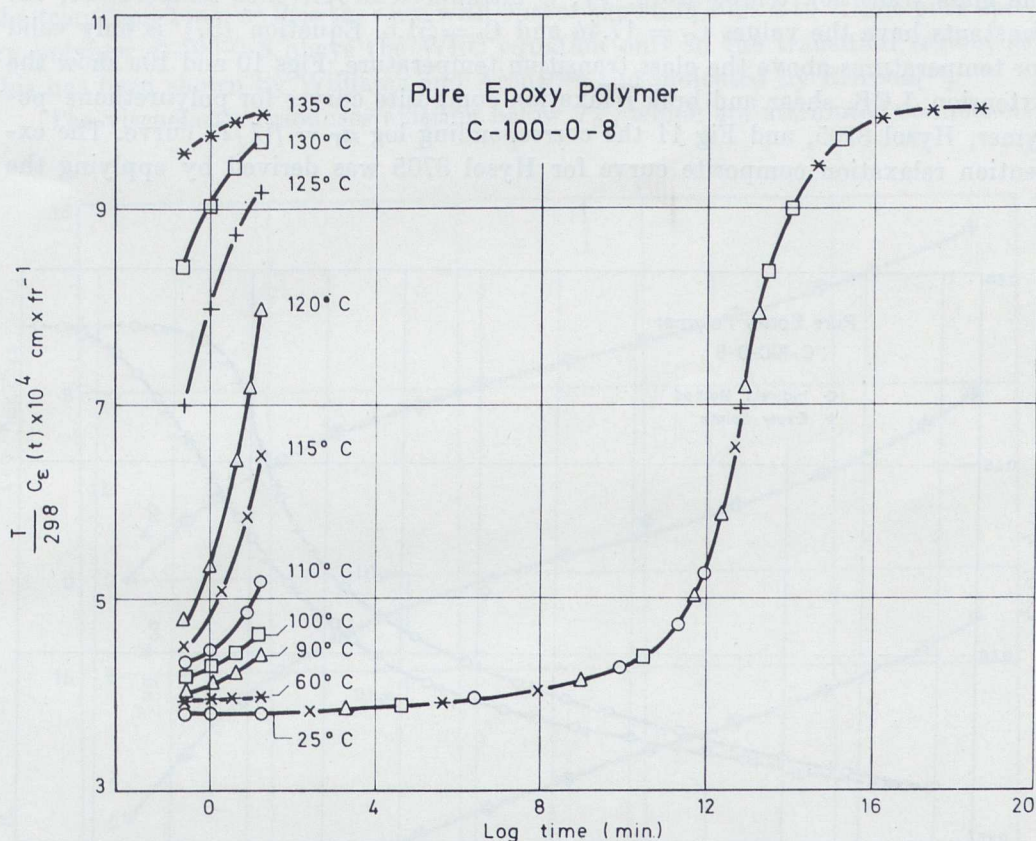


Fig. 7 Isothermal individual curves of the strain optical coefficient for pure epoxy polymer C-100-0-8 and the composite curve derived by applying the method of reduced variables.

Figure 8 presents the lateral contraction ratio composite curves in creep and relaxation for the pure epoxy polymer C-100-0-8^[21]. Both curves are monotonically increasing sigmoid curves whose values of the shift factors a_T are coincident with the values found for the extension compliance and modulus curves, as well as for the stress-optical and strain-optical coefficients characteristic curves. The coincidence of the values for the different shift factors is shown in Fig. 9.

The third criterion of the form of the curve $\log a_T = f(T)$ is of great importance. It has been established that this curve must be a smooth curve without irregularities and fluctuations. The empirical values of a_T must also fit the so-called Williams, Landel and Ferry (WLF) equation^[22]. This empirical equation is given by:

$$\log a_T = \frac{-C_1 (T - T_0)}{(C_2 + T - T_0)}, \quad (57)$$

where C_1 and C_2 are constants depending upon the reference temperature T_0 . If

the glass transition temperature, T_g , is introduced as reference temperature, the constants have the values $C_1 = 17.44$ and $C_2 = 51.6$. Equation (57) is only valid for temperatures above the glass transition temperature. Figs 10 and 10a show the extension, LCR, shear and bulk relaxation composite curves for polyurethane polymer, Hysol 8705, and Fig 11 the corresponding $\log a_T = f(1/T)$ curve. The extension relaxation composite curve for Hysol 8705 was derived by applying the

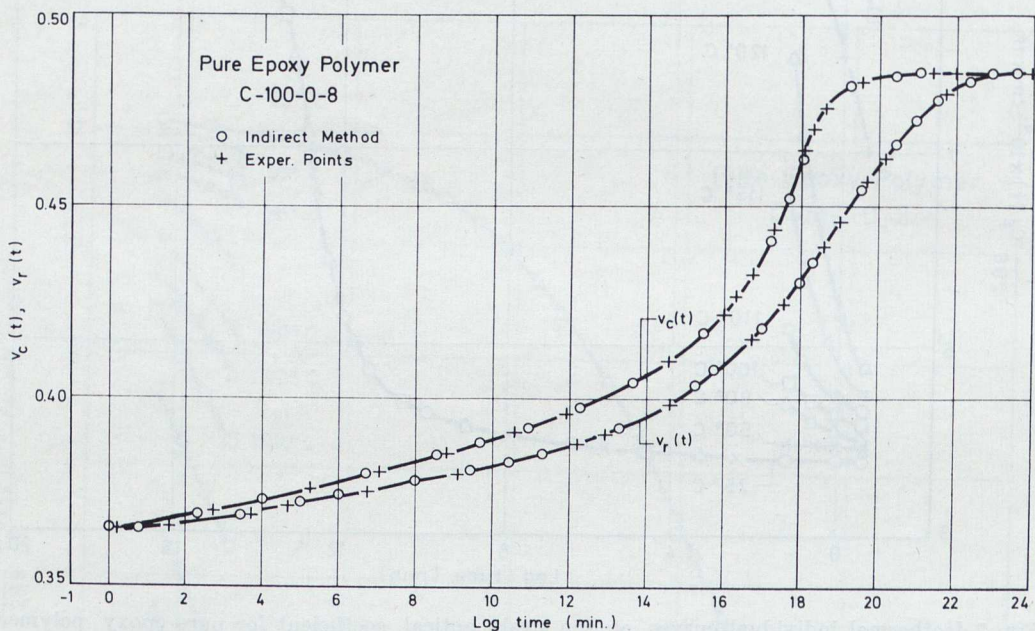


Fig. 8 Lateral contraction ratio composite curves versus logarithmic time for pure epoxy polymer C-100-0-8 in creep and relaxation. Both curves must be coincident. Discrepancies between the two curves which do not exceed 5 percent are due to experimental errors.

method of reduced variables to the isothermal curves of this material shown in Fig. 3. The $\log a_T = f(1/T)$ curve fits exactly the WLF equation for this material, if as reference temperature is taken the temperature $T_R = 273^\circ \text{K}$ (0°C) and the constants $C_1 = 8.86$ and $C_2 = 101.6$. The reference temperature T_R was found to be approximately 50°C above the glass transition temperature T_g , which for Hysol 8705 rubber is approximately $T_g = 223^\circ \text{K}$ (-50°C)^[11]. An excellent coincidence between the experimental values for $\log a_T$ and those obtained from the empirical relation (57) is manifested.

This is one example where the viscoelastic behaviour of a high polymer is expressed by composite curves whose shift factors satisfy with a remarkable precision the WLF equation reduced to a reference temperature. However, there are cases where the reduction is successful only in a restricted zone or extends along

the transition zone, as it is the case with curves shown in Figs 4 to 7. The pure epoxy polymer C-100-0-8 obeys the WLC equation only in the transition region, as this has been shown by Williams and Arenz^[23] and indicated by Brinson^[24].

The viscoelastic responses existing below T_g , which are attributed to motions

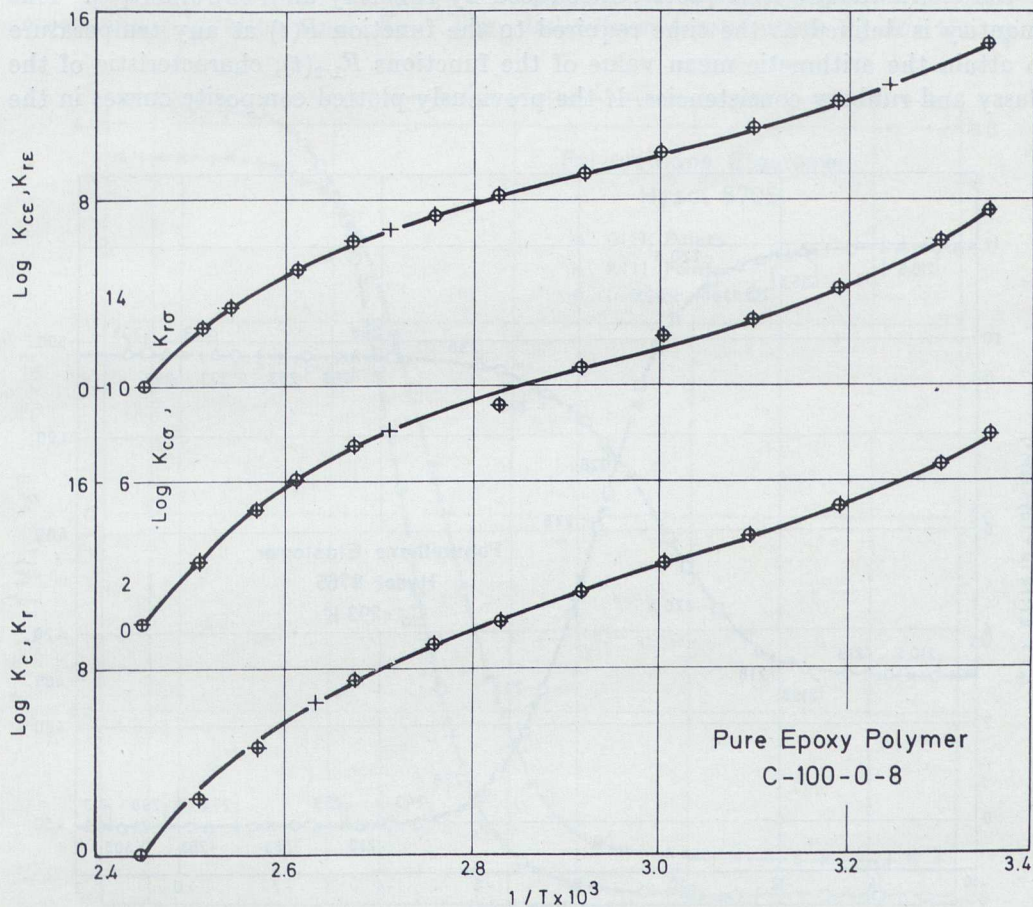


Fig. 9 Logarithms of shift factors $K \equiv a_T$ versus the inverse of absolute temperature for pure epoxy polymer C-100-0-8 (K_C , K_R are shift factors for extension creep compliance and relaxation modulus composite curves, $K_{C\sigma}$, $K_{R\sigma}$ are shift factors for the stress-optical coefficient and $K_{C\epsilon}$, $K_{R\epsilon}$ are shift factors for the strain-optical coefficient composite curves in creep and relaxation).

of side chains, cover a wide spectrum of retardation or relaxation times. These motions cannot be described solely in terms of the friction coefficient ζ_0 . Again, for this region it is assumed that the corresponding retardation or relaxation times have the same temperature dependence. Therefore, the method of reduced variables can be also applied to the glassy zone, but by an entirely different calculation. In this

zone the temperature dependence of the shift factor a_T follows an equation of the simple Arrhenius form:

$$\Delta H_{act} = \pm 2.303R [d \log a_{T_0} / d(1/T)], \quad (57a)$$

where R is the gas constant and $a_{T_0} \equiv K$ is the so-called *characteristic shift factor* or the *characteristic time factor*, introduced by Tobolsky and coworkers^[25]. This quantity is defined as the time required to the function $F(t)$ at any temperature to attain the arithmetic mean value of the functions $F_{1,2}(t)$, characteristic of the glassy and rubbery consistencies. If the previously plotted composite curves in the

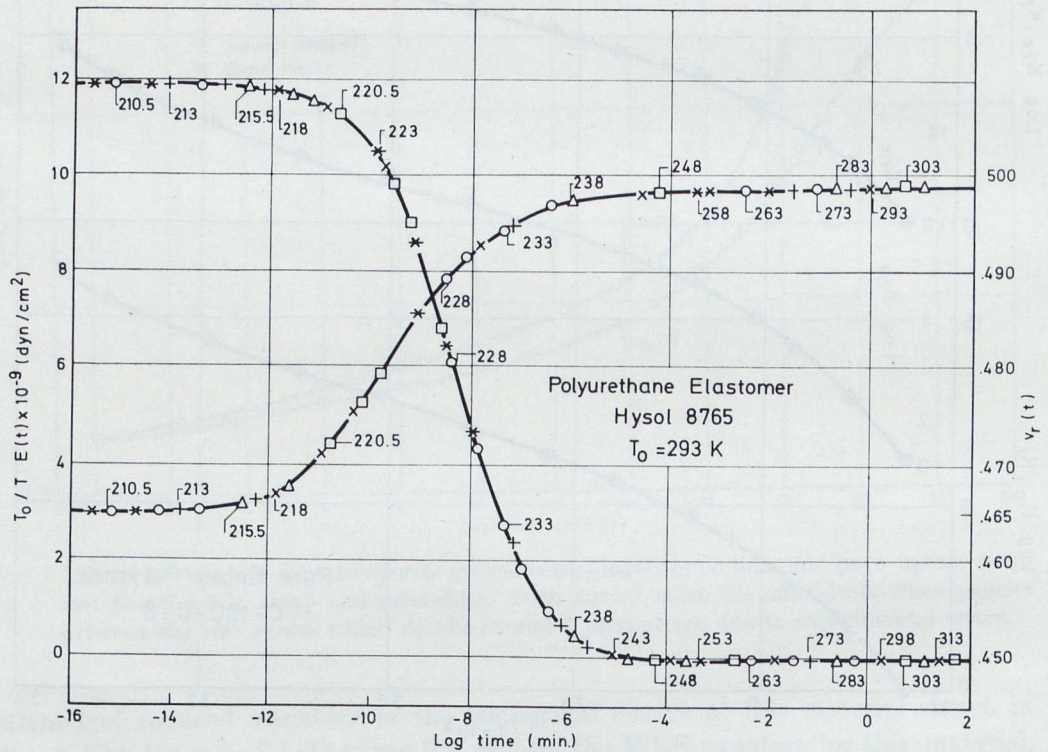


Fig. 10 Extension relaxation and lateral contraction ratio composite curves in semilog scale for polyurethane elastomer Hysol 8705.

form of $F(t/k)$ against $\log(t/k)$ and shown in figs 4-7, are now plotted in the form of $\log F(t/K)$ against $\log(t/K)$, and the origins of each log-time scale are shifted in order to coincide with the defined characteristic times of each curve, the characteristic times derived from creep and relaxation curves (K_c , K_r , K_{cs} , K_{rs} and K_{ce} , K_{re}) are plotted in Fig. 9 against the inverse of the absolute temperature. Fig. 12 shows the dependence of the apparent activation energy ΔH_{act} for the epoxy polymer C-100-0-8 on the inverse of the absolute temperature, as it is calcu-

lated by the Arrhenius equation or its reciprocal form. The Arrhenius equation was used for the calculation of the variation of the apparent activation energy in creep D -curves as well as in all C_ϵ -curves with the «minus» sign, while its reciprocal form used for the corresponding relaxation E -curves and all C_σ -curves (with the «plus» sign)[²⁶]. In all cases ΔH_{act} passes through a definite maximum defining the distinctive temperature T_d for each polymer and the corresponding distinctive creep and relaxation time K_d . The distinctive temperature T_d for the epoxy

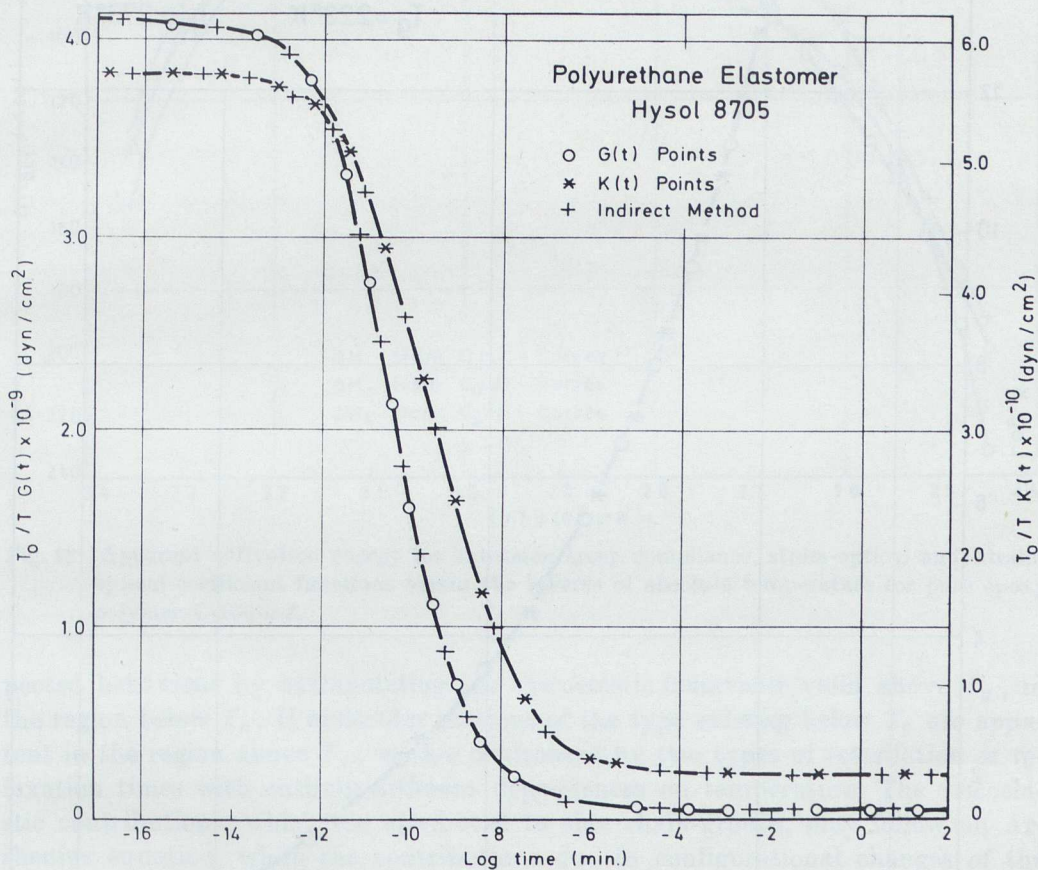


Fig. 10a Shear and bulk relaxation composite curves in semilog scale for polyurethane elastomer Hysol 8705.

polymer C-100-0-8 was found to be approximately 50° C. It is also worthwhile noting that these maxima have only approximately similar values for the extension creep compliance and relaxation modulus curves, as well as for the stress-optical and strain-optical coefficient curves in creep and relaxation. The above experimental evidence, together with the remarks by Brinson[²⁴], indicate that the temperature dependence of viscoelastic response below T_g bears no relation to the ex-

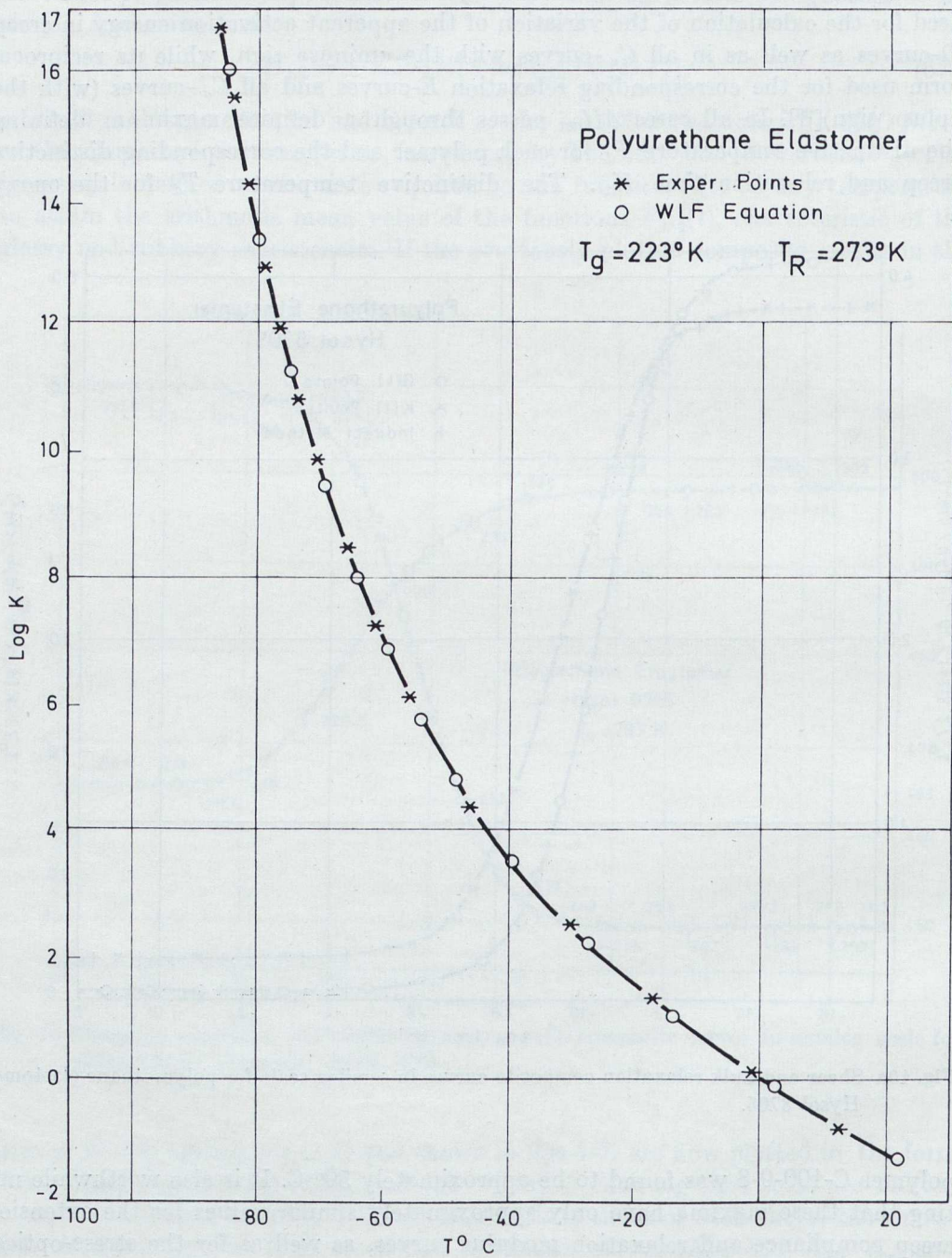


Fig. 11 Logarithm of shift factor $K \equiv a_T$ versus the inverse of the absolute temperature for polyurethane elastomer Hysol 8705 as derived experimentally and compared with the WLF equation.

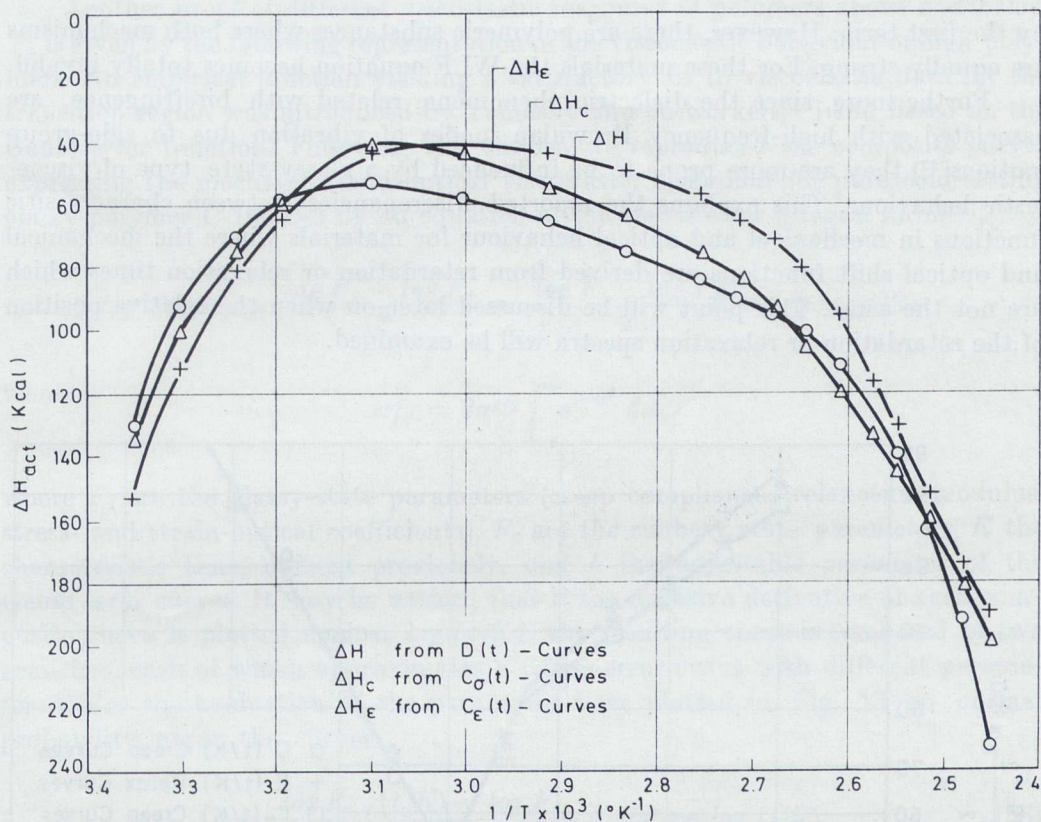


Fig. 12 Apparent activation energy for extension creep compliance, stress-optical and strain-optical coefficient functions versus the inverse of absolute temperature for pure epoxy polymer C-100-0-8.

pected behaviour by extrapolating the viscoelastic behaviour valid above T_g , in the region below T_g . If molecular motions of the type existing below T_g are apparent in the region above T_g , we are confronted by two types of retardation or relaxation times with entirely different dependences on temperature. The viscoelastic contributions, which are attributed to side chain-groups, may follow an Arrhenius equation, while the contributions due to configurational changes of the chain-backbones obey the WLF equation. Anomalies presented by Brinson^[24] in studying the mechanical and optical behaviour of the epoxy polymer Hysol 4290, where the $\log a_T = f(T)$ curves do not coincide with the WLF equation, may be attributed to these two antagonistic mechanisms.

Thus, any measured compliance or modulus is the sum of a contribution from backbone motions, whose retardation or relaxation times follow the WLF equation, and another one from side-chain motions, whose retardation or relaxation times follow the Arrhenius equations. In general, the second contribution becomes very small in the transition region, and it is obscured partly or masked completely

by the first term. However, there are polymeric substances where both mechanisms are equally strong. For these materials the WLF equation becomes totally invalid.

Furthermore, since the dielectric phenomena, related with birefringence, are associated with high-frequency Brownian modes of vibration due to side-group motions^[27] they are more prone to be influenced by a glassy-state type of viscoelastic behaviour. This explains the reported discrepancies between characteristic functions in mechanical and optical behaviour for materials where the mechanical and optical shift functions are derived from retardation or relaxation times which are not the same. This point will be discussed later-on when the relative position of the retardation or relaxation spectra will be examined.

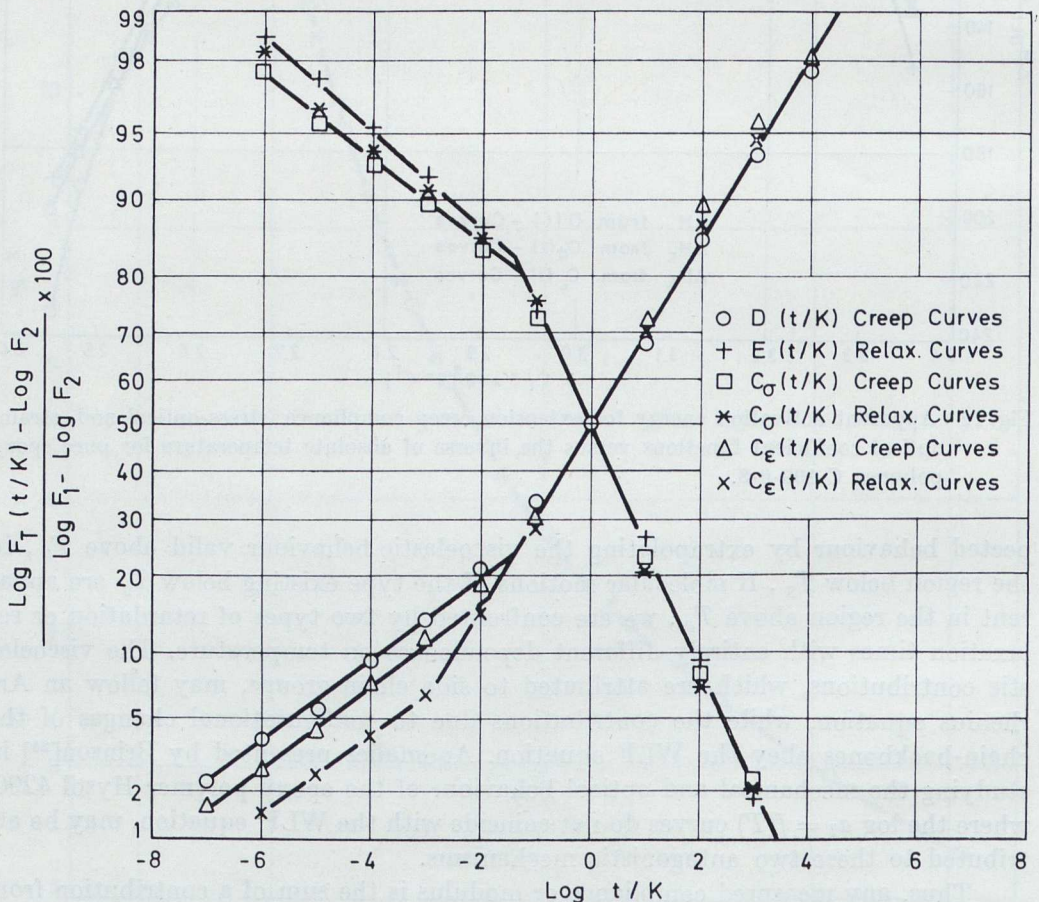


Fig. 13 Difference between the log-value for a characteristic function at a generic point of the composite curve and the corresponding log value for the glassy or rubbery state normalized to the difference in log values for the same function between the glassy and rubbery states versus the log time normalized to the characteristic shift factor K for pure epoxy polymer C-100-0-8.

Another proof of different viscoelastic responses of polymers above and below T_g is given by the following representation of the viscoelastic behaviour of high polymers. An empirical function yielding a satisfactory fit to viscoelastic data for the transition region was introduced by Tobolsky and co-workers^[25] and based on the Gauss error function. Following this theory, we reproduced the composite curves expressing the mechanical and optical viscoelastic behaviour for pure cold-setting epoxy polymer C-100-0-8 by an equation of the Gauss error integral form^[26].

$$\log F(t/K) = \frac{\log F_1 + \log F_2}{2} - \frac{\log F_1 - \log F_2}{2} \operatorname{erf}(h \log t/K)$$

where

$$\operatorname{erf} x = \frac{2}{\sqrt{\pi}} \int_0^x e^{-u^2} du,$$

where F_1 are the glassy-state parameters (creep compliance, relaxation modulus, stress- and strain-optical coefficients), F_2 are the rubbery state parameters, K the characteristic time, defined previously, and h the adjustable parameter of the Gauss error curves. It may be noticed that if the negative derivative of each composite curve is plotted against $\log(t/K)$, the resulting curve is composed of two branches, each of which approximates a Gauss error curve with different parameter h . For the evaluation of the parameter h we plotted in Fig. 13 on normal probability paper the curves:

$$A = \frac{\log F_{c,r}(t/K) - \log F_2}{\log F_1 - \log F_2} \times 100 \text{ vs. } \log(t/K). \quad (58)$$

Each curve in these plots is formed by two distinctive straight lines with different slopes, which correspond to different values of h . The one value is related to the glassy behaviour, while the other value, common for all characteristic quantities, corresponds to the transition and rubbery states. This indicates the different viscoelastic behaviour of a typical rheo-optically simple high polymer in the glassy and transition regions.

Conversion of Characteristic Functions

Viscoelastic studies are always referred to a particular function describing the viscoelastic behaviour of a high polymer in creep or relaxation. The theory of linear viscoelasticity guarantees the uniqueness of the characterization of the mechanical and optical properties and its independence of the type of test used to determine them. This implies the possibility to convert data obtained from various types of tests. Several inversion methods have been developed to determine anyone characteristic function in creep or relaxation from its corresponding function. Moreover, numerical and other approximate methods have been developed

yielding anyone of these characteristic functions from their retardation or relaxation spectra. In this chapter we will examine approximate methods of such conversions.

While transient creep and relaxation experiments are always preferred to study the effects at long times, their application is restricted to the short-time end of the viscoelastic time-scale because of the inertial effects and the impossibility of having a truly instantaneous application of the programmed stress or strain. To integrate the information concerning the viscoelastic behaviour of a polymeric substance by providing data related to the other end of the time scale i.e. to very short times, dynamic or periodic loading patterns may be used. Then, in order to cover a wide time scale adequate to represent the variety of molecular motions in a typical polymer, which ordinarily is spread over 15 decades in the logarithmic time scale, it is often required to combine the above mentioned data. Which method should be used depends to a large extent on the particular functional relationship, which is needed between given independent variables and their functions.

Even this combination of methods contains certain inherent difficulties:

a) The dynamic dependence is commonly measured only on selected regions. This is because forced or free vibrations and wave propagation methods perform satisfactorily only within a rather narrow frequency range.

b) It must be a check between the various transient and dynamic methods used for the elimination of eventual systematic errors.

c) The moduli and compliances functions derived from a test do not always refer to the same deformation process. Hence, a conversion process is required, which yields the value of the characteristic function from another one, related to the same type of loading process (creep-relaxation-recovery). In other cases it is often needed to transform a viscoelastic function belonging to one loading mode (say creep) to its respective function corresponding to the other loading mode (say relaxation). Moreover, the knowledge of the lateral contraction ratio functions in creep and relaxation is sometimes required for the proper interrelation of the other characteristic functions.

A considerable literature has accumulated on the subject concerning the methods, whereby each of the viscoelastic functions may be derived from any other function determined experimentally. Only two main sources of reference need to be mentioned here, that is the comprehensive books by Ferry^[1] and Tobolsky^[11], which the reader is referred to for further more detailed information.

An attempt will be made here to present exact or approximate methods, which allow the conversion of one viscoelastic function to any other. These methods may be classed as follows:

a) methods of inverting a transient or dynamic viscoelastic function to its counterpart.

b) methods of interrelating a transient function with the corresponding dynamic functions.

c) methods of obtaining the retardation (or relaxation) spectra from any transient or the components of any complex dynamic viscoelastic function.

d) methods of converting the retardation spectra to relaxation spectra and vice versa.

e) methods of interrelating the components of any complex dynamic function and the corresponding transient function and

f) methods of calculating any transient creep or relaxation function from another creep or relaxation function.

Besides the preceding basic methods there are other methods dealing with the calculation of more complicated experimental functions which will be excluded from the present study.

While the products of the absolute values for each pair of a complex compliance and its corresponding modulus are equal to unity the interrelation of two corresponding transient compliances and moduli is complicated. Then, the simpler transformations between compliances and moduli are the type:

$$|E^*(\omega)| \cdot |D^*(\omega)| = 1.$$

This relation can readily be derived from relations (21).

Relations (21) may be used to convert the components of a complex dynamic compliance to the components of the corresponding complex dynamic modulus and vice versa. Similar relations to (21), valid for the shear dynamic quantities, were used to calculate the shear storage and loss moduli of a polyurethane elastomer, the Vulcollan 18/40. Landel^[28] has measured the values of the storage and loss dynamic components of the complex shear compliance $J'(\omega)$ and $J''(\omega)$ over a frequency range between 45 and 6,000 cycles/sec. and a temperature range of -16° to 39° C. Composite curves of $J'(\omega)$ and $J''(\omega)$ reduced to a standard temperature of 0.4° C were derived by the method of reduced variables. Using the data of Landel, the storage and loss shear dynamic moduli were determined and plotted in Fig. 14.

In the case of transient types of loading each creep compliance is connected to the corresponding relaxation modulus by the relations (5), which are integral equations of the convolution type. An efficient numerical method for the evaluation of integrals (5) has been introduced by Hopkins and Hamming^[29], in cases where the standard method of solution by application of the Laplace transform is not suitable. This is the case, where the known function is expressed in tabular or graphical form, by measuring this quantity along the whole viscoelastic range and the transform of this function cannot be determined precisely.

The method of Hopkins and Hamming uses finite differences where the integral is changed into a set of simultaneous algebraic equations. For the application of the method the values of the known function (say $E(t)$) normalized to $E(0) = 1$ must be determined in equal intervals by dividing the entire time range into n intervals by the time values t_i , where i are varying between 1 and $(n + 1)$.

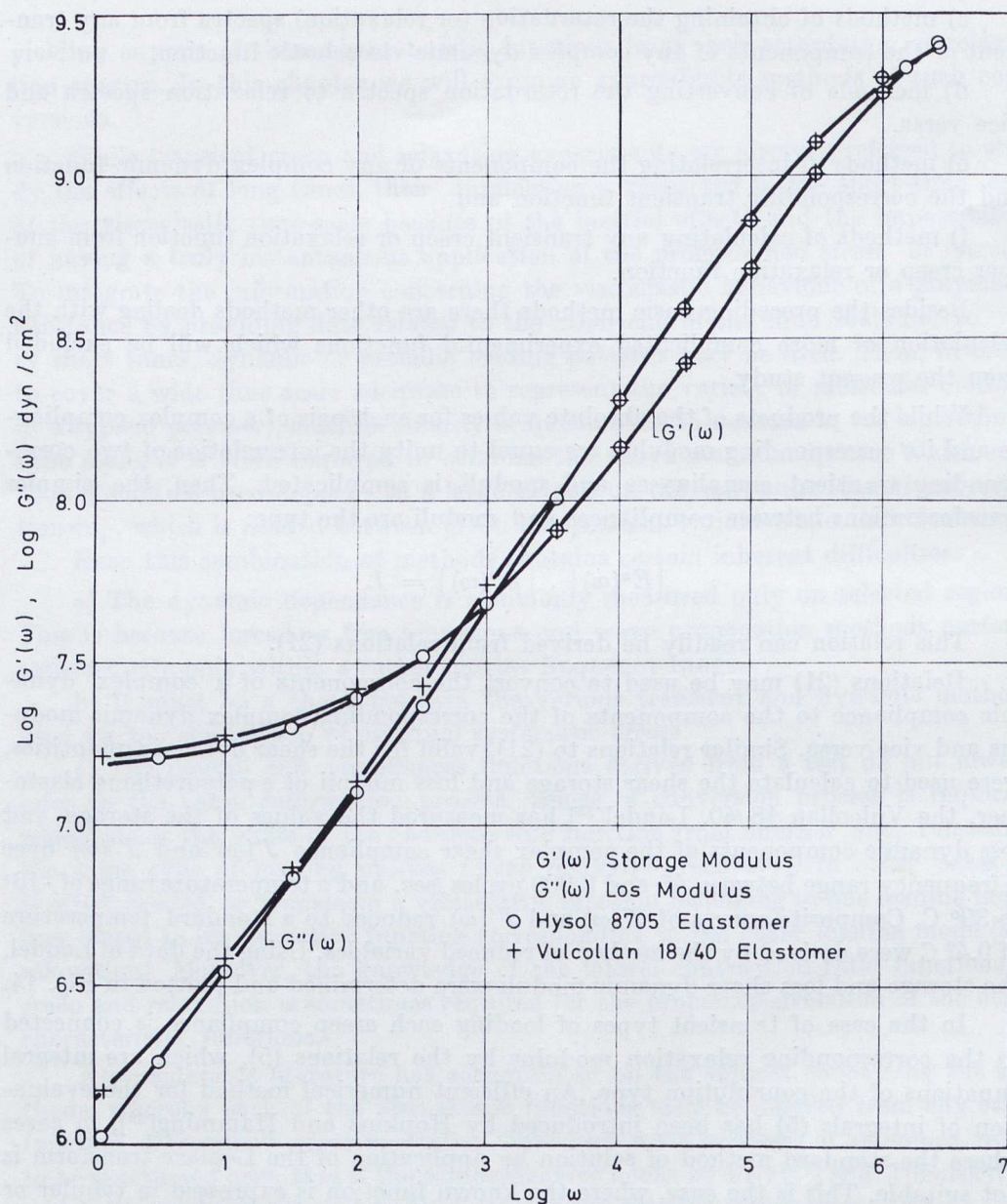


Fig. 14 Storage and loss shear dynamic moduli composite curves versus $\log \omega$ for polyurethane elastomer Hysol 8705 and Vulcollan 18/40 elastomer. The Hysol composite curves were derived from the transient shear modulus and the relaxation spectrum by applying Catsiff and Tobolsky's approximate method. The Vulcollan 18/40 composite curves were derived from the composite curves of the corresponding storage and loss dynamic compliances.

Introducing the integral:

$$f(t) = \int_0^t E(\tau) d\tau, \quad (59)$$

with limit values $f(0) = 0$ and $f'(\tau) = E(\tau)$ and replacing the continuous function $E(\tau)$ by a step function at the intervals i of time, we can determine the function $f(t)$ by using the trapezoid rule of integration. The function $f(t)$ may be expressed as:

$$f(t_{n+1}) = f(t_n) + 1/2 \left[E(t_{n+1}) + E(t_n) \right] \left[t_{n+1} - t_n \right]. \quad (60)$$

Then, the first integral (5) may be written as:

$$t_{n+1} = \sum_{i=1}^{(n+1)} \int_{t_i}^{t_{i+1}} D(\tau) E(t_{n+1} - \tau) d\tau. \quad (61)$$

If, in each of the integrals in the sum, we make the approximation:

$$\int_{t_i}^{t_{i+1}} D(\tau) E(t_{n+1} - \tau) d\tau = -D(t_{i+1/2}) \left[f(t_{n+1} - t_{i+1}) - f(t_{n+1} - t_i) \right].$$

with the time $t_{i+1/2}$ corresponding to the midvalue $1/2(t_{i+1} + t_i)$ and solve for $D(t_{n+1/2})$ we have:

$$D(t_{n+1/2}) = \frac{t_{n+1} - \sum_{i=1}^n D(t_{i+1/2}) \left[f(t_{n+1} - t_i) - f(t_{n+1} - t_{i+1}) \right]}{f(t_{n+1} - t_n)}. \quad (62)$$

We can evaluate the various $D(t_{n+1/2})$ in terms of the values of D 's for time-intervals from 1 to n and to the values of the auxiliary function $f(t_n)$.

The initial value of D is given directly by:

$$D(t_{1/2}) = \frac{t_1}{f(t_1)}. \quad (63)$$

The simple successive solution contained in relations (60) to (63) is originated from the limits of integration of the integral equation, which are 0 and t , and the derived triangular matrix of the finite difference equations.

It was demonstrated by Hopkins and Hamming^[29] that this particular finite-difference representation is extremely stable and the error introduced into every time interval is rapidly attenuated. Moreover, no complications are introduced if the time intervals are varied. Thus, the finite measurements in t intervals of time may be selected conveniently, with increased increments in regions of small varia-

tion of the experimentally determined function. This process tends toward a maintained uniform accuracy all over the time range and a reduction of the number of terms in the finite - difference scheme.

In order to show the possibilities of the method it was applied for the determination of the extension creep compliance of a polyurethane elastomer, the Hysol rubber 8705. The extension relaxation transient modulus of the material was de-

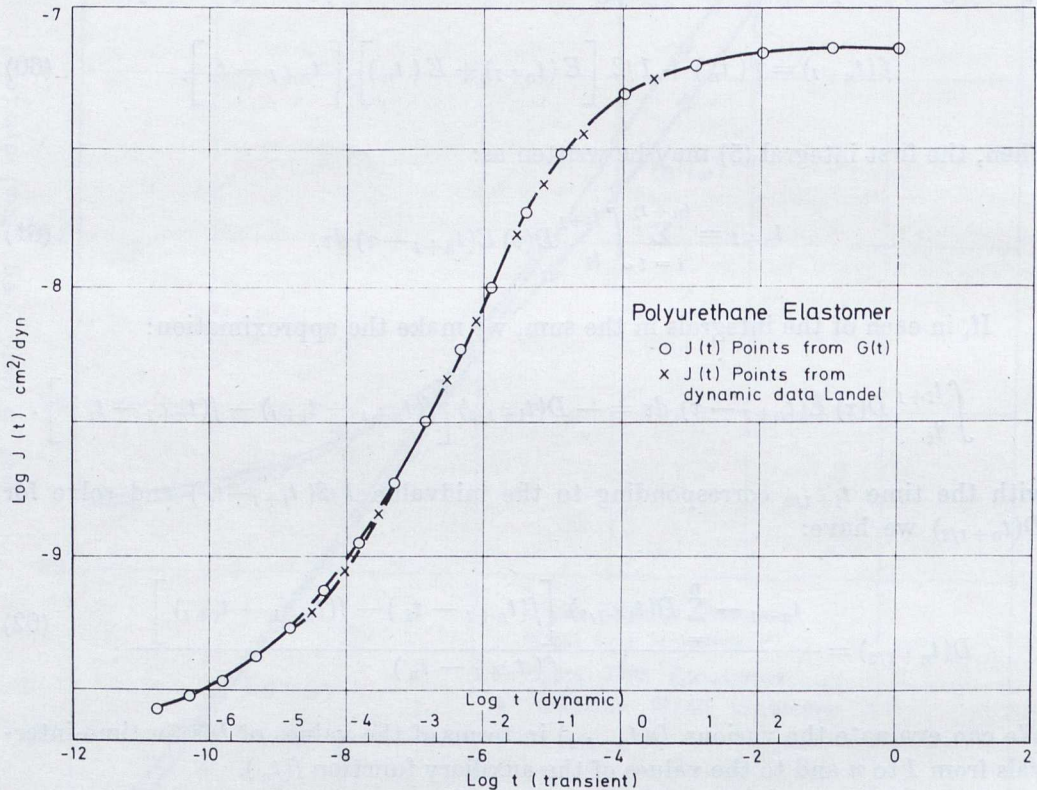


Fig. 15 Composite curves of the transient shear compliance for polyurethane elastomer Hysol 8705 determined from the shear relaxation modulus by numerical inversion of the Duhamel integral (o) and of the transient shear compliance for Vulcollan 18/40 polyurethane elastomer determined from the shear storage and loss dynamic compliances(x).

termined experimentally by applying the principle of reduced variables^[30]. The experimental results coincided with data of $E(t)$ given by Williams and co-workers^[31]. Simultaneously, the lateral contraction ratio function in relaxation was determined by using the differential moiré method and circular gratings of a density of 500 lines per inch, which measured the longitudinal extension, as well as, the lateral contraction in a tension specimen. Fig. 10 shows the extension relaxation modulus function and the lateral contraction ratio function in relaxation, as

they have been derived by the individual relaxation curves at various steps of temperature and application of the principle of reduced variables (see also fig. 3), Fig. 10a depicts the variation of the shear and bulk moduli functions, as they have been derived from the two experimentally determined functions by applying an approximation method described in the following. The values of the shear relaxation modulus function were used to determine the shear compliance function. For this purpose the shear relaxation data were normalized to the initial value of $G(t)$, which was taken to be at a temperature 208° K. The log time scale of the shear relaxation function was converted into a conventional time scale by dividing the log time scale into equal intervals and introducing the notation t ($i = 1$ to $(n+1)$) with $t_1 = 0$, $t_2 = 10^{-17.00}$, $t_3 = 10^{-16.80}$, $t_4 = 10^{-16.60}$ etc).

The function $f(t)$, as it was defined by Eq.(59), was determined at the time-intervals considered by assuming that the $G(t)$ -function remained constant between each interval ($t_n - t_{(n+1)}$). By applying relation (62) for each time-interval, the values of the shear creep compliance were determined. The transient shear compliance function was plotted in Fig. 15.

Each of the relaxation moduli, the inverse of the corresponding compliance

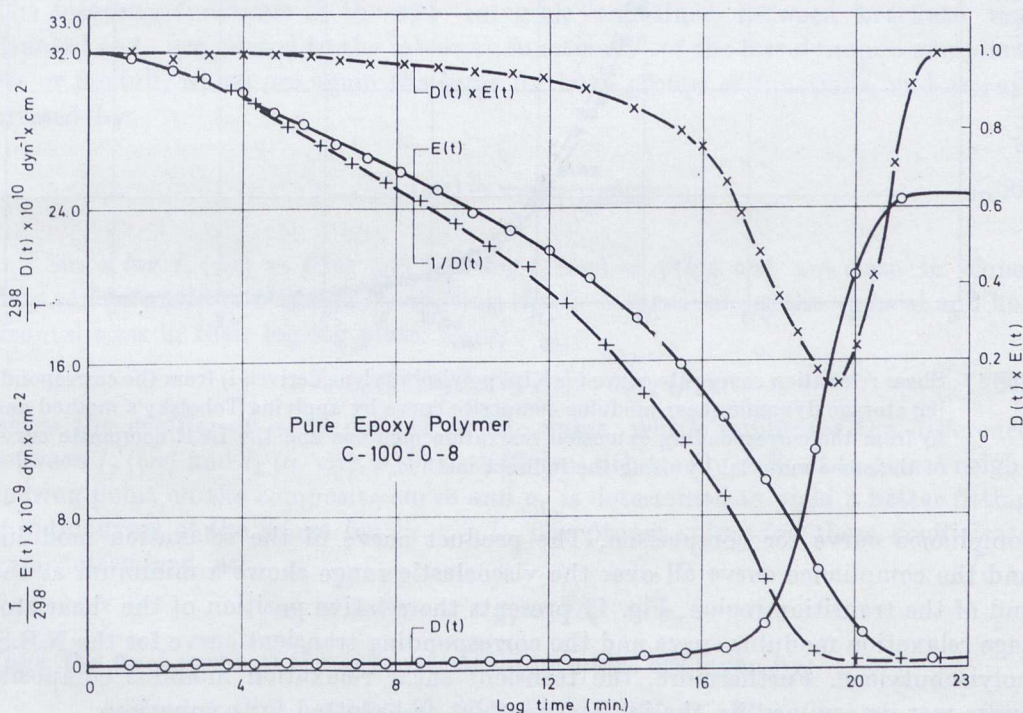


Fig. 16 Extension relaxation modulus composite curve and the inverse of the extension creep compliance curve for pure epoxy polymer C-100-0-8 versus log time. In the same figure the product of extension creep compliance and relaxation modulus transient versus curves log time is plotted for comparison.

and the storage dynamic moduli at a time $t = 1/\omega$ may be taken equal to a first approximation. This equality is valid only at the glassy and rubbery regions. Generally, it is valid that for a given value of the time t , or the circular frequency $\omega = 1/t$, the inverse of any compliance is smaller than the corresponding modulus at the same time and this, in turn, is slightly smaller than the corresponding storage modulus at a frequency $\omega = 1/t$.

Fig. 16 presents the transient relaxation modulus and the creep compliance composite curves for the epoxy polymer C-100-0-8, as well as the inverse of the

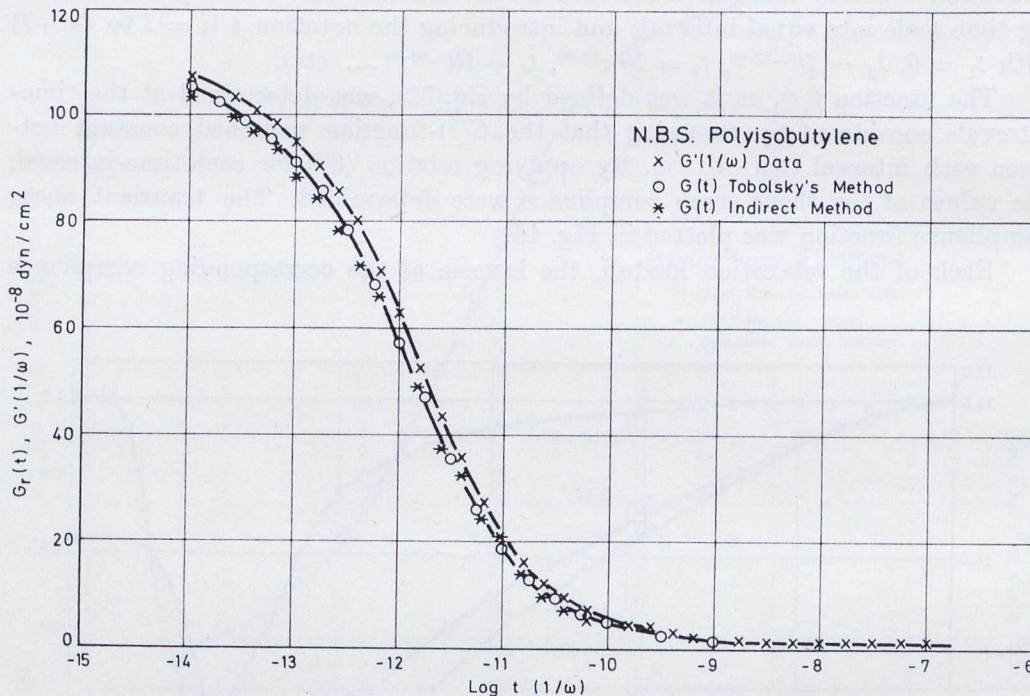


Fig. 17 Shear relaxation composite curve for NBS polyisobutylene derived i) from the corresponding storage dynamic shear modulus composite curve by applying Tobolsky's method and ii) from the corresponding extension relaxation modulus and the LCR composite curve of the same material by using the indirect method.

compliance curve for comparison. The product curve of the relaxation modulus and the compliance curve all over the viscoelastic range shows a minimum at the end of the transition region. Fig. 17 presents the relative position of the shear storage relaxation modulus curve and the corresponding transient curve for the N.B.S. polyisobutylene. Furthermore, the transient shear relaxation modulus composite curve was determined by the indirect method and plotted for comparison.

Where both dynamic components are known, it is possible to calculate the corresponding transient function. Several approximate methods have been developed, all of them based on approximations of the intensity functions and the re-

tardation or relaxation spectra. Thus, Catsiff and Tobolsky have modified a relation due to Marvin^[32] to express any transient relaxation modulus function in terms of the corresponding storage modulus and the respective relaxation spectrum. Smith^[33] gave an analogous expression for the compliances. A common feature of these methods is that they use time or frequency derivatives of experimentally measured quantities.

An alternative and simpler, though equally accurate method, has been developed by Ninomiya and Ferry^[34]. This method interrelates any transient creep or relaxation function directly to the real and imaginary parts of the corresponding dynamic function.

The methods employs the following relations expressing the differences between the storage compliances or moduli and the corresponding transient quantities:

$$-D'(\omega) + D(t)|_{t=1/\omega} = \int_0^{\infty} \left[\frac{\omega^2 \tau^2}{1 + \omega^2 \tau^2} - e^{-(1/\omega\tau)} \right] L(\tau) d(\ln\tau) \quad (64)$$

$$E'(\omega) - E(t)|_{t=1/\omega} = \int_0^{\infty} \left[\frac{\omega^2 \tau^2}{1 + \omega^2 \tau^2} - e^{-(1/\omega\tau)} \right] H(\tau) d(\ln\tau). \quad (65)$$

The intensity functions in the two integrals contained between brackets and denoted as I_r are related to the intensity functions I_i of the loss dynamic compliances or moduli, which are again the same for both groups of functions, and are expressed by:

$$I_i(\omega\tau) = \frac{\omega\tau}{1 + \omega^2 \tau^2}. \quad (66)$$

Since $\log I_r(\omega\tau) = f(\log \omega\tau)$ and $\log I_i(\omega\tau) = \varphi(\log \omega\tau)$ are close in slope, they can be made to coincide by shifting the I_i - curve along the vertical and horizontal axes in their log-log plots. Thus:

$$I_r(\omega\tau) \equiv \alpha_1 I_i(\alpha_1 \omega\tau) - \alpha_2 I_i(\beta_2 \omega\tau) \quad (67)$$

where the coefficient α_1 is defined as the value, which minimizes the difference between $I_r(\omega\tau)$ and $I_i(\alpha_1 \omega\tau)$, β_2 is a coefficient arbitrarily defined to give a neighbouring point on the composite curve and α_2 is determined to yield a better fitting of both curves at the range $\log \omega\tau < -1$. The proper values for these coefficients were determined as:

$$\alpha_1 = 0.400, \quad \beta_1 = 10, \quad \alpha_2 = 0.014$$

Thus, the final forms of the approximation formulas are given by:

$$-D'(\omega) + D(t)|_{t=1/\omega} \approx 0.40 D''(0.40\omega) - 0.014 D''(10\omega) \quad (68)$$

$$E'(\omega) - E(t)|_{t=1/\omega} \approx 0.40 E''(0.40\omega) - 0.014 E''(10\omega) \quad (69)$$

and similarly for the other types of functions.

Relations (68) were used to determine the transient shear compliance $J'(t)$ of a polyurethane elastomer Vulcollan 18/40 from the values of the real and imaginary components of the complex shear compliance $J'(\omega)$ and $J''(\omega)$ measured by Landel^[28]. Using the data by Landel the transient shear compliance function was determined and plotted in Fig. 15. Although the material used by Landel was different than the Hysol polyurethane elastomer 8705, the coincidence of the two $J(t)$ -composite curves is remarkable.

Various approximation methods have been developed to derive the retardation or relaxation spectra from the corresponding compliances or moduli viscoelastic functions.

The so-called first approximations use derivatives of experimentally measured quantities with respect to time or frequency, depending on the type of the quantity measured experimentally^[1]. The second approximations use in addition the first derivatives of the first approximations of the spectra, by assuming that the corresponding spectrum satisfies an analytic relation of a power^[35] or logarithmic^[36] form.

Schwarzl and Staverman^[8,9] have proposed general formulas yielding calculations of the spectra to any degree of approximation, by determining first and higher order derivatives at different points along the creep or relaxation curves. The method of Ferry and Williams^[35] yields also a system of approximations. According to their method the first and second order approximations of the spectra in terms of the transient and storage or loss dynamic compliances and moduli are expressed by:

$$\begin{aligned} L_{1e}(\tau) &= M(-m) D(t) \left. \frac{d \log D(t)}{d \log t} \right|_{t=\tau} \\ H_{1e}(\tau) &= -M(m) E(t) \left. \frac{d \log E(t)}{d \log t} \right|_{t=\tau} \end{aligned} \quad (70)$$

$$\begin{aligned} L'_{1e}(\tau) &= -AD' \left[\frac{1}{\omega} \right] \left. \frac{d \log D'(1/\omega)}{d \log \omega} \right|_{1/\omega=\tau} \\ H'_{1e}(\tau) &= AE'(1/\omega) \left. \frac{d \log E'(1/\omega)}{d \log \omega} \right|_{1/\omega=\tau} \end{aligned} \quad (71)$$

$$\begin{aligned} L''_{1e}(\tau) &= BD''(1/\omega) \left[1 - \left| \frac{d \log D''(1/\omega)}{d \log \omega} \right| \right] \Big|_{1/\omega=\tau} \\ H''_{1e}(\tau) &= BE''(1/\omega) \left[1 - \left| \frac{d \log E''(1/\omega)}{d \log \omega} \right| \right] \Big|_{1/\omega=\tau} \end{aligned} \quad (72)$$

where:

$$M(m) = \frac{1}{\Gamma(m+1)} \quad (73)$$

with $\Gamma(m+1)$ the well-known gamma function which for integral values of m yields $\Gamma(m+1) = m!$, and $(-m)$ the slope of the doubly logarithmic plot of the curves $L = f(t)$ and $H = f(t)$. Moreover, the other factors A and B are defined as follows:

$$A = (2-m) / 2\Gamma \left[2 - \frac{m}{2} \right] \Gamma \left[1 + \frac{m}{2} \right] \quad (74)$$

and

$$B = (1 + |m|) / 2\Gamma \left[\frac{3}{2} - \frac{|m|}{2} \right] \Gamma \left[\frac{3}{2} + \frac{|m|}{2} \right]. \quad (75)$$

Usually the log-time scale is divided into equal sub-intervals. Then, from the tentative first curves $L = f(t)$ and $H = f(t)$ the slope $(-m)$ is determined and the corresponding values of M , A and B are found, by using relations (73-75) for the existing values of the tabulated functions M , A and B .

A slightly different system of approximations, proposed by Schwarzl and Staverman^[9] expresses higher approximations of the spectra by:

$$\begin{aligned} L_{2e}(\tau) &= \left. \frac{dD(t)}{d \ln t} - \frac{d^2 D(t)}{d (\ln t)^2} \right|_{t=2\tau} \\ H_{2e}(\tau) &= \left. -\frac{dE(t)}{d (\ln t)} - \frac{d^2 E(t)}{d (\ln t)^2} \right|_{t=2\tau}, \end{aligned} \quad (76)$$

where, both first and second derivatives of $D(t)$ or $E(t)$ must be evaluated at each point of the corresponding composite curve and the values of the spectra determined correspond to the point $\tau = t/2$. Similarly for the spectra derived from the storage and loss quantities we have:

$$\begin{aligned} L'_{3e}(\tau) &= \left. -\frac{dD'(1/\omega)}{d(\ln \omega)} + \frac{1}{4} \frac{d^3 D'(1/\omega)}{d(\ln \omega)^3} \right|_{1/\omega=\tau}, \\ H'_{3e}(\tau) &= \left. \frac{dE'(1/\omega)}{d(\ln \omega)} - \frac{1}{4} \frac{d^3 E'(1/\omega)}{d(\ln \omega)^3} \right|_{1/\omega=\tau} \end{aligned} \quad (77)$$

and

$$\begin{aligned} L''_{2e}(\tau) &= \left[\frac{2}{\pi} \right] \left[D''(1/\omega) - \frac{d^2 D''(1/\omega)}{d(\ln \omega)^2} \right] \Big|_{1/\omega=\tau} \\ H''_{2e}(\tau) &= \left[\frac{2}{\pi} \right] \left[E''(1/\omega) - \frac{d^2 E''(1/\omega)}{d(\ln \omega)^2} \right] \Big|_{1/\omega=\tau}, \end{aligned} \quad (78)$$

where the primes and the double-primes in the spectra express the quantities derived from the storage and loss dynamic quantities. Relations (76) to (78) are derived from relations (38) to (40) given previously. Formulas (70) to (78) may be extended to the other types of compliances and moduli by an appropriate change of the respective quantities.

In order to illustrate the various methods of approximating the spectra, the following calculations were programmed in a digital computer. First and second

approximations of the shear modulus transient spectrum of Hysol elastomer 8705 were determined from the transient shear compliance composite curve, which was derived by conversion of the shear relaxation modulus curve. These two curves were plotted in Fig. 18. In the same figure the retardation spectra of the Vulcollan 18/40 polyurethane elastomer were plotted, as they were derived from the shear storage and loss dynamic compliances given by Landel, by applying relations (71.1) and (72.1).

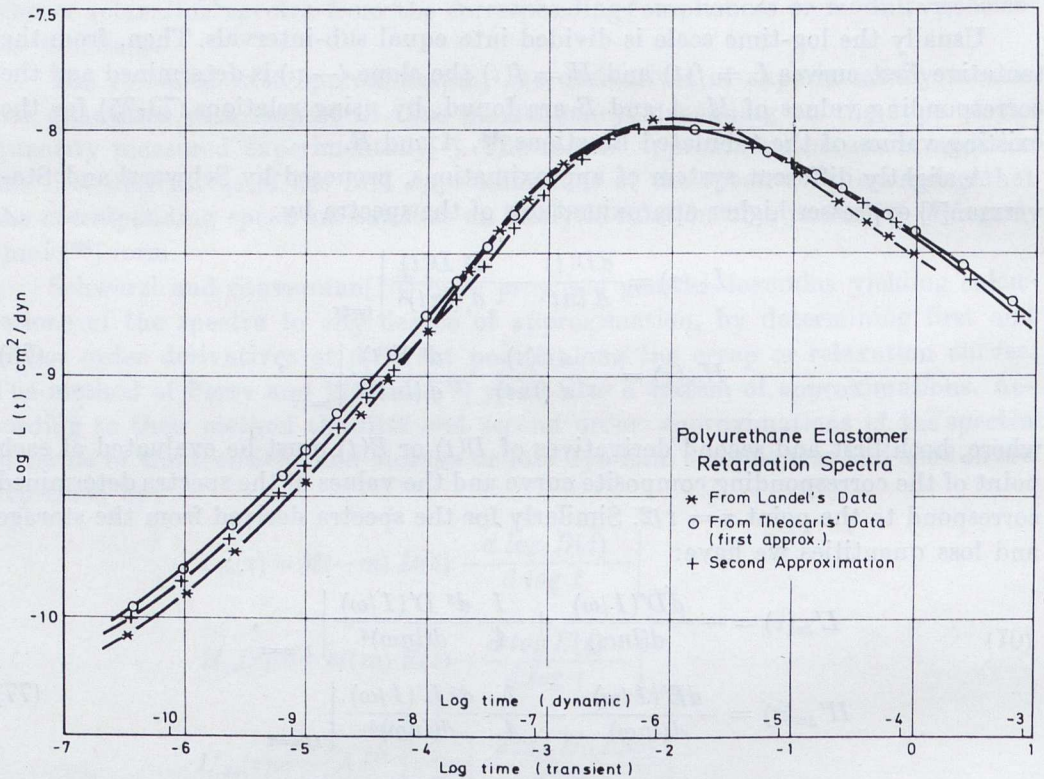


Fig. 18 First approximations of retardation spectra derived from shear storage or loss compliances for Vulcollan 18/40 polyurethane elastomer and first and second approximations of the retardation spectra derived from the transient shear compliance composite curve for Hysol 8705 polyurethane elastomer.

To calculate one spectrum from the other when a transient function is known we use the relations (41) and (42), which after a rearrangement, may be written as:

$$L_e(\tau) = \frac{H_e(\tau)}{\left\{ E(t) + H_e(\tau) \left[\frac{\pi}{2} \left[\csc \frac{m\pi}{2} - \sec \frac{m\pi}{2} \right] - \Gamma(m) + 1.37 \right] \right\}^2 + \pi^2 H_e^2(\tau)} \quad (79)$$

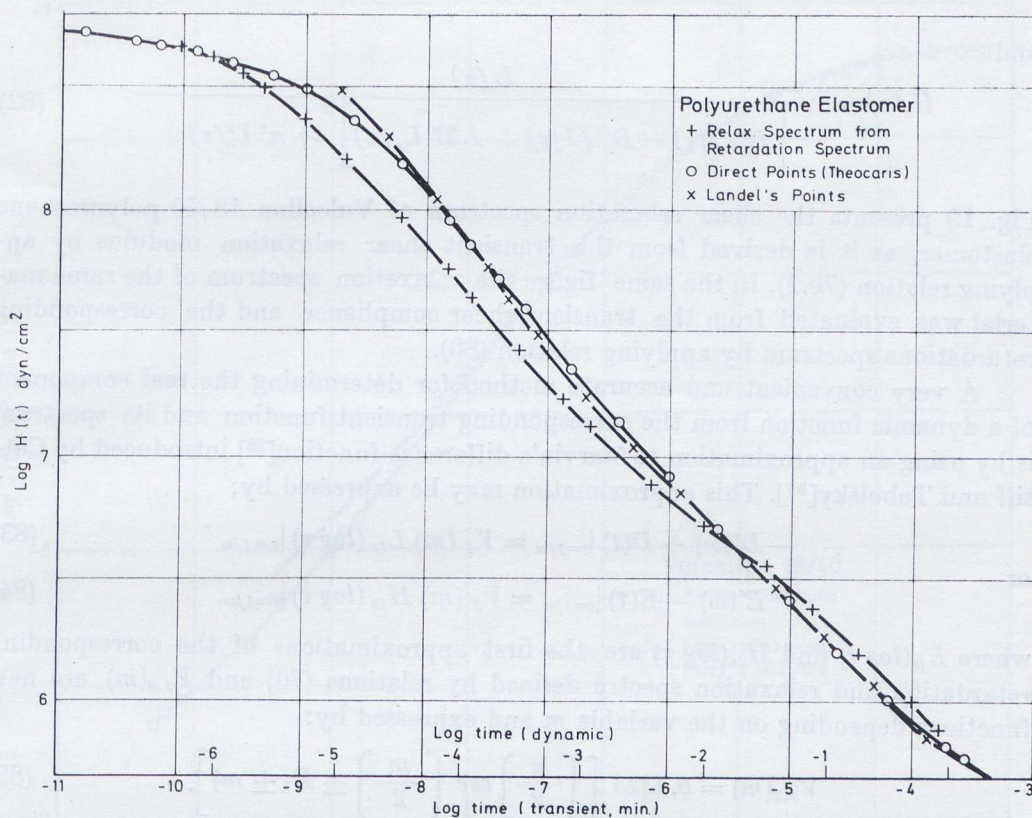


Fig. 19 Shear relaxation spectrum derived from the corresponding shear retardation spectrum and the shear relaxation spectrum derived from the transient shear modulus composite curve for Hysol 8705 polyurethane elastomer. This spectrum is compared to the shear relaxation spectrum for the Vulcollan 18/40 polyurethane elastomer.

$$H_e(\tau) = \frac{L_e(\tau)}{\left\{ D(t) + L_e(\tau) \left[\frac{\pi}{2} \left[\csc \frac{m\pi}{2} - \sec \frac{m\pi}{2} \right] + \Gamma(-m) + 1.37 \right] \right\}^2 + \pi^2 L_e^2(\tau)} \quad (80)$$

where, again, m is the negative slope of the log plot of each spectrum, measured at the point considered.

To calculate one spectrum from the other, when dynamic data are known, we use the formulas, which again are derived from relations (41) and (42):

$$L_e(\tau) = \frac{H_e(\tau)}{\left[E'(1/\tau) - E'' \left(1/\tau \right) + 1.37 H_e(\tau) \right]^2 + \pi^2 H_e^2(\tau)} \quad (81)$$

and

$$H_e(\tau) = \frac{L_e(\tau)}{\left[D'(1/\tau) - D''(1/\tau) + 1.37 L_e(\tau) \right]^2 + \pi^2 L_e^2(\tau)} \quad (82)$$

Fig. 19 presents the shear relaxation spectrum of Vulcollan 18/40 polyurethane elastomer, as it is derived from the transient shear relaxation modulus by applying relation (70.2). In the same figure the relaxation spectrum of the same material was evaluated from the transient shear compliance and the corresponding retardations spectrum by applying relation (80).

A very convenient and accurate method for determining the real component of a dynamic function from the corresponding transient function and its spectrum is by using an approximation to Marvin's difference function^[32] introduced by Catsiff and Tobolsky^[37]. This approximation may be expressed by:

$$-D'(\omega) + D(t)|_{t=1/\omega} \approx V_1(m) L_{1e}(\log \tau)|_{\tau=1/\omega} \quad (83)$$

or

$$E'(\omega) - E(t)|_{t=1/\omega} \approx V_2(m) H_{1e}(\log \tau)|_{\tau=1/\omega}, \quad (84)$$

where $L_{1e}(\log \tau)$ and $H_{1e}(\log \tau)$ are the first approximations of the corresponding retardation and relaxation spectra defined by relations (70) and $V_{1,2}(m)$ are new functions depending on the variable m and expressed by:

$$V_{1,2}(m) = 0.4343 \left[\left[\frac{\pi}{2} \right] \csc \left[\frac{m}{2} \right] \pm \Gamma(\pm m) \right]. \quad (85)$$

The functions $V_{1,2}(m)$ either may be easily calculated or their values taken from the tabulated values of m . The tabulated values of $V(m)$ are given in Refs. 11 and 37. Relations (83) and (84) are derived from relations (64) and (65) by a judicious approximation of the intensity functions.

Similarly, it can readily be proved that the following approximation exists, which relates the loss dynamic quantities to the corresponding transient spectra:

$$D''(1/\omega) \approx -\sec \left[\frac{m\pi}{2} \right] L_{1e}(\log \tau) \quad (86)$$

$$E''(1/\omega) \approx \frac{\pi}{2} \sec \left[\frac{m\pi}{2} \right] H_{1e}(\log \tau). \quad (87)$$

Similar relations exist for the compliances and moduli derived from the other types of loading.

The above mentioned approximate method of Catsiff and Tobolsky was applied to the evaluation of the storage and loss dynamic components of the shear relaxation modulus of the polyurethane elastomer Hysol 8705 from the tabulated transient shear modulus. These components are depicted in Fig. 14. Fig. 17 presents the $G(t)$ -curve for Polyisobutylene as derived from the $G'(1/\omega)$ -curve measured by Ferry et al^[51].

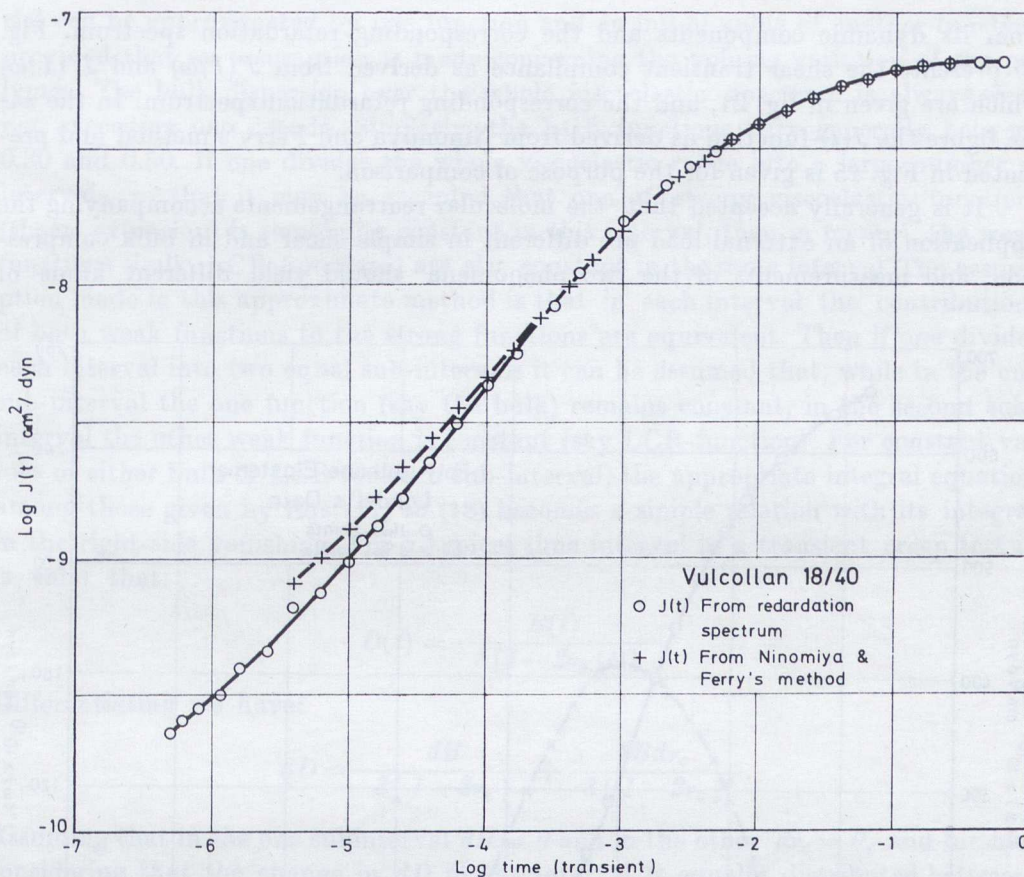


Fig. 20 Transient shear compliance composite curve for Vulcollan 18/40 polyurethane elastomer computed from the storage and loss dynamic shear compliances and the retardation spectrum. This curve is compared with the transient shear compliance composite curve calculated from the storage and loss dynamic shear compliances given in fig. 21 by applying Ninomiya and Ferry's method.

Another useful approximation yielding the transient compliance or modulus functions from their dynamic components and the corresponding retardation or relaxation spectra may be derived from Eqs. (79) and (80) respectively. These relations are given by:

$$D(t) = D'(1/\omega) - D''(1/\omega) - L_{1e}(\tau) \left[\frac{\pi}{2} \left(\csc \frac{m\pi}{2} - \sec \frac{m\pi}{2} \right) + \Gamma(-m) \right] \quad (88)$$

$$E(t) = E'(1/\omega) - E''(1/\omega) - H_{1e}(\tau) \left[\frac{\pi}{2} \left(\csc \frac{m\pi}{2} - \sec \frac{m\pi}{2} \right) - \Gamma(m) \right]. \quad (89)$$

A relation similar to (88), yielding the shear compliance, was used for the determination of this quantity for the Vulcollan 18/40 polyurethane elastomer

from its dynamic components and the corresponding retardation spectrum. Fig. 20 presents the shear transient compliance as derived from $J'(1/\omega)$ and $J''(1/\omega)$ which are given in fig. 21, and the corresponding retardation spectrum. In the same figure the $J(t)$ -function as derived from Ninomiya and Ferry's method and presented in Fig. 15 is given for the purpose of comparison.

It is generally accepted that the molecular rearrangements accompanying the application of an external load are different in simple shear and in bulk compression, and measurements of the two phenomena should yield different kinds of

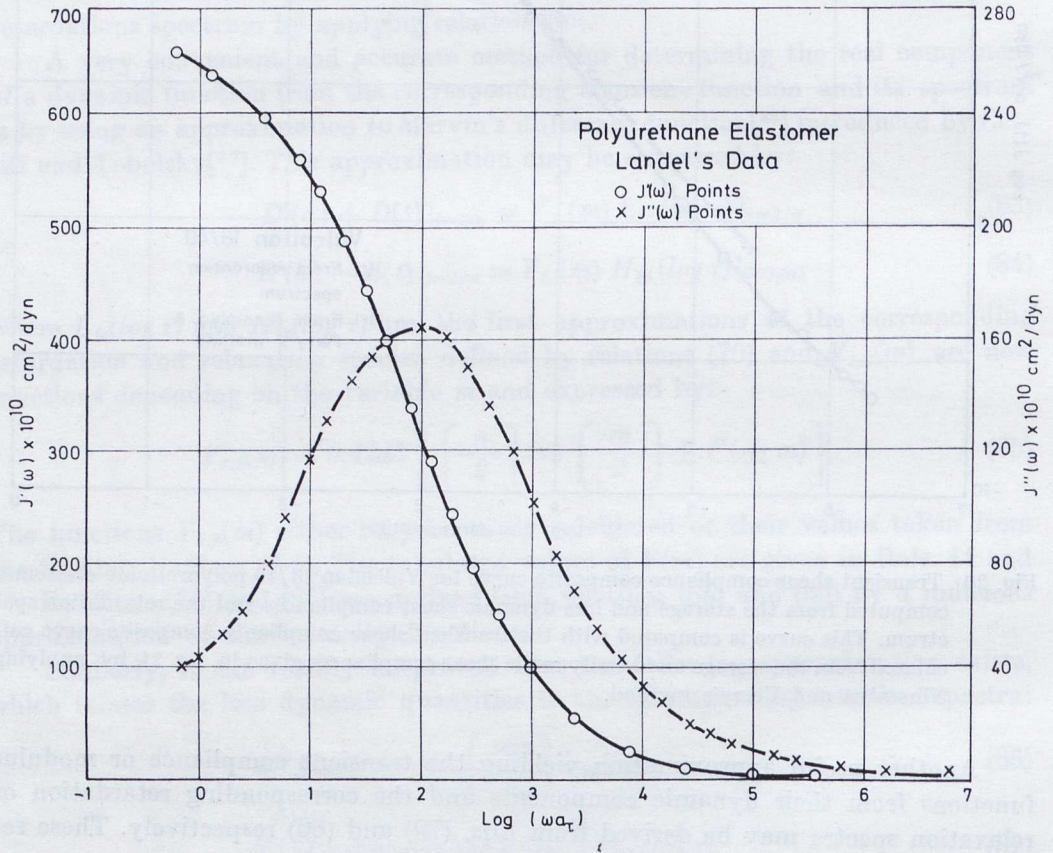


Fig. 21 Storage and loss shear compliance composite curves Vulcollan 18/40 polyurethane elastomer as derived from Landel's data of isothermal curves by applying the method of reduced variables.

information about the molecular motions and interactions. This implies that two characteristic functions describing these phenomena must be expressed by two independent linear differential or integral operator relations. However, it has been recently shown^[5,38] that these two functions which must be known along the whole viscoelastic range in order to determine the viscoelastic behaviour of the mate-

rial can be approximated by one function and an initial value of another function, provided that an assumption is made concerning the volume variation of the polymer. The bulk dispersion over the whole viscoelastic spectrum is always weak not exceeding one decade. Similarly, the LCR functions vary generally between 0.30 and 0.50. If one divides the whole viscoelastic range into a large number of intervals, so that it may be accepted that one of strong viscoelastic functions (shear, extension) is remaining constant in this interval, then, a fortiori, the weak functions (bulk, LCR-functions) are also constant in the same interval. The assumption made in this approximate method is that in each interval the contributions of both weak functions to the strong functions are equivalent. Then if one divides each interval into two equal sub-intervals it can be assumed that, while in the one sub-interval the one function (say the bulk) remains constant, in the second sub-interval the other weak function is constant (say LCR-function). For constant values of either bulk or LCR for each sub-interval, the appropriate integral equation among those given by Eqs. (11) to (18) becomes a simple relation with its integral in the right-side vanishing. For a typical time interval in a transient creep test it is valid that:

$$D(t) = \frac{B(t)}{3[I - 2\nu_c(t)]}.$$

Differentiating we have:

$$dD = \frac{dB}{3(I - 2\nu_c)} + \frac{2Bd\nu_c}{3(I - 2\nu_c)^2}.$$

Assuming that in the one subinterval $dB = 0$ and in the other $d\nu_c = 0$, and further considering that the change in dD in the interval is equally distributed between $B(t)$ and $\nu_c(t)$ we have for the one subinterval

$$\frac{dD}{2} = \frac{dB}{3(I - 2\nu_c)} \quad \text{for } \nu_c = \text{const} (d\nu_c = 0).$$

For the second subinterval, where $dB = 0$, since $B = \text{const.}$, it is valid that:

$$\frac{dD}{2} = \frac{2Bd\nu_c}{3(I - 2\nu_c)^2}.$$

Equating the two last relations, separating variables, and integrating, it can be found that:

$$B(t)[I - 2\nu_c(t)] = B_o(I - 2\nu_{c0}), \quad (90a)$$

where B_o and ν_{c0} are the initial values for the bulk modulus and LCR at the glassy or rubbery state.

For the corresponding transient relaxation test it can be respectively found that:

$$K(t) = \frac{K_o}{(I - 2\nu_{r0})} [I - 2\nu_r(t)]. \quad (90b)$$

Relations (90a) and (90b) interrelate the weak viscoelastic functions in a transient mode of loading. While Eq. (90a) is a parabola, relation (90b) is a straight line^[30,38,39]. Approximate relations (90) may replace any other assumption like the incompressibility or the constancy in bulk deformation along the whole viscoelastic range.

Therefore, if one of the strong transient viscoelastic functions (shear or extension) is known all over the viscoelastic range, an initial value for one of the weak functions (bulk deformation or LCR) and the appropriate assumption expressed by one of relations (90) suffice for the complete viscoelastic characterization of the material. Thus, if the logarithmic scale is divided into a number of n intervals labelled between I and $(n+I)$, so that the maximum variation of the known function $D(t)$ (or $E(t)$), or $J(t)$ (or $G(t)$), in any of these intervals is very small, then, a fortiori, the variations of the corresponding $B(t)$ (or $K(t)$) and $\nu_{c,r}(t)$ -functions in the same intervals may be considered as constant. In this case the functions $B(t)$ and $\nu_c(t)$ are given by^[44]:

$$\log \left[\frac{1}{2} - \nu_c(t_{2n}) \right] = \sum_{i=1}^n \left[\log D(t_{2i-1}) - \log D(t_{2i}) \right] + \log \left[\frac{1}{2} - \nu_{c0} \right] \quad (91)$$

$$\log B(t_{2n}) = \sum_{i=1}^n \left[\log D(t_{2i}) - \log D(t_{2i-1}) \right] + \log B_0.$$

where the initial values $D_0 = D(t_1)$, $\nu_0 = \nu(t_1)$ and $B_0 = B(t_1)$ are the values of these quantities at the glassy or rubbery range, where they are interrelated by the elastic relationships. Moreover, the quantities $D(t_{2i})$ express the values of the extension compliance at the interval t_{2i} and they are replaced by the values of function at the end of the interval. Taking successively $n = 1, 2, 3, \dots$ in the set of equations (91), we obtain relations from which we can evaluate the pairs of quantities $\nu_c(t_2)$, $B(t_2)$, $\nu_c(t_3)$, $B(t_3)$,....., each equation determining the next value of either of these quantities in terms of the values of the other quantity and the experimentally determined values of the function $D(t)$. The calculation process must start simultaneously for both equations (91), and the lower or upper bound for each quantity is obtained by starting the calculation process with the one or the other initial value. This finite difference approximation found to be extremely stable by the results obtained is cases where the $D(t)$ and $E(t)$ -functions are smooth, continuously increasing or decreasing functions as it is the case with all cross-linked polymers. The evaluation of the bounds of both characteristic functions was programmed for a digital computer. Flexibility of the number of log-time sub-intervals was provided so that discrepancies between bounds to be minimized by an appropriate choice of the time increment.

The values of the lateral contraction ratio in relaxation for the Hysol 8705 elastomer, obtained by this indirect method, were compared with the existing experimental values. They were plotted in Fig. 22. The coincidence of the results is

remarkable and proves the validity of the indirect method. Moreover, the shear and bulk transient modulus functions determined by this approximate method were plotted in Fig. 14. The shear modulus function thus determined was used for the

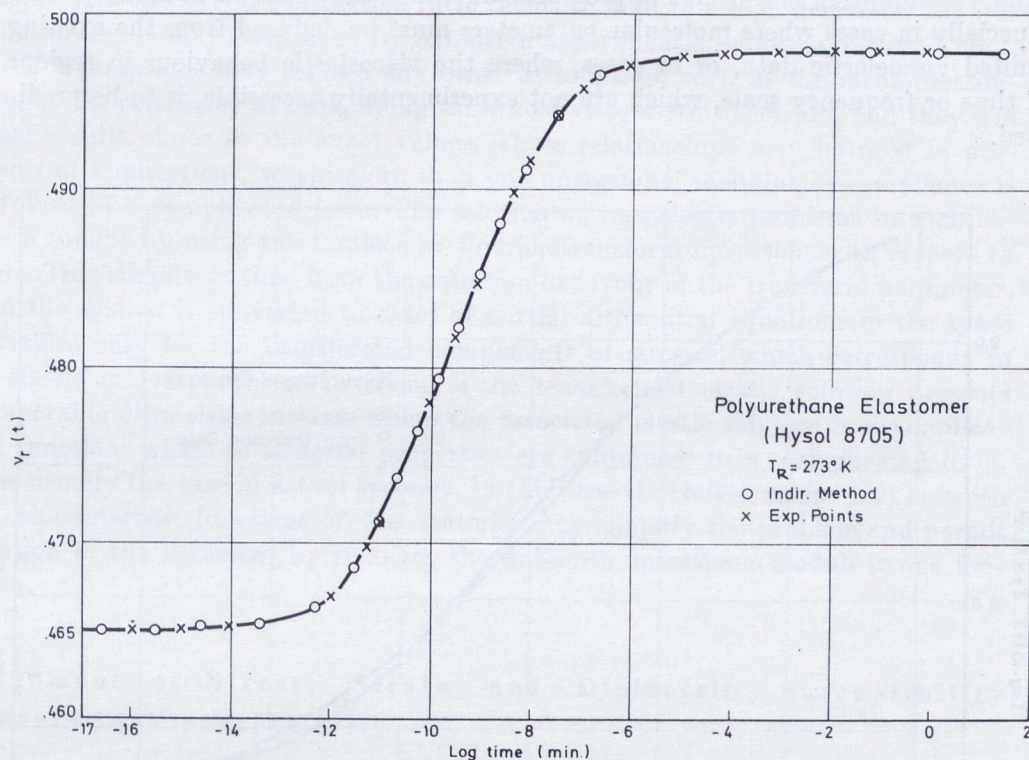


Fig. 22 Lateral contraction ratio composite curve for Hysol 8705 polyurethane elastomer determined experimentally by applying the method of reduced variables and compared with results obtained by using the indirect method.

evaluation of the relaxation spectrum $H_{Is}(t)$, which was satisfactorily compared in Fig. 19 with the relaxation spectrum computed from the retardation spectrum and Landel's data.

Moreover, in Fig. 23, the shear modulus function for the Hysol 8705 elastomer, as derived from the abovementioned approximate method, was compared to the transient shear relaxation modulus functions derived from Ninomiya and Ferry's method (formula 69). Again, the two curves representing the same function, as it was derived from two different methods, showed a remarkable coincidence.

Most viscoelastic solids exhibit a mechanical and optical behaviour, which is characterized by a broad creep or relaxation spectrum spread over many decades of the log time scale. As it has been previously mentioned, it is necessary to dispose two characteristic functions for the complete description of the viscoelastic be-

haviour of the materials. For totally incompressible materials, as is essentially the case for high polymers at the rubbery region, the mean normal stress is independent of the vanishing dilatation and only one relation is needed. But the incompressibility assumption is a coarse approximation, which may lead to misconceptions, especially in cases where molecular parameters must be deduced from the existing limited viscoelastic data, or in cases, where the viscoelastic behaviour in regions of time or frequency scale, which are not experimentally accessible, is to be predicted.

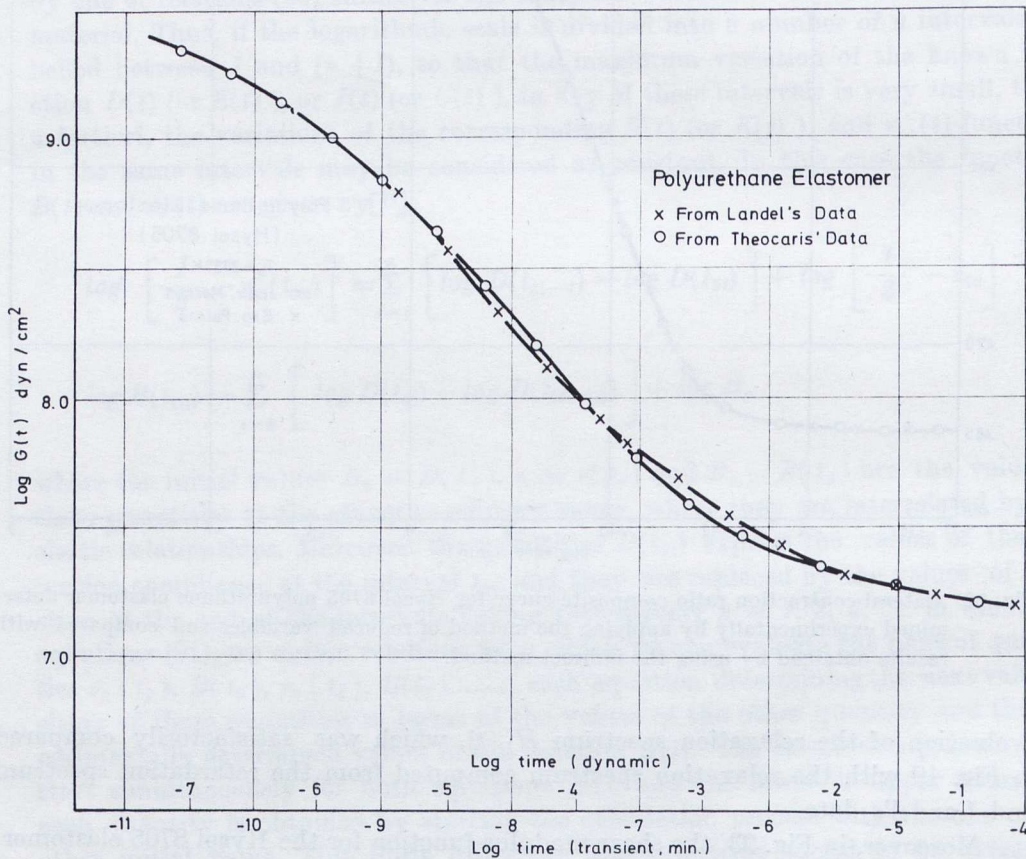


Fig. 23 Transient shear relaxation modulus composite curves for Hysol 8705 and Vulcollan 18/40 polyurethane elastomers. The first curve is derived from the corresponding extension relaxation composite curve and an initial value of the LCR at the rubbery state while the second curve is derived from Ninomiya and Ferry's approximation method.

It is assumed in the indirect method that an equivalent contribution of the bulk modulus and the LCR function to the variation of the main characteristic function in the two steps of the interval holds. Since, the bulk and the lateral con-

traction ratio functions are the only functions, which depend uniquely on the change of volume, this equivalent contribution is a reasonable one.

The linear and parabolic relationships between the bulk modulus and compliance and the lateral contraction ratio seems to hold to a high degree of approximation as it may be proved by extensive experimental evidence^[30,38,39]. Thus, these assumptions may replace any other assumption, such as the incompressibility, or the constancy of bulk, along the whole viscoelastic spectrum, and they will yield results closer to the exact values. These relationships may be used in problems of applications, where more than one operational modulus or compliance is involved in a complicated form. The solution of viscoelastic problems in such cases is sought by using the Laplace or Fourier transform operation with respect to time. This eliminates time from the equation in favour of the transform parameter, and the system is converted to a set of partial differential equations in the space variables only for the transformed components of stresses, which corresponds to an elastic analysis problem. Inversion of the transformed elastic solution presents insuperable difficulties in cases where the associated elastic solution is a complicated function, where the material properties are contained in a complicated form, as is usually the case in actual systems. In this case the relationships (90) between two characteristic functions of the material may simplify the problem and permit solution of the inversion, by reducing the unknown operational moduli to one function.

Alignment of Stress, Strain, and Dielectric Susceptibility Tensors in Viscoelasticity

It has been established that for a perfectly elastic material, the principal stress-, strain- and dielectric susceptibility-directions (for the transparent polymers used in photoelasticity) are always coincident. Since there is always an immediate response in strain or stress, and birefringence for a suddenly applied external load, or prescribed displacement, in a perfectly elastic material, the equilibrium state for stress, strain and birefringence is reached instantaneously, as soon as the externally applied load or displacement is established in the body. Photoelasticity, based on this simple principle, allows the study of elastic stress and displacement fields by using the birefringence created in a transparent model, submitted to similar stress or displacement configurations as in the prototype, which according to the Maxwell-Neumann law is directly proportional to the externally applied type of disturbance in the body. Therefore, in perfectly elastic materials the stress-, strain- and birefringence-isoclinics (that is the lines along which the orientation of principal stresses, strains or birefringence is constant) are confounded into one family of curves.

For the case of a material presenting a viscoelastic behaviour and subjected to any type of loading or displacement the correspondence between stress-, strain-

and dielectric susceptibility-tensors is not in advance known to be so simple, as for perfectly elastic materials. Even for a rheo-optically simple material, the interrelation of these three tensors is not very simple especially in the transition region.

However, in an one-dimensional geometry the axes of principal stress, strain and birefringence are known to be aligned, but this alignment is not necessarily the case in a general two-or three-dimensional photoviscoelastic test configuration. It is, therefore, necessary to explore the phase angle relationships between principal mechanical axes and principal optical axes in a convenient two-dimensional photoviscoelastic test configuration. It should be mentioned here that any eventual birefringence lag established during the experiment does not constitute a material characterization parameter, since birefringence depends on the particular loading programme of the viscoelastic material, on the geometric characteristics of the specimen, and on the optical set-up used in tests. On this aspect it could be correct to replace the birefringence tensor by the dielectric susceptibility tensor, or the refractive index tensor, which could then be independent of the particular characteristics of the experimental set-up and the geometry of the specimen used in the tests. But since birefringence is what we measure in a photoelastic test, we use in the followings this quantity, having always in mind the above remarks. Thus, it is necessary to use a test for measuring birefringence for which continuous collinearity between the mechanical and optical principal axes is not assured by reason of geometry and loading modes.

It was Mindlin^[40], who first considered the case of a photoviscoelastic material. Mindlin assumed small strains, so that the material obeyed Boltzmann's superposition principle and, furthermore, he postulated that the birefringence created in the material was due only to elastic elements. In this way he admitted the basic hypothesis that the relation between birefringence and stress is of a similar form as the relation between stress and strain. The same hypothesis was introduced in 1964 by Dill^[41], who accepted that the dielectric susceptibility tensor x_{ij} can be explicitly determined by the strain history of the body. He linearized this relation for simplicity and thus restricted this hypothesis to small strains.

The optical properties of high polymers used in photoelasticity was the subject of correlated studies with the mechanical properties of these materials. The stress-optical and the strain-optical coefficient functions, which relate the birefringence with the applied stress or strain in rheo-optically simple materials, proved to be monotonically varying with time, temperature or frequency^[42]. It has been shown that the time-temperature superposition principle, or the principle of reduced variables, is valid also for the optical viscoelastic properties, provided that this principle is valid for the mechanical properties of the substance^[17,21,30,38]. Furthermore, it has been proved experimentally that approximately the same time or shift factors are valid for optical and mechanical properties, and the WLF equation for optical characteristic properties is similar to the corresponding equation for mechanical properties of the high polymer. Williams and Arenz^[23] and Dill^[41,43] have given, among others, expressions in integral form interrelating

birefringence or better the dielectric susceptibility with the time-varying stresses and strains. These relations express mathematically what it has been already proved experimentally for the optical viscoelastic behaviour of polymers^[17,21,30,38].

All these studies are based on the main assumption that the relation between stress and birefringence, that is the stress-optical law, is of the same form as the stress-strain law for the material. This is not precisely true, especially at the transition region. If one examines the retardation or relaxation spectra of the composite curves in creep or relaxation versus log time, one can easily deduce that the first relaxing spectrum is the shear compliance or modulus, followed by the extension, bulk and LCR ratio spectra^[44,45]. Similar remarks are valid for the mechanical and optical behaviour of viscoelastic materials, as they can be derived from refs. 17, 18, 19, 20, 24, 26, 38 and 46.

However, the most extensive study for the proof of the non-coincidence of the stress-, strain-, and dielectric susceptibility-tensors was made by van Geen^[47], who showed that the stress, strain, and birefringence isotropic points in a two-dimensional viscoelastic stress field are in general non coincident, and only under certain and specified conditions may coincide. In spite of the relatively large number of papers dealing with this phenomenon and published by van Geen, (see list of references in refer. 47), he did not consider any quantitative evaluation of these discrepancies between the appropriate tensors and he restricted his studies to the proof of the various aspects of this non-coincidence.

In order to investigate the eventual coincidence of the three types of isoclinics in a typical viscoelastic material, a specimen geometry and load configuration were selected which yield an exact theoretical solution for the instantaneous principal stress and principal strain directions. The specimen was a thin circular disc, which was loaded equally by concentrated forces applied along two orthogonally oriented diameters of the disc. While the side (horizontal) loads were applied permanently, the vertical loads could be applied or removed rapidly at a preselected time instant^[55].

The material used for the specimens was a cold-setting epoxy polymer (Shell Epon 628), plasticized by adding 60 percent by weight of the epoxy prepolymer a Thiokol LP3 polysulfide plasticizer. The mixture was hardened by adding 8 percent TETA hardener in a glass mould after it has been thoroughly mixed and properly degassed. The cast plate was cured and annealed, so that during the period of experiments the polymer was stable and without any residual fringes.

It has been previously shown^[17-21] that epoxy resins (pure or plasticized) behave admirably as linear viscoelastic substances up to a certain limit of loading (different for each region of the viscoelastic spectrum) obeying Boltzmann's time-temperature superposition principle and the principle of reduced variables. Furthermore, the WLF equation is applicable in the transition region of these polymers and the same molecular mechanism determines the mechanical and optical properties of the material, so that composite curves expressing mechanical and optical characteristic functions are similar. Therefore, this type of material is ideal

for the study of the eventual non-coincidence of stress-, strain- and dielectric susceptibility tensors at the transition region, because if this non-coincidence exists for this rheo-optically simple material, a fortiori, the same behaviour may be expected for any other viscoelastic substance presenting a more complicated rheologic behaviour.

Since addition of plasticizer in the epoxy polymer merely shifts the composite curves of the material towards lower temperature levels, while it does not appreciably alter its characteristic viscoelastic properties, the plasticized epoxy polymer was selected because it presents a rubbery plateau at a temperature of 80°C and a glassy state at -10°C , which are very convenient temperatures to achieve experimentally. The material selected presents compliances and moduli at the glassy and rubbery states which are essentially constant. Furthermore, under conditions

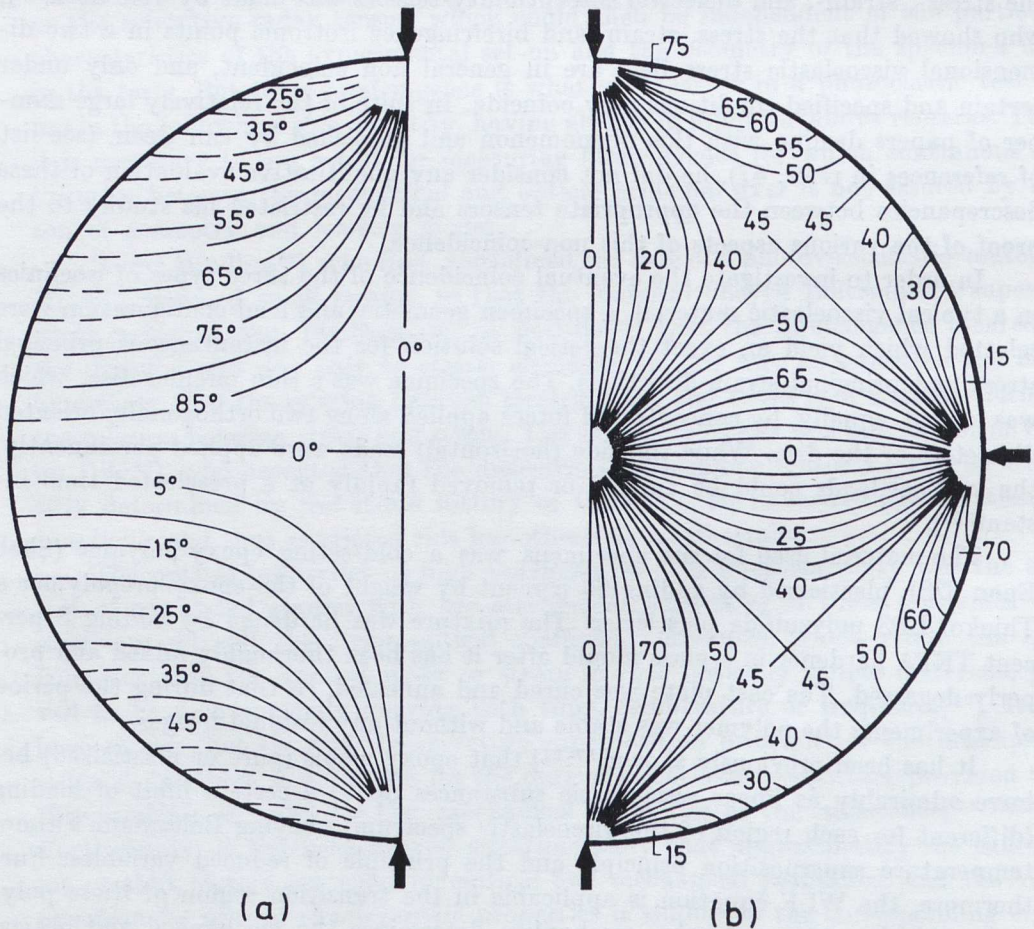


Fig. 24 The isoclinics for a disc subjected either to a diametral compression (a), or to four equal-load compression (b).

of viscoelastic equilibrium the birefringence-isoclinics coincided with the stress- and strain-isoclinics derived from the corresponding elastic solution.

For the study of the relative position of the three types of isoclinics in the transition region of the material, where the principal directions of stress, strain and birefringence change rapidly and drastically, we make use of the fact that when the four-load configuration abruptly changes to a two-load configuration the isoclinic pattern is changing from Fig. 24a to Fig. 24b. These two patterns correspond to two-load and four-load isoclinic ensembles for the corresponding elastic case. The same appearance of isoclinics is valid for the glassy and rubbery states, where in a very short period of time the one configuration changes to the other, as the one pair of loads is suddenly removed, after some time-interval was elapsed from the first application of the four-load pattern.

Indeed, it has been observed that when the material was at its glassy state (temperatures below zero) or at its rubbery plateau (temperatures above 75°C) the birefringence isoclinics changed from the four-load equilibrium configuration to the two load state in approximately the time interval elapsed for the change of the loading configuration in the disc. Therefore, it is reasonable to conclude that the birefringence isoclinics corresponded to the principal stress directions and consequently to the principal strain directions. On the contrary, at the transition region this correspondence did not happen and the birefringence isoclinics were changing slowly although the application or removal of the one pair of loads was always abrupt.

The testing programme adopted in our experiments consisted of a sudden application of the four compressive and equal loads P_x and P_y along the coordinate axes Ox and Oy of the circular disc ($P_x = P_y$) at time $t = 0$ under isothermal conditions. The loads were kept constant (creep test) for a time interval t_c equal to time necessary for reaching equilibrium in the disc. At time $t = t_c$ the vertical pair of loads P_y was released and the disc was left to recover for another interval $t_e = 16'$. We call the first time interval from $t = 0$ until $t = t_c$ the *creep interval* and the second time interval from $t = t_c$ until $t = (t_c + t_e)$ the *recovery interval*.

For the case when the two pairs of loads are equal, ($k = P_y / P_x = 1$), it is well known that a single isotropic point S_0 appears at the centre of the disc. If $P_y < P_x$, a pair of isotropic points S_1 and S_2 appears along the y -axis symmetrically placed to the centre O of the disc. The distance δ^* , which expresses the distance δ between S_1 and S_2 normalized to the diameter D of the disc is expressed by the simple relation^[48]:

$$\delta^* = \left[\frac{1 - k^{1/2}}{1 + k^{1/2}} \right]^{1/2} . \quad (92)$$

Fig. 25 presents the variation of the distance δ^* between the singularities S_1 and S_2 , as the ratio k varies between zero and unity.

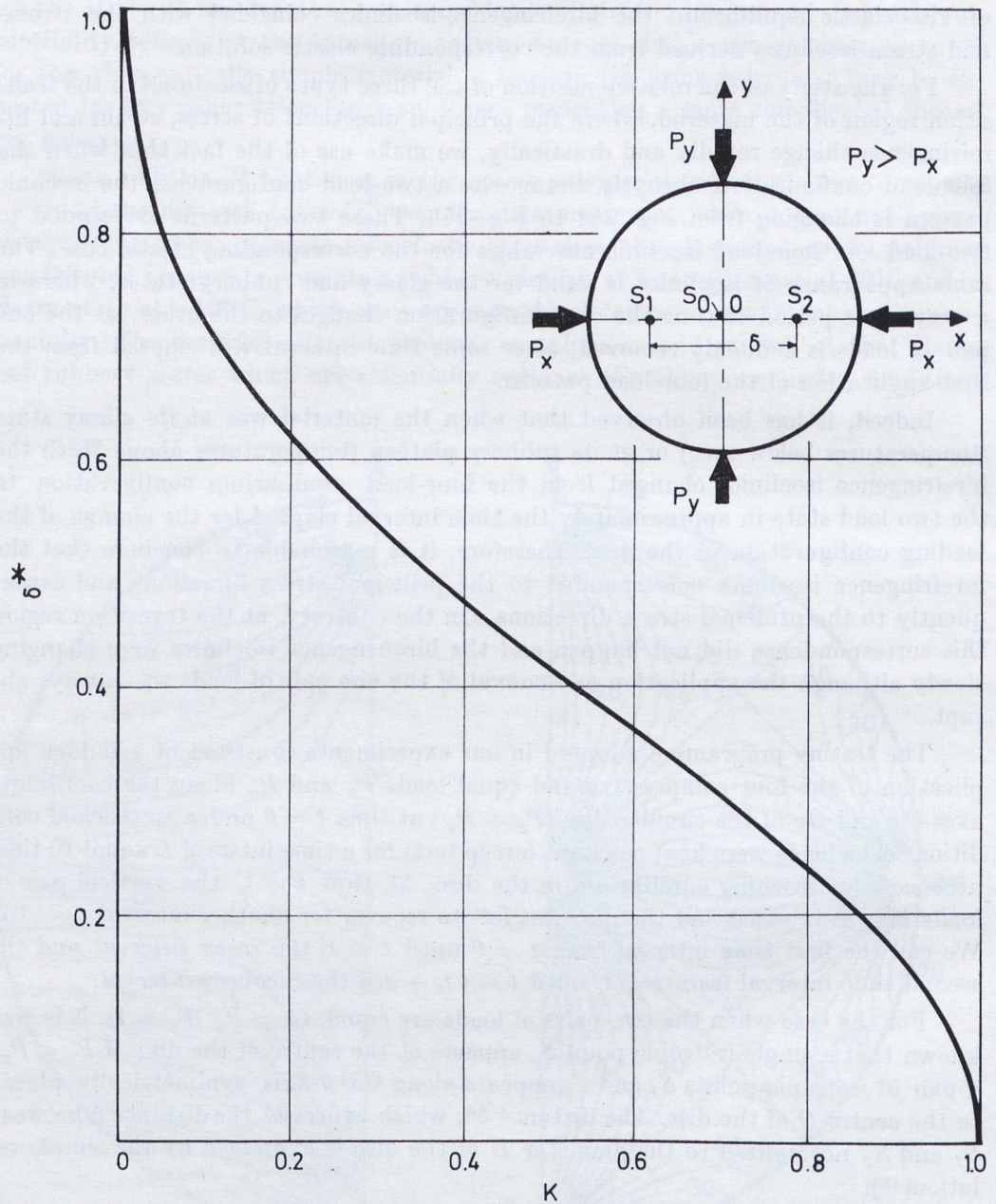


Fig. 25 Variation of distance δ^* between isotropic points normalized to the diameter of the disc versus the ratio K of the applied compressive loads P_x and P_y .

For a disc made of a linear viscoelastic substance, and considering time as a suppressed parameter, the stresses along the y -axis at $t = 0$ are given by:

$$\sigma_{xc} = -\frac{4P_x}{\pi d} \left[\frac{R^3}{(y^2 + R^2)^2} \right] + \frac{P_x + P_y}{\pi d R} \quad (93)$$

$$\sigma_{yc} = -\frac{2P_y}{\pi d} \left[\frac{1}{(R-y)} + \frac{1}{(R+y)} \right] + \frac{P_x}{\pi d R} \left[\frac{R^2 - y^2}{R^2 + y^2} \right] + \frac{P_y}{\pi d R}.$$

where d is the thickness and R the radius of the disc.

For the recovery interval the components of stresses along the y -axis of the disc are given by:

$$\begin{aligned} \sigma_{xe} &= \left\{ -\frac{4P_x}{\pi d} \frac{R^3}{(y^2 + R^2)^2} + \frac{P_x + P_y}{\pi d R} \right\} - \left\{ \frac{P_y}{\pi d R} \right\} \\ \sigma_{ye} &= \left\{ -\frac{2P_y}{\pi d} \left[\frac{1}{(R-y)} + \frac{1}{(R+y)} - \frac{1}{2R} \right] + \frac{P_x}{\pi d R} \left[\frac{R^2 - y^2}{R^2 + y^2} \right]^2 \right\} + \quad (94) \\ &+ \left\{ \frac{2P_y}{\pi d} \left[\frac{1}{(R-y)} + \frac{1}{(R+y)} - \frac{1}{2R} \right] \right\}. \end{aligned}$$

In these relations each curled bracket, for each component of stress, corresponds to different time origins and therefore they must not be merged as it could be done for the purely elastic case.

In order to obtain the corresponding viscoelastic solutions and since the applied loads are step functions with time and the material behaves as a rheo-optically simple substance, the correspondence principle may be applied. According to this principle all functions are assumed to be time dependent and the creep compliances and the lateral contraction ratio functions entering in the expressions for the strain components are time dependent functions defined by their corresponding composite curves.

The components of strains at the recovery interval are given by:

$$\begin{aligned} \varepsilon_{xe} &= D_c (t_c + t) \left[\left\{ -\frac{4P_x}{\pi d} \frac{R^3}{(y^2 + R^2)^2} + \frac{P_x + P_y}{\pi d R} \right\} - \nu_c (t_c + t) \left\{ \right. \right. \\ &\left. \left. \left\{ -\frac{2P_y}{\pi d} \left[\frac{1}{(R-y)} + \frac{1}{(R+y)} - \frac{1}{2R} \right] + \frac{P_x}{\pi d R} \left[\frac{R^2 - y^2}{R^2 + y^2} \right]^2 \right\} \right] + \\ &+ D_c (t) \left[\left\{ -\frac{P_y}{\pi d R} \right\} - \nu_c (t) \left\{ \frac{2P_y}{\pi d} \left[\frac{1}{(R-y)} + \frac{1}{(R+y)} - \frac{1}{2R} \right] \right\} \right] \quad (95) \\ \varepsilon_{ye} &= D_c (t_c + t) \left[\left\{ -\frac{2P_y}{\pi d} \left[\frac{1}{(R-y)} + \frac{1}{(R+y)} - \frac{1}{2R} \right] + \frac{P_x}{\pi d R} \left[\frac{R^2 - y^2}{R^2 + y^2} \right]^2 \right\} - \right. \\ &\left. - \nu_c (t_c + t) \left\{ -\frac{4P_x}{\pi d} \frac{R^3}{(y^2 + R^2)^2} + \frac{P_x + P_y}{\pi d R} \right\} \right] + \\ &+ D_c (t) \left[\left\{ \frac{2P_y}{\pi d} \left[\frac{1}{(R-y)} + \frac{1}{(R+y)} - \frac{1}{2R} \right] \right\} - \nu_c (t) \left\{ -\frac{P_y}{\pi d R} \right\} \right]. \end{aligned}$$

In these relations $D_c(t_c + t)$ and $v_c(t_c + t)$ are the values for the extension creep compliance and the creep LCR function for the material at time $(t_c + t)$, where t is the time elapsed in the recovery period, and $D_c(t)$ and $v_c(t)$ are the values of the same characteristic functions corresponding to the time t , elapsed in the recovery period only. If the time t_c corresponds to the retardation time of the ma-

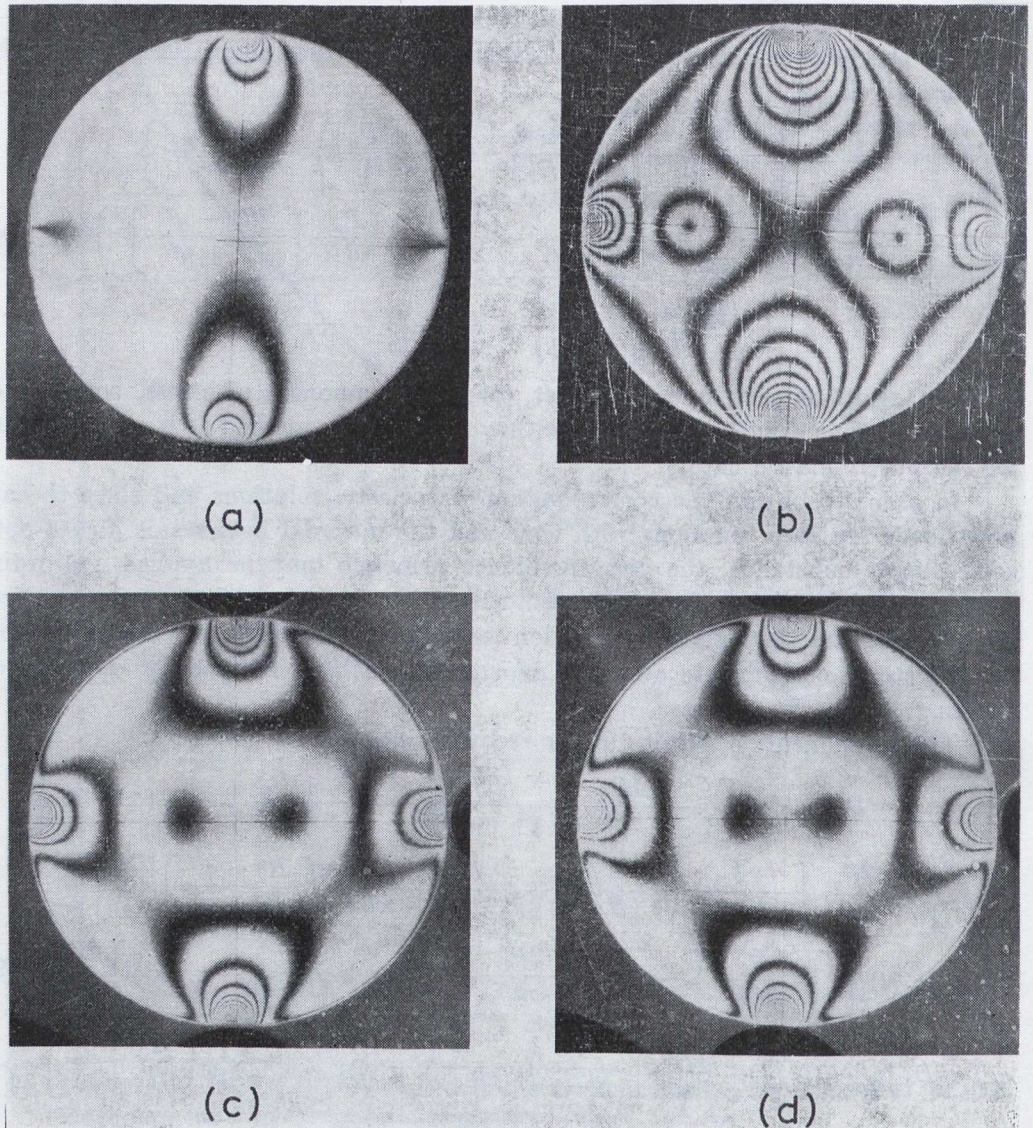


Fig. 26 Typical isochromatic patterns for a disc made of a plasticized epoxy polymer, subjected to a four-equal load configuration until viscoelastic equilibrium is reached and then submitted to a recovery period by releasing the one pair of loads. The patterns correspond to recovery times $t = 8$ min, 16 min, 16 min and 2 min respectively and the corresponding temperatures of the tests were $T = 75^\circ, 40^\circ, 25^\circ$ and 10°C .

terial at the temperature of test, then $D_c(t_c + t) = D_\infty$ and $\nu_c(t_c + t) = \nu_c(\infty)$ that is the equilibrium compliance and the equilibrium LCR value.

In order to find the position to the strain-isotropic points along the y -axis for $P_x = P_y$ and their relative position to the corresponding birefringence isotropic points, which are defined experimentally from the photoelastic test in creep and subsequent recovery of the disc, it is necessary to equate the two components

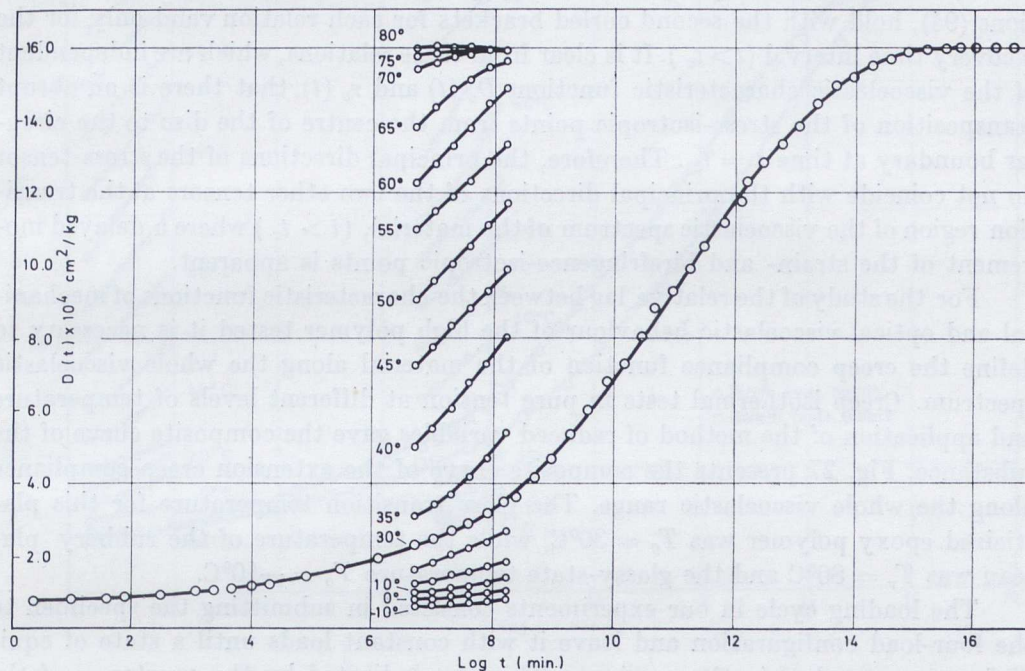


Fig. 27 Individual isothermal creep curves for the extension creep compliance at various steps of temperature and the composite $D(t)$ -curve derived by applying the principle of reduced variables versus log time.

of strain at each time instant. Equating relations (95.1) and (95.2) and solving we obtain, after some algebra, that:

$$\frac{P_x}{P_y} \left[\frac{1 - (y/R)^2}{1 + (y/R)^2} \right]^2 = \left[1 - \frac{D_c(t)}{D_c(t_c + t)} \cdot \frac{[1 + \nu_c(t)]}{[1 + \nu_c(t_c + t)]} \right]. \quad (96)$$

In the case when the two loads are equal ($P_x = P_y$) and the LCR function does not change drastically, that is when $\nu_c(t) = \nu_c(t_c + t)$, relation (96) becomes:

$$\left[\frac{1 - (y/R)^2}{1 + (y/R)^2} \right]^2 = \left[1 - \frac{D_c(t)}{D_c(t_c + t)} \right] \quad (97)$$

Solving relations (96) or (97) with respect to y , we define the distance $\pm y$ along the y -axis in both sides of the origin O , where the isotropic points are lying

for each time-interval during recovery. These are compared with the corresponding birefringence-isotropic points found experimentally by photoelasticity. Fig. 26 presents a typical photoelastic pattern for a disc made of cold-setting plasticized epoxy resin C-100-60-8 at temperatures $T = 75^\circ, 40^\circ, 25^\circ, 10^\circ\text{C}$, where the times t_c were taken equal to the retardation times of the material and $t = 8$ min., 16 min., 16 min. and 2 min respectively.

For the stress isotropic points the components of stresses, expressed by relations (94), hold with the second curled brackets for each relation valid only for the recovery time interval ($t > t_c$). It is clear from these relations, which are independent of the viscoelastic characteristic functions $D_c(t)$ and $\nu_c(t)$, that there is an abrupt transposition of the stress-isotropic points from the centre of the disc to the circular boundary at time $t = t_c$. Therefore, the principal directions of the stress-tensor do not coincide with the principal directions of the two other tensors at the transition region of the viscoelastic spectrum of the material, ($t > t_c$) where a delayed movement of the strain- and birefringence-isotropic points is apparent.

For the study of the relative lag between the characteristic functions of mechanical and optical viscoelastic behaviour of the high polymer tested it is necessary to define the creep compliance function of the material along the whole viscoelastic spectrum. Creep isothermal tests in pure tension at different levels of temperature and application of the method of reduced variables gave the composite curve of the substance. Fig. 27 presents the composite curve of the extension creep compliance along the whole viscoelastic range. The glass transition temperature for this plasticized epoxy polymer was $T_g = 30^\circ\text{C}$, while the temperature of the rubbery plateau was $T_r = 80^\circ\text{C}$ and the glassy-state temperature $T_o = -10^\circ\text{C}$.

The loading cycle in our experiments consisted in submitting the specimen to the four-load configuration and leave it with constant loads until a state of equilibrium was reached in the specimen. This was indicated by the constancy of the fringe patterns with time and the constancy of the applied pairs of loads without operating at the electric regulators. The experiment started at a temperature very close to the rubbery state, where viscoelastic equilibrium was reached very quickly. The creep period for this and subsequent tests was limited. As soon as viscoelastic equilibrium was achieved, the recovery period was started by the instantaneous release of the one pair of loads (the horizontal loads)^[55]. The position of the birefringence isotropic points was recorded for each time interval in the log time scale. Furthermore, the position of the strain-isotropic points was determined by putting in relations (96) or (97) $D_c(t) = D_\infty$ and $\nu_c(t) = \nu_\infty$ (that is the values of these functions at the rubbery state) and $D_c(t_c + t)$ and $\nu_c(t_c + t)$ the corresponding values from the isothermal individual creep curve at the time interval considered. The recovery experiments lasted always 16', and measurements were taken at 1/2', 1', 2', 4', 8' and 16' in a logarithmic scale.

As soon as the experimental cycle was terminated, the temperature was dropped by 5°C , the specimen left to recover, and the four loading configuration started again. This constant loading lasted until again equilibrium is reached, which for

lower temperature levels necessitated a longer time period. When viscoelastic equilibrium was established the recovery loading cycle started, which again lasted for 16' and measurements of the position of the birefringence isotropic points were executed in the same time intervals.

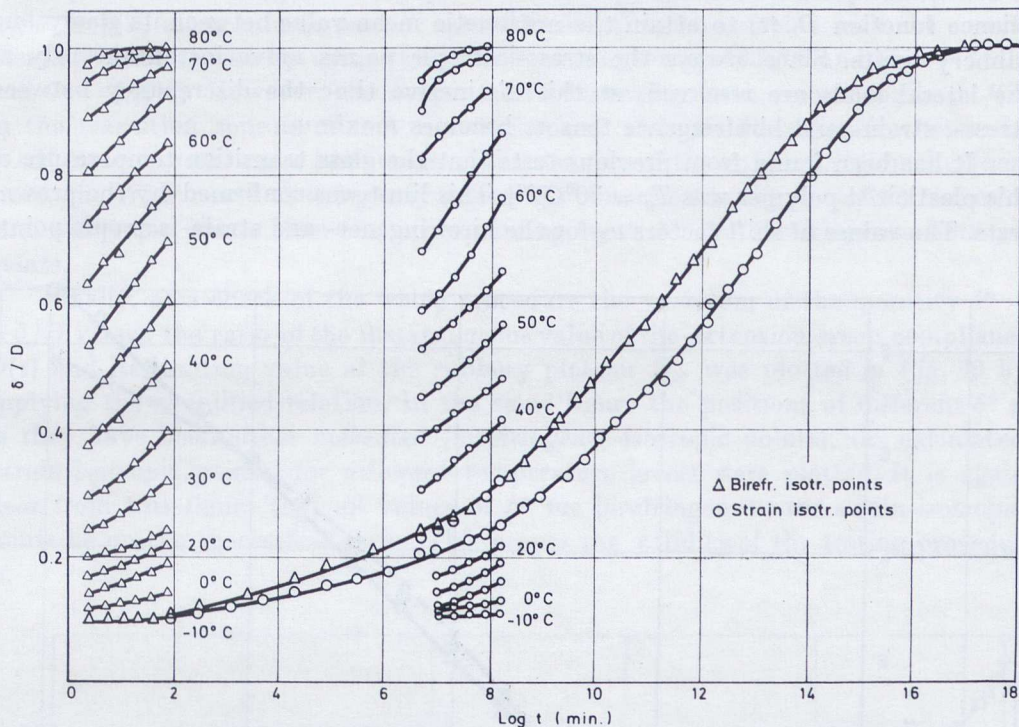


Fig. 28 Individual isothermal curves for the relative positions of isotropic points expressed by the distance $\delta^* = \delta/D$ corresponding to birefringence (Δ) and strains (\circ).

Fig. 28 presents the individual isothermal curves of the relative positions of isotropic points $\delta^* = \delta/D$ corresponding to birefringence (Δ) and strains (\circ). Since the relative position of the individual curves suggests the application of the method of reduced variables, this method was applied to the experimental and analytical data for the distance between birefringence- and strain-isotropic points. Application of the method of reduced variables to the individual isothermal curves for $\delta^* = f(\log T)$ gave the composite curves shown in Fig. 28. It is clear from the relative position of these two composite curves that in the glassy and rubbery states of the polymers there is a satisfactory coincidence of the birefringence- and strain-isotropic points. Since the response of the material at these extreme states was almost instantaneous, it is reasonable to accept that in these regions all three tensors are coincident.

However, as soon as we withdraw from these two limiting states, there is an

increasing discrepancy between the (δ/D) -composite curve for birefringence-isotropic points and the corresponding curve for strain-isotropic points. This discrepancy becomes maximum for the distinctive creep time K_d , as it has been defined by Tobolsky[11]. This time corresponds to the distinctive Temperature T_d . These two quantities are defined as the time or temperature required to the creep compliance function $D_c(t)$ to attain the arithmetic mean value between its glassy and rubbery limits. Since always the stress-isotropic points move instantaneously as the lateral loads are removed, at this distinctive time the discrepancy between stress-, strain- and birefringence tensors becomes maximum.

It has been found from previous tests that the glass transition temperature of this plasticized polymer was $T_g = 30^\circ\text{C}$ [20]. This limit was confirmed by the present tests. The values of shift factors a_T for the birefringence- and strain-isotropic points

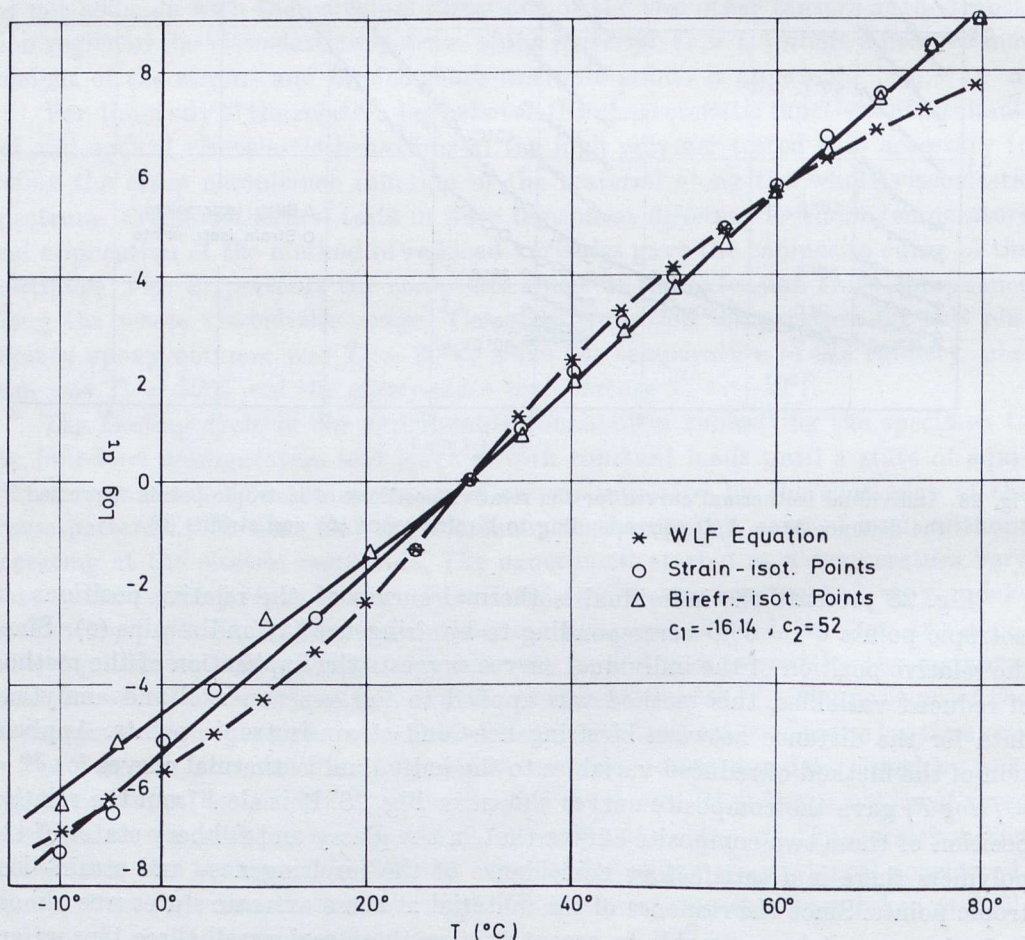


Fig. 29 The logarithm of the shift factor a_T versus temperature for composite curves $\delta^* = f(\log t)$ corresponding the birefringence (Δ)-and strain (\circ)-isotropic points. The corresponding WLF equation for $T = 30^\circ\text{C}$ was also plotted for comparison.

were determined and the curves $\log a_T = f(T)$ for both composite curves were plotted in Fig. 29. It is clear from this figure that above T_g both $\log a_T = f(T)$ curves for birefringence and strain-isotropic points coincide. Below T_g , that is in the glassy region of viscoelastic behaviour, the birefringence-isotropic points values of a_T lie in a different curve than the strain-isotropic points values of a_T . Both curves $\log a_T = f(T)$ along a large part of their transition region coincide with the corresponding curve traced by using the WLF equation for $T_g = 30^\circ\text{C}$ and $C_1 = -16.14$ and $C_2 = 56$ [11]. However, the unique curve expressing both curves $\log a_T = f(T)$ in the transition zone is almost a straight line and the discrepancies with the WLF curve become more important at the vicinity of the rubbery region. Furthermore, the WLF curve at the glassy region lies closer to the $\log a_T = f(T)$ curve for strain-isotropic points than the corresponding curve for the birefringence-isotropic points.

Finally, as a check of the whole procedure the variation of the quantity $\delta^* = \delta/D$ versus the ratio of the instantaneous value of the extension creep compliance $D(t)$ and its limiting value at the rubbery plateau D_∞ was plotted in Fig. 30 by applying the simplified relation. In the same figure the positions of different δ^* 's, as they have been either measured (birefringence-isotropic points), or calculated (strain-isotropic points) for different temperature levels were plotted. It is again clear from this figure that all values of δ^* for birefringence- and strain-isotropic points lie on the theoretical curve. This proves the validity of the testing procedure.

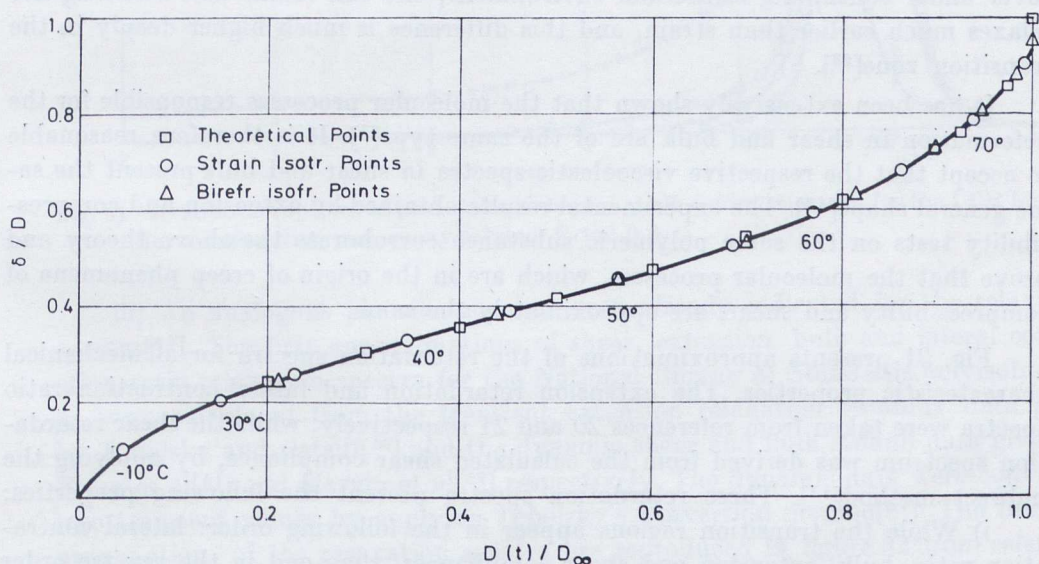


Fig. 30 Variation of the normalized distance δ^* of birefringence- and strain-isotropic points versus the ratio of the instantaneous values of the creep compliance normalized to its rubbery plateau value. The positions of this quantity δ^* for different values of $D(t)/D_\infty$ were plotted as they have derived from relation (97) (small squares).

It is worthwhile mentioning here that the use of the simplifying relation (97), instead of the accurate form of Eq. (96), where the values of LCR function along the viscoelastic range were taken as constant, does not influence the results more than at maximum 3 percent for values of lateral contraction ratio between 0.5 (rubbery state of polymer) and 0.365 (glassy state). It is therefore indifferent which one of these two relations was used for our calculations.

It has been shown that, even for a rheo-optically simple polymer, as it is the plasticized Epoxy polymer used in our tests, where the optical viscoelastic behaviour presumably follows the mechanical behaviour of the substance, there is always in the transition zone a lagging in time of the mechanical viscoelastic phenomenon relatively to the corresponding optical phenomenon. For non rheo-optically simple polymers, where the mechanism defining the optical viscoelastic behaviour is of a different form than the mechanism determining the mechanical behaviour, it is expected that this difference in optical and mechanical viscoelastic behaviour will be much stronger in the transition zone.

Thus, although it is stated that for linear viscoelastic substances the same values of the shift factor a_T must superpose all viscoelastic functions^[1], this principle is only approximately true. Previous experimental evidence proves this fact^[45], ^[49]. Indeed, if one runs simultaneous creep or relaxation tests under isothermal conditions and in simple tension, up to a certain limit of loading, which may be or may be not the viscoelastic equilibrium limit, and then leaves the specimen to recover under continuing isothermal environment, one can found that birefringence relaxes much earlier than strain, and this difference is much higher deeply in the transition zone^[53].

It has been extensively shown that the molecular processes responsible for the deformation in shear and bulk are of the same type^[1]. It is therefore, reasonable to accept that the respective viscoelastic spectra in shear and bulk present the same general shape^[49]. The experimental results obtained by extension and compressibility tests on the same polymeric substance corroborate the above theory and prove that the molecular processes, which are in the origin of creep phenomena of compressibility and shear, are approximately the same.

Fig. 31 presents approximations of the retardation spectra for all mechanical characteristic properties. The extension retardation and lateral contraction ratio spectra were taken from references 20 and 21 respectively, while the shear retardation spectrum was derived from the calculated shear compliance, by applying the indirect method^[17]. These retardation spectra present the following properties:

i) While the transition regions appear in the following order: lateral contraction ratio, bulk, extension and shear compliances, they end in the reverse order except the lateral contraction ratio function, which enters first in the rubbery region. The broadest transition region appears for the lateral contraction ratio function and the shortest for the shear compliance. Moreover, the inflection points of these curves, that is the maxima of the corresponding retardation spectra, are pre-

sented in the following order in the time scale: lateral contraction ratio, bulk, extension and shear compliance.

ii) The width of the bell-shape protrusions of the curves, representing the respective retardation spectra, is greater for the lateral contraction ratio function and it diminishes progressively, from bulk to extension and to shear retardation spectra.

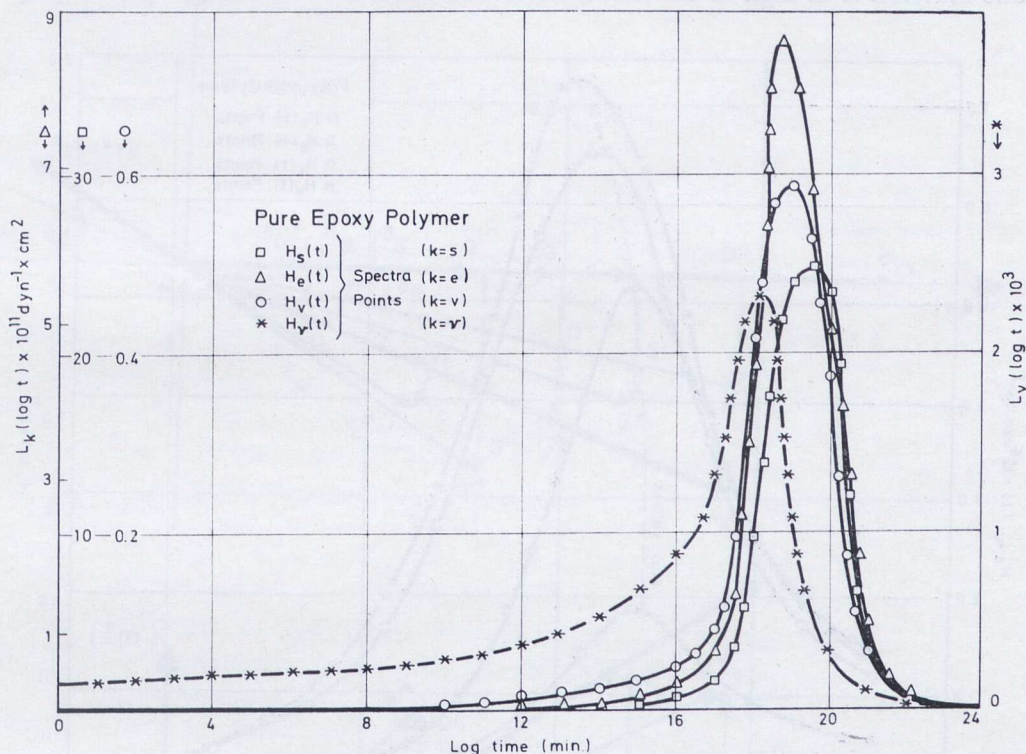


Fig. 31 Retardation spectra in pure shear, extension, bulk deformation and for the LCR function for a cold-setting pure epoxy polymer C-100-0-8.

iii) An analogous phenomenon has been already indicated for the relaxation spectra^[49]. The first approximations of shear, extension, bulk and lateral contraction ratio relaxation spectra for the National Bureau of Standards polyisobutylene were calculated from the transient extension relaxation modulus data given by Tobolsky and Catsiff^[50] and the dynamic shear and bulk moduli data given by Ferry et al^[51] and Marvin et al^[52] respectively. The dynamic data were converted into transient values by applying Tobolsky's conversion method^[37]. The first approximation of the relaxation spectra are reproduced in figure 32 from reference 49. From this figure it is again clear that the rate of relaxation is decreasing from shear modulus to extension modulus, to bulk modulus and to lateral contraction ratio relaxation function. The maxima of the relaxation spectra are following the

order: shear, extension, bulk moduli and finally the lateral contraction ratio function.

Furthermore, the bulk compliance for NBS-PIB goes through a dispersion increasing from about $2.5 \times 10^{-11} \text{ cm}^2/\text{dyn.}$ to $20.5 \times 10^{-11} \text{ cm}^2/\text{dyn.}$ The ratio of the extreme values of this dispersion region in the short and the long time ranges is of the order of eight. The corresponding ratio of the dispersion region in shear for the same material is as high as 85. Thus, while the viscoelastic behaviour of the poly-

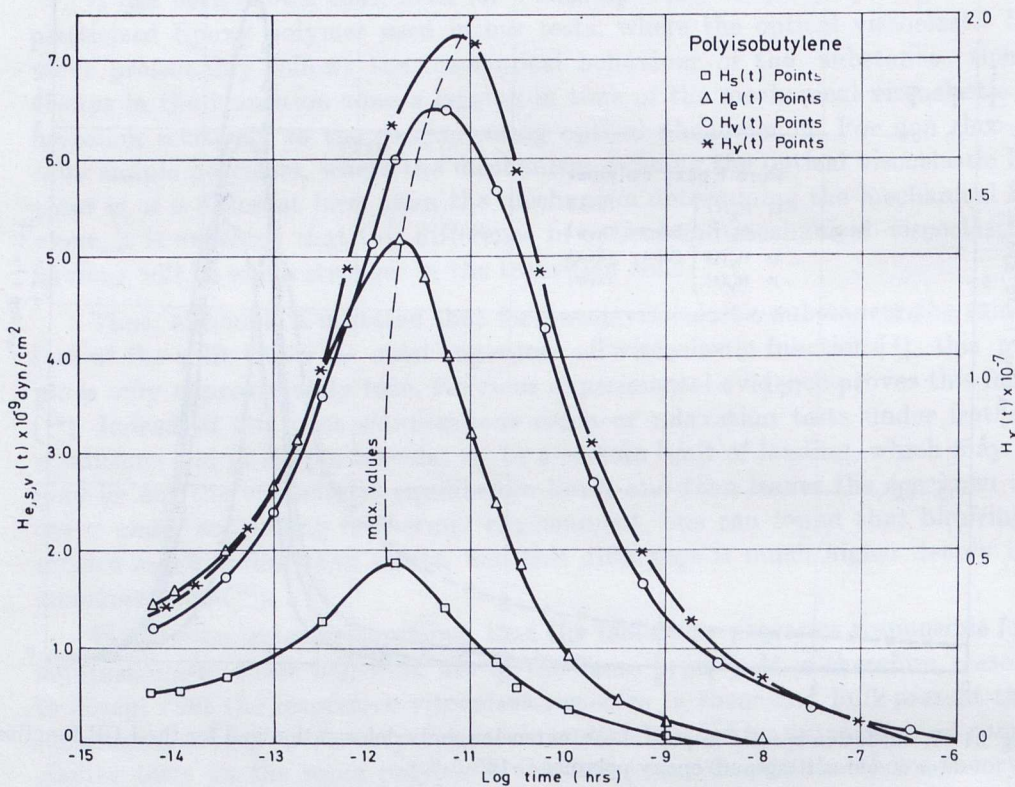


Fig. 32 Relaxation spectra in pure shear, extension, bulk deformation and for the LCR function for the NBS polyisobutylene.

mer in shear and bulk is qualitatively the same and it is governed by the same molecular mechanisms, there are certain quantitative differences of the behaviour of the material which differentiate the two deformation modes.

Indeed, it could be reasoned that at the glassy region, where a complete absence of any configurational rearrangements of the chain-backbones of the molecule is happening, the scission and interchange mechanisms create the same results in bulk, as in shear deformation. The distribution of retardation times for both types of deformation is therefore similar. Optical phenomena, which are related to side-groups movements and scission, follow closely the shear and bulk deformation

mechanisms. Above the glass transition temperature long-range configurational changes in the chain-backbones result in a considerable increase of the shear compliance. The bulk compliance and optical phenomena depend only on the scission and interchange between cross-links in the network. Therefore, they do not present

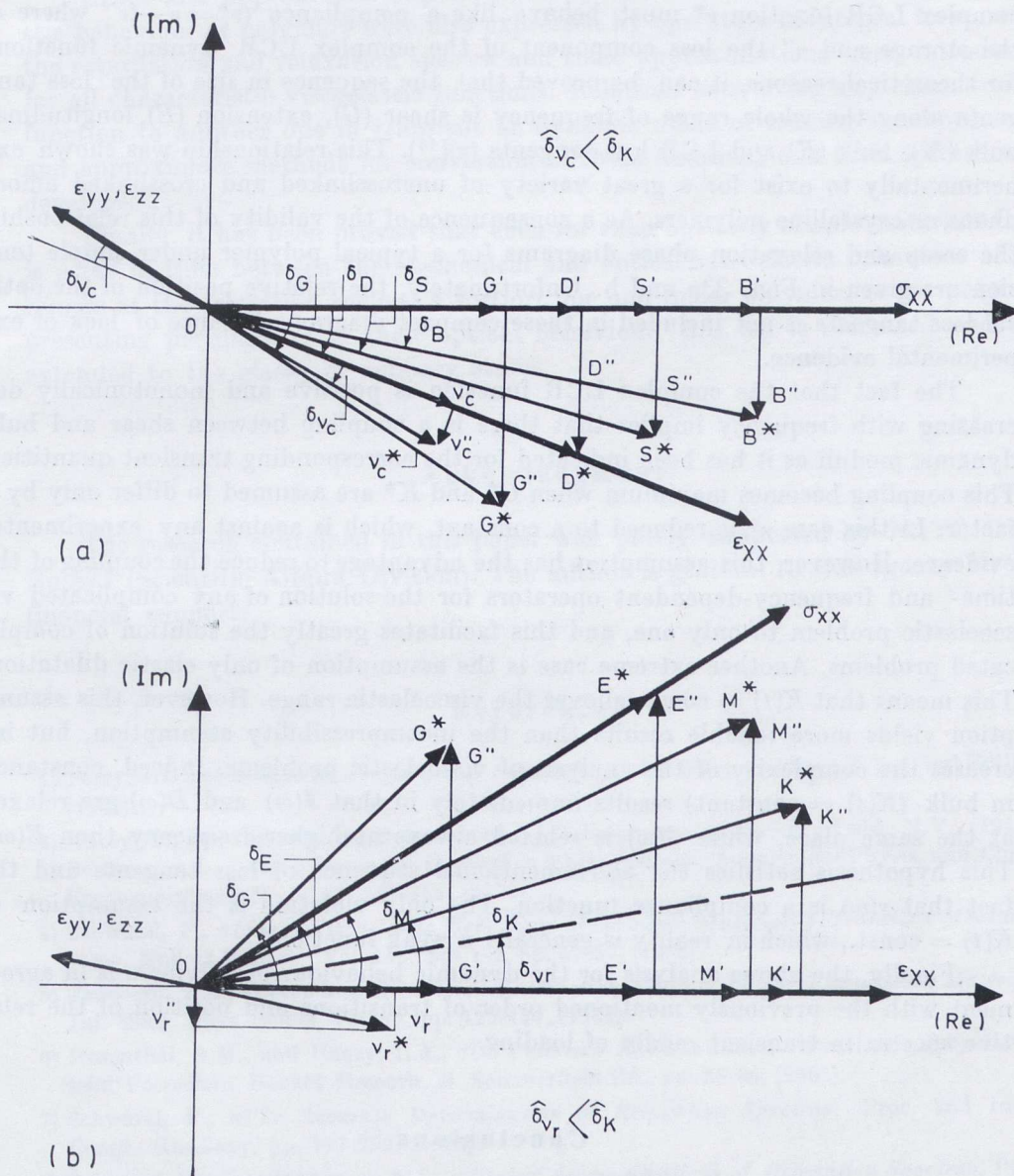


Fig. 33 Typical creep (a) and relaxation (b) phase diagrams for a cross-linked polymer subjected to simple tension. The relative position of complex, storage and loss moduli as well as the phase angles are indicated.

a very strong dispersion like the shear compliance and their mechanisms deviate from the mechanisms of shear deformation, which is the main contributor to mechanical characteristic properties of high polymers.

Similar reasoning has been developed for the relative position of the characteristic functions of dynamic moduli and compliances. Based on the fact that the complex LCR function ν^* must behave like a compliance ($\nu^* = \nu' - i\nu''$ where ν' the storage and ν'' the loss component of the complex LCR dynamic function) for theoretical reasons, it can be proved that the sequence in size of the loss tangents along the whole range of frequency is shear (G), extension (E), longitudinal bulk (M), bulk (K) and LCR loss tangents (ν)^[45]. This relationship was shown experimentally to exist for a great variety of uncrosslinked and crosslinked amorphous or crystalline polymers. As a consequence of the validity of this relationship the creep and relaxation phase diagrams for a typical polymer under simple tension are given in Figs. 33a and b. Unfortunately, the relative position of the optical loss tangents is not included in these compact diagrams because of lack of experimental evidence.

The fact that the complex LCR function is positive and monotonically decreasing with frequency implies that there is a coupling between shear and bulk dynamic moduli as it has been indicated for the corresponding transient quantities. This coupling becomes maximum when G^* and K^* are assumed to differ only by a factor. In this case ν^* is reduced to a constant, which is against any experimental evidence. However, this assumption has the advantage to reduce the coupling of the time- and frequency-dependent operators for the solution of any complicated viscoelastic problem to only one, and this facilitates greatly the solution of complicated problems. Another extreme case is the assumption of only elastic dilatation. This means that $K(t) = \text{const.}$ all over the viscoelastic range. However, this assumption yields more reliable results than the incompressibility assumption, but increases the complexity of the analysis of viscoelastic problems. Indeed, constancy in bulk ($K(t) = \text{constant}$) results immediately in that $J(\omega)$ and $D(\omega)$ are relaxed at the same place, while $G(\omega)$ is relaxed always at higher frequency than $E(\omega)$. This hypothesis satisfies the abovementioned sequence of loss tangents and the fact that $\nu(\omega)$ is a compliance function. The only violation is the assumption of $K(t) = \text{const.}$, which in reality is generally a weak function.

Finally, the above analysis for the dynamic behaviour of polymers is in agreement with the previously mentioned order of transitions and position of the relative spectra in transient modes of loading.

Conclusions

In this review the mechanical and optical viscoelastic behaviour of rheo-optically simple substances was presented in the linear region of loading. It was demonstrated that Boltzmann's superposition principle, the principle of reduced varia-

bles (or time-temperature superposition principle), together with the validity of the WLF equation, either in the transition, or along the whole viscoelastic spectrum, constitute a general method for condensed representation of the mechanical and optical properties of polymers.

Exact and approximate expressions for the mechanical and optical viscoelastic behaviour of polymers were also expressed by operators in integral form, while the retardation and relaxation spectra and their approximations were introduced, for all characteristic viscoelastic functions. Relations converting any characteristic function to another one in transient or dynamic mode of loading were presented and approximate methods for conversion of these functions and their spectra were developed.

Finally, it has been proved that even for rheo-optically simple materials there is a lag in time between the mechanical and optical viscoelastic behaviour of polymers at the transition region. A fortiori, for non-linear polymers or for polymers presenting peculiarities in their optical behaviour, this lag is increased and also extended to the glassy or rubbery states.

Acknowledgment

The research contained in this paper was partly supported by NATO Grant No 577 (Scientific Affairs Division). The author is grateful to this agency for this financial support.

References

- 1) Ferry, J.D., «*Viscoelastic Properties of Polymers*», John Wiley and Sons N.Y. (First Edition), (1961).
- 2) Alfrey, T., Jr., «*Mechanical Behavior of High Polymers*», Interscience Publ., N.Y., (1948).
- 3) Boltzmann, L., «*Zur Theorie der elastischen Nachwirkung*», Annalen der Physik und Chemie, Ergänzungsband No 7, pp. 624-654, (1876).
- 4) Schwarzl, F., «*Linear Viscoelastic Behaviour of Isotropic Materials I. Transient Measurements*», Kolloid Zeitsch., Vol. 148, Nos 1-2, pp. 47-57, (1956).
- 5) Theocaris, P.S., «*Creep and Relaxation Contraction Ratio of Linear Viscoelastic Materials*», Jnl. Mech. Phys. Solids, Vol. 12, pp. 125-138, (1964).
- 6) Rosenthal, A.M., and Henry, L.A., «*On Poisson's Ratio in Linear Viscoelastic Propellants*», Solid Propellant Rocket Research, M. Sommerfield Ed., pp. 33-66, (1961).
- 7) Schwarzl, F., «*The Accurate Determination of Relaxation Spectra*», Proc. 2nd Intern. Congr. Rheology, pp. 197-202, (1954).
- 8) Schwarzl, F., and Staverman, A.J., «*Higher Approximations of Relaxation Spectra*», Physica, Vol. 18, pp. 791-798, (1952).
- 9) Schwarzl, F., and Staverman, A.J., «*Higher Approximation Methods for the Relaxation Spectrum from Static and Dynamic Measurements of Viscoelastic Materials*», Appl. Sci. Research, Sect. A, Vol. 4, pp. 127-140, (1953).

- 10) Gross, B., «*Mathematical Structure of the Theories of Viscoelasticity*», Hermann & Cie, Paris, (1953).
- 11) Tobolsky, A.V., «*Properties and Structure of Polymers*», John Wiley & Sons, N. York, (1962).
- 12) Leadermann, H., «*Elastic and Creep Properties of Filamentous Materials*», Textile Foundation, Wash. D.C. p. 76, (1943).
- 13) Ferry, J.D., «*Mechanical Properties of Substances of High Molecular Weight. VI Dispersion in Concentrated Polymer Solutions and its Dependence on Temperature and Concentration*», Jnl. Amer. Chem. Society, Vol. 72, pp. 3746-3752, (1950).
- 14) Tobolsky, A.V., and Andrews, R.D., «*Systems Manifesting Superposed Elastic and Viscous Behavior*», Jnl. Chem. Phys., Vol. 13, No 1, pp. 3-27, (1945).
- 15) Andrews, R.D., and Tobolsky A.V., «*Elastoviscous Properties of Isobutylene. IV Relaxation Time Spectrum and Calculation of the Bulk Viscosity*», Jnl. Polymer Sci., Vol. 7, Nos 2,3 pp. 221-242, (1951).
- 16) Rouse, P.E., Jr., «*A Theory of the Linear Viscoelastic Properties of Dilute Solutions of Coiling Polymers*», Jnl. Chem. Phys., Vol. 21, pp. 1272-1280, (1953).
- 17) Theocaris, P. S., «*Viscoelastic Properties of Epoxy Resins Derived from Creep and Relaxation Tests at Different Temperatures*», Brown Univ., Div. of Engrg. Report NSF-G 8188/1 (April 1960). See also Rheologica Acta, Vol. 2, No 2, pp. 92-96, (1961).
- 18) Theocaris, P.S., «*The Rheologic Behavior of Epoxy Resins in their Transition Region*», Brown Univ., Div. of Engrg., Report NSF-G 8188/3 (May 1960).
- 19) Theocaris, P.S., Discussion on the paper «*Extended Frozen Stress Method*», by J. Schwaighofer (Prof. Paper 3351). Proc. Am. Soc. Civil Engrs., 89 EM 4, 73-77, (1963).
- 20) Theocaris P.S., and Hadjijoseph, Chr., «*Viscoelastic Behavior of Plasticized Epoxy Polymers in Their Transition Region*», Proc. Fourth Intern. Congr. Rheology, Inters. Publ., Vol. 3, pp. 485-500, (1965).
- 21) Theocaris, P.S., and Hadjijoseph, Chr., «*Transient Lateral Contraction Ratio in Creep and Relaxation*», Kolloid Zeitsch. and Zeitsch. für Polymere, Vol. 202, No 2, pp. 133-139, (1965).
- 22) Williams, M.L., Landel, R.F., and Ferry, J.D., «*The Temperature Dependence of Relaxation Mechanics in Amorphous Polymers and Other Glass-forming Liquids*», Jnl. Amer. Chem. Soc., 77, pp. 3701-3707, (1955).
- 23) Williams, M.L., and Arenz, R.J., «*The Engineering Analysis or Linear Photoviscoelastic Materials*», Experimental Mechanics, Vol. 4, No 9, pp. 249-262, (1964).
- 24) Brinson, H.F., «*Mechanical and Optical Viscoelastic Characterization of Hysol 4290*» Exp. Mechanics, Vol. 8, No 12, pp. 561-566, (1968).
- 25) Bischoff, J., Catsiff, E., and Tobolsky, A.V., «*Elastoviscous Properties of Amorphous Polymers in the Transition Region I.*», Jnl. Amer. Chem. Soc., Vol. 74, pp. 3378-3381, (1952).
- 26) Theocaris, P.S., «*Rheologic Behavior of Epoxy Resins in the Transition Region*», Jnl. Appl. Polymer Sci., Vol. 8, pp. 399-412, (1964).
- 27) Bueche, F., «*The Viscoelastic Properties of Plastics*», Jnl. Chem. Phys., Vol. 22, No 4, pp. 603, (1954).
- 28) Landel, R.F., «*Mechanical Properties of a Polyurethane Elastomer in the Rubber to Glass Transition Zone*», Jnl. Colloid Sci., Vol. 12, pp. 308-320, (1957).
- 29) Hopkins, I.L., and Hamming, K.W., «*On Creep and Relaxation*», Jnl. Appl. Phys., Vol. 28, pp. 906-909, (1957).
- 30) Theocaris, P.S., «*Relaxation Response of Polyurethane Elastomers*», Jnl. Polymer Sci., Part A, Vol. 3, pp. 2619-2635, (1965). See also Rubber Chem. and Techn., Vol. 39, No 2, pp. 375-388 (1966).

- 31) Lindsey, G.H., Schapery, R.A., Williams, M.L., and Zak, A.R., «*The Triaxial Tension Failure of Viscoelastic Materials*», ARL Report 63-152, (Sept. 1963).
- 32) Marvin, R.S., «*A New Approximate Conversion Method for Relating Stress Relaxation and Dynamic Modulus*», Phys. Rev., Vol. 86, p. 644, (1952).
- 33) Smith, T.L., «*Approximate Equations for Interconverting the Various Mechanical Properties of Linear Viscoelastic Materials*», Trans. Soc. Rheology, Vol. 2, pp. 131-151, (1958).
- 34) Ninomiya, K., and Ferry, J.D., «*Some Approximate Equations Useful in the Phenomenological Treatment of Linear Viscoelastic Data*», Jnl. Coll. Sci., Vol. 14, pp. 36-48, (1959).
- 35) Ferry, J.D., and Williams, M.L., «*Second Approximation Methods for Determining the Relaxation Time Spectrum of a Viscoelastic Material*», Jnl. Coll. Sci., Vol. 7, pp. 347-353, (1952).
- 36) Andrews, R.D., «*Correlation of Dynamic and Static Measurements of Rubber Like Materials*», Ind. Engrg. Chemistry, Vol. 44, pp. 707-715, (1952).
- 37) Catsiff, E., and Tobolsky, A.V., «*Stress Relaxation of Polyisobutylene in the Transition Region*», Jnl. Coll. Sci., Vol. 10, pp. 375-392, (1955).
- 38) Theocaris, P.S., «*Basic Affinities Between the Characteristic Functions of Linear Viscoelastic Materials*», Rheologica Acta, Vol. 3, No 4, pp. 294-310, (1964).
- 39) Theocaris, P.S., «*Affine Transformations of Viscoelastic Functions*», Rev. Roum. Sci. Techn., Mécanique Appl., Vol. 11, No 4, pp. 953-975, (1966).
- 40) Mindlin, R.D., «*A Mathematical Theory of Photoviscoelasticity*», Jnl. Appl. Phys., Vol. 20, pp. 206-216, (1949).
- 41) Dill, E.H., «*On Phenomenological Rheo-Optic Constitutive Relations*», Jnl. Polym. Sci., Part C, Vol. 5, pp. 67-74, (1964).
- 42) Theocaris, P.S., and Mylonas, C., «*Viscoelastic Effects in Birefringent Coatings*» Jnl. Appl. Mech., Vol. 28, Trans. ASME, Vol. 83, pp. 601-607, (1961). See also discussion in Jnl. Appl. Mech., Vol. 29, No 3, pp. 599-603, (1962).
- 43) Dill, E.H., «*On the Theory of Photoviscoelasticity*», Univ. Washington, Dept. Aeron. and Astron., Rep. 63-1, (1963).
- 44) Theocaris, P.S., «*Phenomenological Analysis of Linear Viscoelastic Media*», Kolloid Zeitsch. and Zeitsch. für Polymere, Vol. 209, No 1, pp. 34-43, (1966). See also: Revue Roumane Sci. Techn., Méc. Appl., Vol. 11, No 5, pp. 1185-1197, (1966).
- 45) Theocaris, P.S., «*Interrelation Between Dynamic Moduli and Compliances in Polymers*», Kolloid Zeitsch. und Zeitsch. für Polymere, Vol. 235, No 1, pp. 2182-2188, (1969).
- 46) Theocaris, P.S., «*A Review of the Rheo-optical Properties of Linear High-Polymers*», Exp. Mech., Vol. 5, No 4, pp. 105-114, (1965).
- 47) Van Geen, R., «*Effect Photoélastique et matériaux adéquantes en photoélasticimétrie*», Sciences et Techniques de l'Armement, Mémorial de l'Artillerie Française, Vol. 45, No 2, pp. 381-476, (1971).
- 48) Iosipescu, N., and Teleman, S., «*Contributie la Studiul Puncterol Singulare Produse la un Disc Circular*», Buletin Stiintific (Sectiunea de Stiinte Matematice si Fizice), Vol. 6, No 2, pp. 437-447, (1954) (in Roumanian).
- 49) Theocaris, P.S., «*Transient Creep Behaviour of Cross-Linked Polymers in Bulk Deformation*», Kolloid Zeitsch. and Zeitsch. für Polymere, Vol. 236, No 1, pp. 59-76, (1970).
- 50) Tobolsky, A.V., and Catsiff, E., «*Elastoviscous Properties of Polyisobutylene (and Other Amorphous Polymers) from Stress-Relaxation Studies IX. A Summary of Results*» Jnl. Polymer Sci., Vol. 19, pp. 111-121, (1956).
- 51) Ferry, J.D., Grandine, L.D., and Fitzgerald, E.R., «*The Relaxation Distribution Function of Polyisobutylene in the Transition from Rubber-like to Glass-like Behavior*», Jnl. Appl. Phys., Vol. 24, pp. 911-916, (1953).

- 52) Marvin, R.S., Aldrich, R., and Sack, H.S., «*The Dynamic Bulk Viscosity of Polyisobutylene*», Jnl. Appl. Phys., Vol. 25, pp. 1213-1218, (1954).
- 53) Theocaris, P.S., «*Time Dependence of Creep Recovery in Cross-Linked Polymers*» Rheologica Acta, Vol. 6, No 3, pp. 246-251, (1967).
- 54) Tobolsky, A.V., and Catsiff, E., «*Reduced Equation for Viscoelastic Behavior of Amorphous Polymers in the Transition Region*», Jnl. Amer. Chem., Soc., Vol. 76, pp. 4204-4208, (1954).
- 55) Theocaris, P.S., «*Time Lag in Mechanical and Optical Responce of Polymers*», Polymer, Vol. 15, No 11, pp. 655-660, (1974). See also, «*A Phenomenological Study of the Coincidence of Stress—, Strain—, and Birefringence Tensors in Rheologically Simple Materials*», Trons. Soc. Rheology, Vol. 18, No 4, pp. 607-683, (1974).